

MICROSCOPIC STUDY OF NUCLEAR LEVEL DENSITY

A THESIS SUBMITTED TO
THE GRADUATE SCHOOL OF NATURAL AND APPLIED SCIENCES
OF
MIDDLE EAST TECHNICAL UNIVERSITY

BY

MEHRDAD GHOLAMI

IN PARTIAL FULFILLMENT OF THE REQUIREMENTS
FOR
THE DEGREE OF DOCTOR OF PHILOSOPHY
IN
DEPARTMENT OF CHEMISTRY

JULY 2007

I hereby declare that all information in this document has been obtained and presented in accordance with academic rules and ethical conduct. I also declare that, as required by these rules and conduct, I have fully cited and referenced all material and results that are not original to this work.

Name, Last Name: Mehrdad Gholami

Signature :

ABSTRACT

MICROSCOPIC STUDY OF NUCLEAR LEVEL DENSITY

Gholami, Mehrdad

Ph.D., Department of Department of Chemistry

Supervisor : Prof.Dr. Mehmet Kıldır

July 2007, 113 pages

Level densities and spin cut-off factors have been investigated within the microscopic approach based on BCS Hamiltonian. In particular the spin cut-off parameters have been calculated at neutron binding energies over a large range of nuclear mass using the BCS theory. The results are compared with their corresponding macroscopic values. It is found that the values of $\sigma^2(E)$ do not increase smoothly with A as expected based on macroscopic theory. Instead, the values of $\sigma^2(E)$ show structures reflecting the angular momentum of the shell model orbitals near the Fermi energy.

The spin cut-off parameter $\sigma^2(E)$ has also been computed from the knowledge of nuclear level density, at neutron binding energy, B_n and the average s-wave neutron spacing, $(\sigma^2(E) = \frac{1}{2}\rho(B_n) < D_{1/2+} >)$. The values of $\sigma^2(E)$ are compared with their corresponding values from the model calculations.

The influence of the isospin in nuclear level density in particular the isospin cut-off parameter has also been investigated and are compared with their corresponding spin cut-off parameters.

Keywords: spin cut-off factor, the microscopic approach.

ÖZ

ATOM ÇEKİRDEKLERİ ENERJİ YÜZEY YOĞUNLUKLARININ MİKROSCOPIK MODELLE İNCELENMESİ

Gholami, Mehrdad

Doktora, Kimya Bölümü

Tez Yöneticisi : Prof. Dr. Mehmet Kıldır

Haziran 2007, 113 sayfa

Atom çekirdekleri enerji yüzey yoğunlukları ve açısal momentum dağılım faktörleri, BCS Hamilton'una dayanan mikroskopik modelle incelenmiştir. Özellikle, açısal momentum dağılım faktörlerinin çekirdeklerin nötron bağlanma enerjisindeki değerleri, geniş kütle aralığındaki atom çekirdekleri için hesaplanmıştır. Bulunan değerler makroskopik modelde elde edilen değerleriyle karşılaştırılmış, ancak makroskopik modelde beklenen düzgün artış gözlenmemiştir. Buna karşın açısal momentum dağılım faktörlerinin, çekirdeğin tabakalı yapısı modeline göre Fermi enerjisi civarındaki orbitallerin açısal momentum değerleriyle ilişkilendirilebilen, bir yapı gösterdiği sonucuna varılmıştır.

Açısal momentum dağılım faktörlerinin nötron bağlanma enerjisindeki değerleri, $\sigma^2(E)$, hesaplanan atom çekirdeği enerji yüzey yoğunlukları ve deneysel s-dalga nötron aralıkları yardımıyla elde edilmiştir, $(\sigma^2(E) = \frac{1}{2}\rho(B_n) < D_{1/2+} >)$. Böylece elde edilen değerler hesap sonuçlarıyla karşılaştırılmıştır.

Ayrıca, isospin kuantum sayının atom çekirdekleri enerji yüzey yoğunlukları üzerine etkisi incelenmiş ve özellikle isospin dağılım faktörlerinin hesaplanarak bulunan değerleri, açısal momentum dağılım faktörleri değerleriyle karşılaştırılmıştır.

Anahtar Kelimeler: açısal momentum dağılım faktörü, mikroskopik model

TO MY DEAR WIFE, DAUGHTER, FATHER AND MOTHER IN LAW

ACKNOWLEDGMENTS

I would like to express my sincere gratitude and appreciation to my supervisor Prof. Dr. M. Kildir , for his constant help, guidance and encouragement during the course of my research. I would also like to thank Prof. Dr. A. N. Behkami for his help and guidance as a co-advisor.

I am also greatly indebted to my wife, Shima for her support and encouragements which were always a relief in all hardships and to my lovely daughter, Rima.

Finally, I appreciate all the members of the Chemistry Department for their help during my studies at Middle East Technical University.

TABLE OF CONTENTS

ABSTRACT	iv
ÖZ	vi
DEDICATON	viii
ACKNOWLEDGMENTS	ix
TABLE OF CONTENTS	x
LIST OF TABLES	xii
LIST OF FIGURES	xiii
CHAPTER	
1 INTRODUCTION	1
2 METHODS AND MODELS FOR CALCULATING NUCLEAR LEVEL DENSITIES	13
2.1 The combinatorial method	13
2.2 The partition function method	16
2.3 The Equidistant Model	18
2.4 Fermi Gas Model	19
2.5 Spin Dependence	20
2.6 Spin Cut-off Factor	22
2.7 Residual Interaction	23
2.8 Shell Model	24
2.9 Deformed Nuclei	25
3 BCS MODEL	27
3.1 Basic Formulas	27
3.2 Energy Gap and Critical Temperature	30
3.3 Excitation Energy and Entropy	34
3.4 Odd Particle System	39
3.5 Nuclear State and Level Density	41
3.6 Spin Cut-off Factor	47
3.7 Nuclear Isospin	51
3.8 Isospin Dependent Nuclear Level Density	54

4	CALCULATIONS AND RESULTS	56
4.1	Introduction	56
4.2	Method of calculations	57
4.3	Calculations of the spin cut-off parameter	57
4.3.1	Calculations of σ^2 , Using Microscopic Model	57
4.3.2	Calculations of σ^2 , from the Level Spacing Information	76
4.4	Isospin Dependent Nuclear Level Density	81
4.5	Isospin Cut-off Parameter	85
5	SUMMARY AND CONCLUSIONS	103
	REFERENCES	105
	VITA	110

LIST OF TABLES

TABLES

Table 3.1 Energies of single particle levels with their spins for ^{244}Am nucleus.	42
Table 3.2 Symmetries of the two nucleon system.	52
Table 4.1 Comparison of Spin Cut-off Parameter, σ^2 from different methods for even-even nuclei.	59
Table 4.2 Comparison of Spin Cut-off Parameter, σ^2 from different methods for odd-odd nuclei.	63
Table 4.3 Comparison of Spin Cut-off Parameter, σ^2 from different methods for odd-A nuclei.	67
Table 4.4 The Spin Cut-off Parameter, σ^2 at neutron binding energy for odd-A Spherical Nuclei.	77
Table 4.5 Calculated Level Density for ^{30}P for various isospin.	82
Table 4.6 Calculated Level Density for ^{32}S for various isospin.	82
Table 4.7 The Isospin Cut-off parameters calculated using a , E_0 , and B_n values from Ref [71] and Ref [72].	86

LIST OF FIGURES

FIGURES

Figure 1.1 The total number of levels as a function of U for ^{56}Mn , ^{55}Fe , ^{56}Fe , ^{57}Fe and ^{58}Fe	3
Figure 1.2 The total number of levels as a function of U for ^{56}Mn , ^{55}Fe , ^{56}Fe , ^{57}Fe and ^{58}Fe	6
Figure 1.3 The total number of levels as a function of U for ^{56}Mn , ^{55}Fe , ^{56}Fe , ^{57}Fe and ^{58}Fe	8
Figure 1.4 The total number of levels as a function of U for ^{56}Mn , ^{55}Fe , ^{56}Fe , ^{57}Fe and ^{58}Fe	9
Figure 2.1 Typical excited configuration for an equidistantly spaced Fermi system of one kind of particles. At the excitation energy of $7d$, two particles are excited and two hole have been created.	15
Figure 2.2 The exact state density per unit single particle spacing $\omega(s)$ for a Fermi system of one kind of particle with equidistant single particle levels vs. excitation energy s in units of spacing, d	15
Figure 3.1 Temperature dependence of the neutron and proton gap parameters for ^{243}Cm	32
Figure 3.2 Temperature dependence of the neutron and proton gap parameters for ^{244}Am	33
Figure 3.3 Excitation energy for ^{243}Cm as a function of temperature. The neutron and proton components are shown separately.	35

Figure 3.4	Excitation energy for ^{244}Am as a function of temperature. The neutron and proton components are shown separately.	36
Figure 3.5	Relation between the entropy, S and temperature, T for ^{243}Cm .	37
Figure 3.6	Relation between the entropy, S and temperature, T for ^{244}Am .	38
Figure 3.7	Occupation probabilities of double degenerate single particle levels at excitation energy of 2.0 MeV, for ^{244}Am	40
Figure 3.8	The single particle energy levels of ^{244}Am	44
Figure 3.9	Relation between the state density, ω and excitation energy for ^{243}Cm	45
Figure 3.10	Relation between the state density, ω and excitation energy for ^{244}Am	46
Figure 3.11	The spin distribution for ^{20}F . The histogram showing the experimental spin distribution and the solid curve is a fit.	48
Figure 3.12	The Spin Cut-off parameter from microscopic theory. The individual contributions of neutron and proton are shown for ^{243}Cm .	49
Figure 3.13	The Spin Cut-off parameter from microscopic theory. The individual contributions of neutron and proton are shown for ^{244}Am .	50
Figure 3.14	The lowest levels of the three possible two nucleon systems. None of the S= 0, I= 1 levels are stable.	53
Figure 4.1	Comparison of Spin Cut-off Parameter, σ^2 from different methods for even-even nuclei.	62
Figure 4.2	Comparison of Spin Cut-off Parameter, σ^2 from different methods for odd-odd nuclei.	66
Figure 4.3	Comparison of Spin Cut-off Parameter, σ^2 from different methods for odd-A nuclei.	74
Figure 4.4	Comparison of Spin Cut-off Parameter, σ^2 at Neutron Binding Energy.	75

Figure 4.5 The Spin Cut-off Parameter, σ^2 at Neutron Binding Energy for Odd-A Spherical Nuclei.	80
Figure 4.6 Level density of ^{30}P as a function of energy and isospin. . . .	83
Figure 4.7 Level density of ^{32}S as a function of energy and isospin. . . .	84
Figure 4.8 The Isospin Cut-off parameter plotted as a function of mass number, A . The parameters of a , E_0 , and B_n are taken from Ref [71].	99
Figure 4.9 The Isospin Cut-off parameter plotted as a function of mass number, A . The parameters of a , E_0 , and B_n are taken from Ref [72].	100
Figure 4.10 Comparison of the Isospin Cut-off parameter for two different sets of parameters a , E_0 , and B_n	101
Figure 4.11 Comparison of the Isospin Cut-off parameter multiplied by a using parameters of a , E_0 , and B_n from Ref [71] with that of Spin Cut-off parameter from the BCS theory.	102

LIST OF SYMBOLS

Nomenclatures	Definitions
A	mass number
a	level density parameter
α, β and γ	Lagrange multipliers
B_n	neutron binding energy
$\langle D_{1/2^+} \rangle$	s-wave neutron spacing
Δ	pairing energy
d	single particle level spacing
E	the total energy
E_0	back shift energy
E_g	the energy of ground state
E_k	quasi particle energy
ϵ_k	energy of single particle level
ϵ_F	Fermi energy
G	strength of pairing
g	single particle level density
g_0	single particle level density at Fermi energy
h	Plank constant
I	isospin
I_z	isospin projection
\mathfrak{S}	moment of inertia
J	total angular momentum
λ	chemical potential

Nomenclatures	Definitions
M	projection of the total angular momentum
M_c	critical value of angular momentum
m_n	mass of a nucleon
$\langle m^2 \rangle$	average squared of single particle spin projections
$\langle m_i^2 \rangle$	average squared of nucleon isospin projections
n_k	occupational probability
ω	density of nuclear states which takes into account $2J + 1$ degeneracy of levels
p	momentum
P	number of projections on the space fixed axis
R	nuclear radius
r_0	radius of a nucleon
ρ	density of nuclear levels irrespective of their angular momentum degeneracy
S	entropy
σ^2	spin cut-off parameter
T	nuclear temperature
T_c	critical temperature
t	thermodynamic (statistical) temperature
U	excitation energy
U_{eff}	excitation energy corrected for pairing
V	nuclear volume
Z	grand partition function

CHAPTER 1

INTRODUCTION

The levels of the nucleus can be divided into two energy regions, namely the low energy and high energy excitations. This division arises naturally from the different approaches employed for their analysis; the spectroscopical approach for the low energy levels and the statistical approach for the high energy levels. The low-lying nuclear excited levels are small in number, well separated, and rather simple in structure. With increasing excitation energy, the spacing between the levels is progressively reduced and the nature of the excitations becomes very complicated [1]. From the statistical point of view the most relevant quantity describing the statistical nuclear properties is the level density of the system, expressed as a function of various constants of motion such as angular momentum, excitation energy, number of protons and neutrons or simply mass number, since the density of levels as a function of constants of motion is the starting point to extract quantities such as entropy and temperature [2].

The most outstanding feature of the total density of levels experimentally measured is its extremely rapid increase with excitation energy. This is apparent in high-resolution experiments, where only at the lowest excitation energies it is possible to resolve the peaks corresponding to the transitions to the discrete levels of the residual nucleus. At a few MeV of excitation energy these peaks partly overlap and then merge in the continuum. This is also evident when one compares the spacing of slow neutron resonances (occurring at an excitation energy equal to the neutron binding energy, around 7-8 MeV) with the spacing

of levels at very low excitation energy (≈ 1 MeV). The slow neutron resonance density is $10^5 - 10^6$ times greater than the low-energy level density [3]. This extremely rapid increase is characteristic of the systems where the excitation energy is distributed among many degrees of freedom, as it is expected in the nuclear case when several nucleons may be excited simultaneously. As an illustration of this rapid increase of the number of levels in Figure 1.1, the total number of levels $N(U)$ is plotted as a function of excitation energy U for ^{29}P [4], which is such a light element that the individual levels are known to quite high excitation.

The calculation of the density of states for a Fermi gas amounts to counting the number of different ways in which the excitation energy, U ,

$$U = E - E_g \tag{1.1}$$

can be distributed among the single particle states. In Eqn. (1.1) E is the total energy and E_g is the total ground state energy of the Fermion system. When the logarithmic derivative of the state density, $\omega(U)$ with respect to U is referred to the reciprocal of nuclear temperature,

$$\frac{d[\ln\omega(U)]}{dU} = \frac{1}{T} \tag{1.2}$$

the constant level density expression is obtained. A simple thermodynamic arguments suggest an exponential dependence of the level density on the excitation energy U [5]

$$\rho(U) = \frac{1}{T} \exp(U/T) \tag{1.3}$$

This expression has been widely used to analyze the spectra of particles emitted in statistical reactions and it reproduces the energy dependence of the emitted particle yield to an accuracy comparable with that obtained by use of more elaborate expressions of $\rho(U)$, or even better, as in the case of quasi-magic nuclei [6].

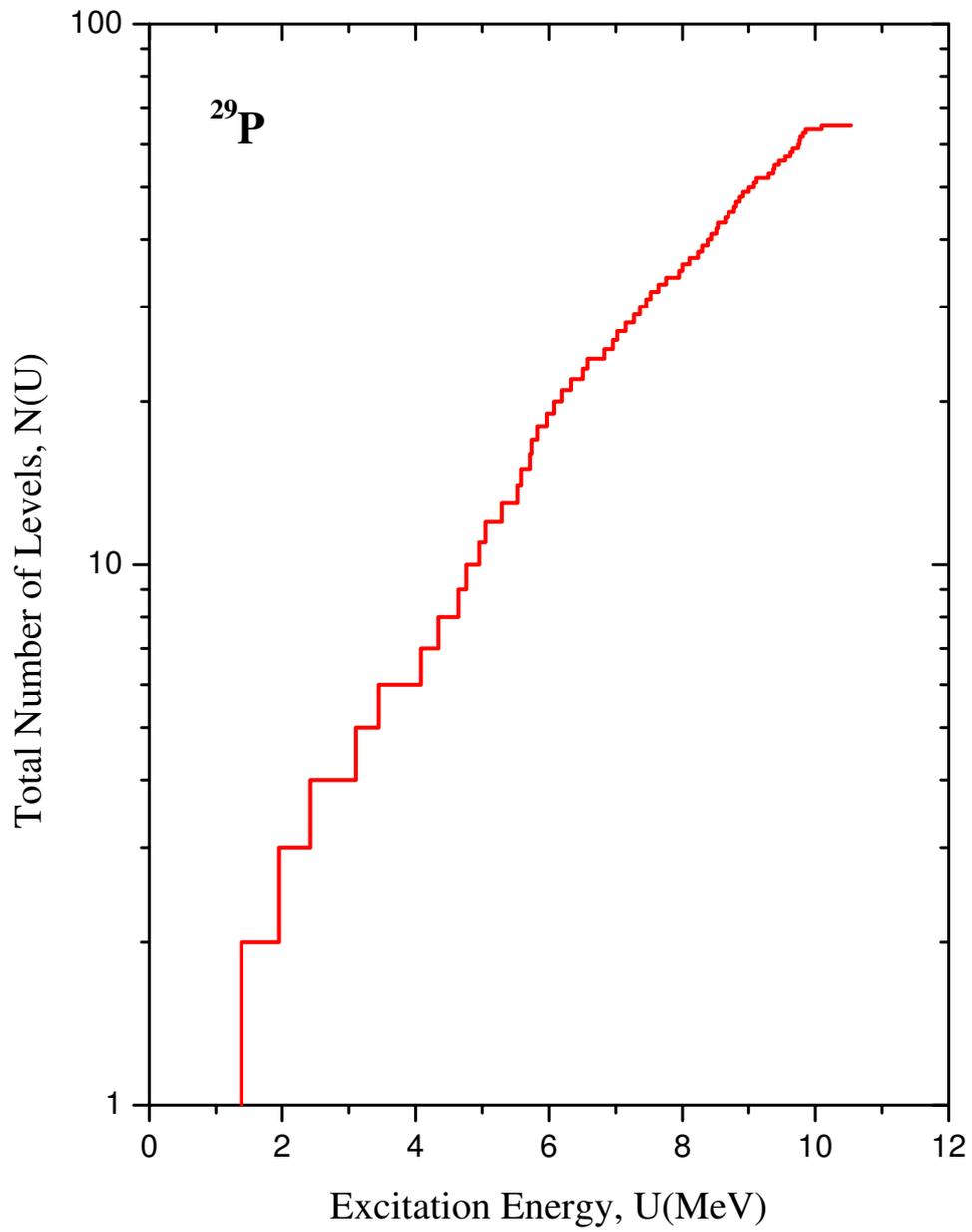


Figure 1.1: The total number of levels as a function of U for ^{56}Mn , ^{55}Fe , ^{56}Fe , ^{57}Fe and ^{58}Fe .

Gilbert *et al.* [7] showed that a constant temperature expression reproduces, at low energies, the experimental level densities better than the Fermi gas model, and later analysis of Fischer *et al.* [8] and von Egidy *et al.* [9] confirm its adequacy up to excitation energies around the neutron binding energy.

On the other hand Holbrow and Barschall [10] analysing neutron spectra from the reaction $^{103}\text{Rh}(p, n)^{103}\text{Pd}$, at different incident energies and the same interval of emitted neutron energy, found evidence for an increase of nuclear temperature with increasing excitation energy, which is contrary to that predicted by constant temperature expression.

A more elaborate expression for the energy dependence of the level density is provided by the *equidistant spacing* model in which independent Fermions are assumed to be distributed among equally spaced single particle levels with spacing d . This model of nucleus is clearly not realistic in many respects, since it neglects the residual interactions between the nucleons (so that the total energy of nucleus is simply obtained by adding the energies of the constituent nucleons) and it gives highly degenerate excited states. However, in a real nucleus the single particle levels are split into a number of components by the residual interactions. This splitting greatly increases the number of nuclear states. However, although this is indeed the case, it is not of practical importance if one is primarily interested in calculating the cross section of a reaction to the continuum region of the residual nucleus. In this case what is important is the total spectroscopic strength of the states, and this is independent of whether they are split or not. Since this splitting affects the actual number of levels, it could appreciably increase the level density obtained by direct counting of resolved levels at low excitations. However, such counts become impracticable at quite low energies and in most cases are not given for high weight for determining the constants in the level density formula. Analysis of the experimental data shows that, for most nuclei, a rather accurate expression for the single particle level

spacing d is provided by the Fermi gas model

$$d = \frac{2\varepsilon_F}{3A} \quad (1.4)$$

where ε_F is the Fermi energy and A is the mass number. In the next chapter it will be shown that the energy and mass dependence of the state density for a system composed of neutrons and protons in the equidistance spacing model is:

$$\omega(A, U) = \frac{\sqrt{\pi} \exp(2(aU)^{1/2})}{12a^{1/4}U^{5/4}} \quad (1.5)$$

where $a = \pi^2 g_0/6$, and $g_0 = g_n + g_p$ is the average total single Fermion level density. Using the energy dependence of the state density one easily finds the relation between excitation energy and nuclear temperature as

$$\frac{1}{T} = \left(\frac{a}{U}\right)^{1/2} - \frac{5}{4U} \quad (1.6)$$

The reciprocal of thermodynamic (statistical) temperature t is defined as the first derivative of entropy, S with respect to excitation energy. In the equidistant spacing model, the excitation energy is related to the thermodynamic temperature by

$$U = at^2 \quad (1.7)$$

and using for a the expression provided by the Fermi gas model, one obtains

$$T \simeq t = \left(\frac{U}{a}\right)^{1/2} = \frac{2}{\pi} \varepsilon_F^{1/2} \left(\frac{U}{A}\right)^{1/2} \quad (1.8)$$

in agreement with the energy and mass dependence found, using Eqn. (1.3), in the analysis of the experimental data of the Holbrow and Barschall [10].

Extensive analyses of the experimental data (for instance, Erba *et al.* [11]; Facchini and Saetta Menichella [12]) show that for excitation energies around $5 - 10 \text{ MeV}$ and for the nuclei far from magic regions, a varies linearly with A (or with N and Z), as shown in Figure 1.2 :

$$a \approx \frac{A}{k} \quad \text{MeV}^{-1} \quad (1.9)$$

It is found that $k \approx 7.5 - 8$, which in the Fermi gas model corresponds to $\varepsilon_F \approx 20 \text{ MeV}$.

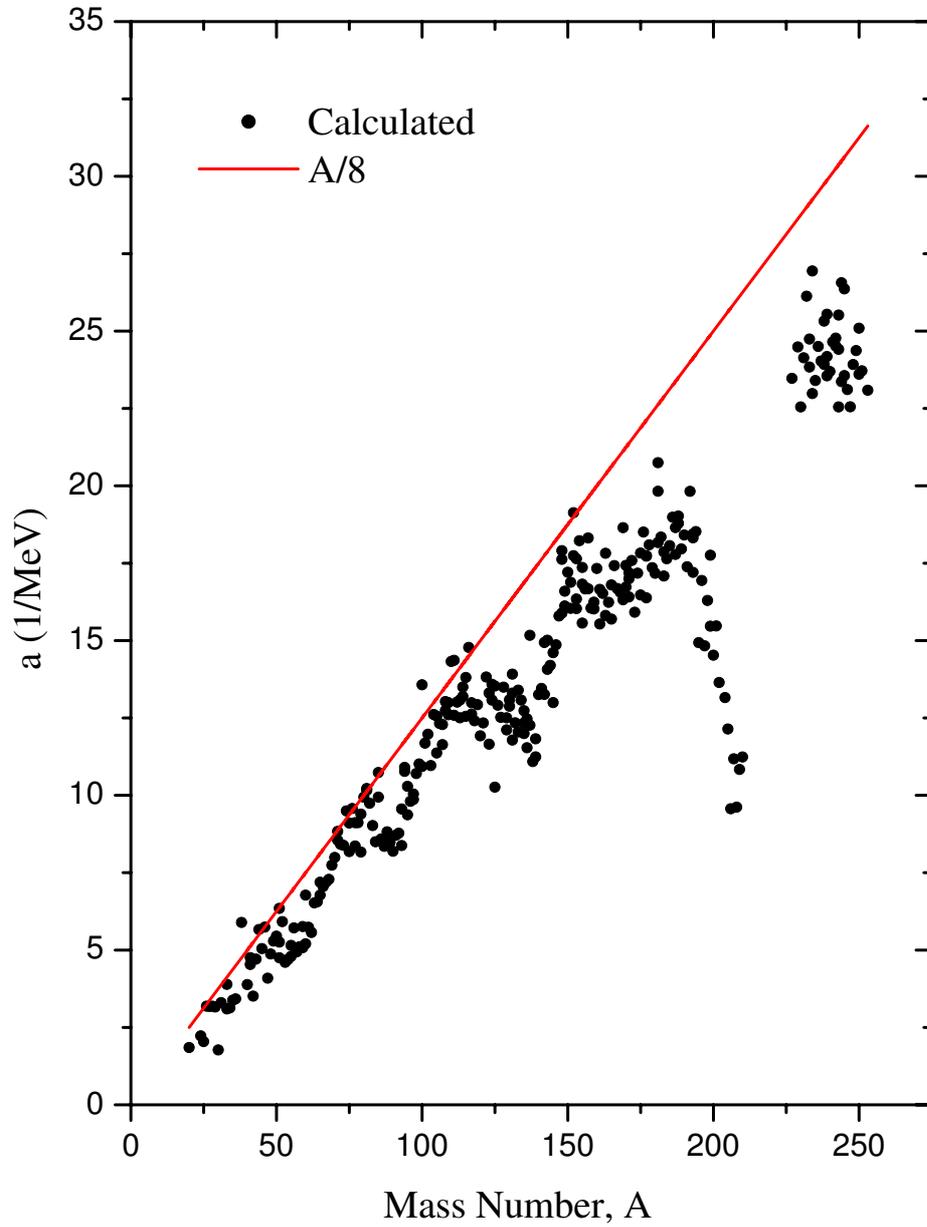


Figure 1.2: The total number of levels as a function of U for ^{56}Mn , ^{55}Fe , ^{56}Fe , ^{57}Fe and ^{58}Fe .

The figure shows, for the nuclei in near-magic regions, large deviations occur from the simple Fermi gas model estimate Eqn. (1.9). These lower values of a are strongly correlated with the ground state shell correction to the nuclear potential energy [13]. They are due to the larger average spacing of single nucleon levels around the Fermi energy for magic nuclei or, better, to the energy gap occurring in the single nucleon level sequence at the filling of the shell. These shell effects tend to disappear with increasing the excitation energy, since at higher energies the nucleon levels to be considered for evaluating the state density may have energies quite different from the Fermi energy, and their average spacing approaches again that predicted by the Fermi gas model. Figure 1.3 shows the total numbers of levels $N(U) = \sum_J \int_0^U \rho(U) dU$ for isobars of cobalt, nickel, and copper. One may easily compare level density of magic nucleus, N_i , with those of neighboring nuclei.

Another structure effect in the level densities is apparent when one compares the level densities of odd-odd, even-odd, and even-even neighboring nuclei. In Figure 1.4 are shown the total numbers of levels for isotopes of manganese and iron. One may easily see that at the same excitation energy the odd-odd ${}^{56}_{25}\text{Mn}_{31}$ has a level density greater than those of the even-odd ${}^{55}_{26}\text{Fe}_{29}$ and ${}^{57}_{26}\text{Fe}_{31}$, which in turn are greater than that of the even-even ${}^{58}_{26}\text{Fe}_{32}$. The effect may also be observed in higher excitation energies, for instance when one measures the slow neutron resonance spacings.

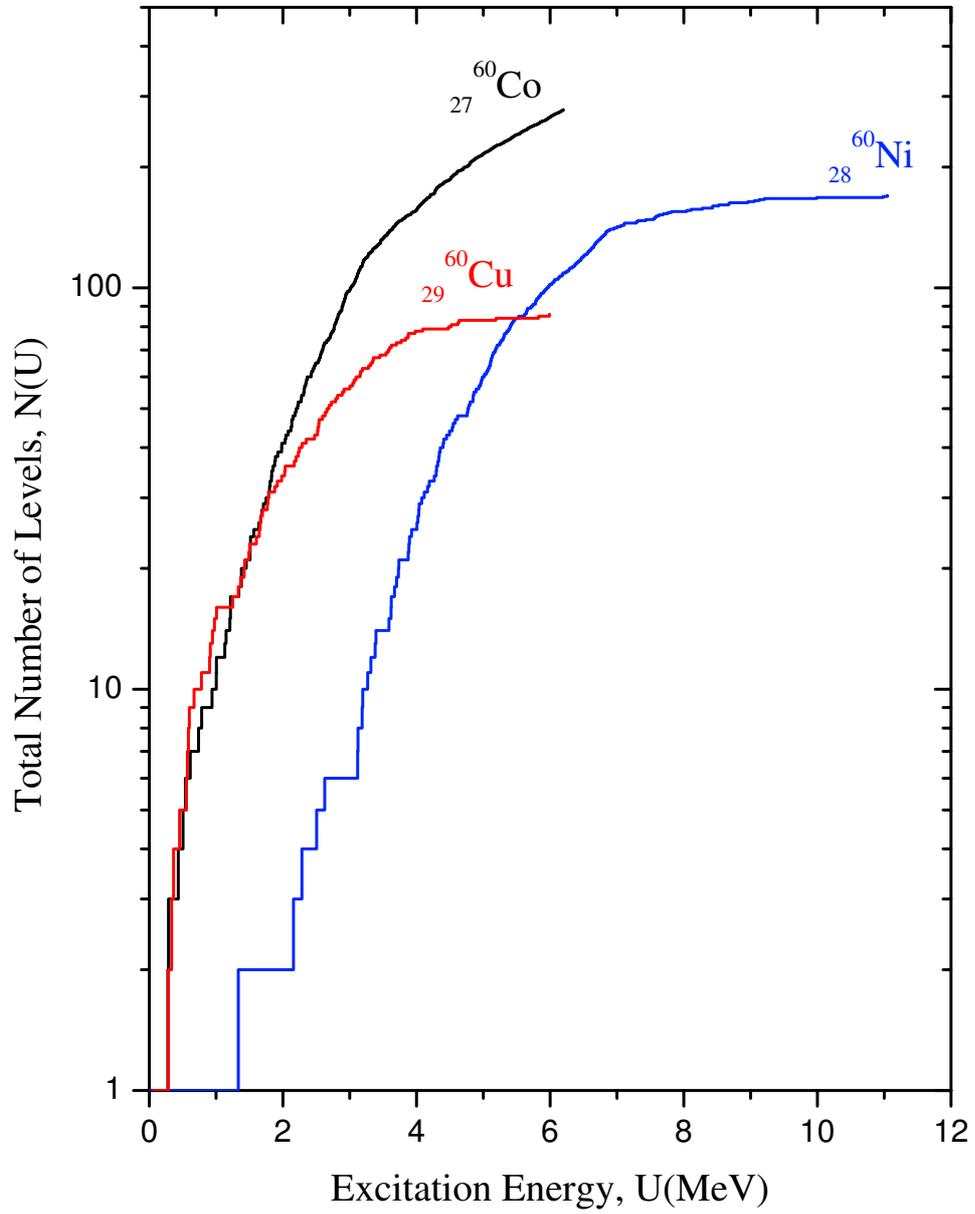


Figure 1.3: The total number of levels as a function of U for ${}^{56}\text{Mn}$, ${}^{55}\text{Fe}$, ${}^{56}\text{Fe}$, ${}^{57}\text{Fe}$ and ${}^{58}\text{Fe}$.

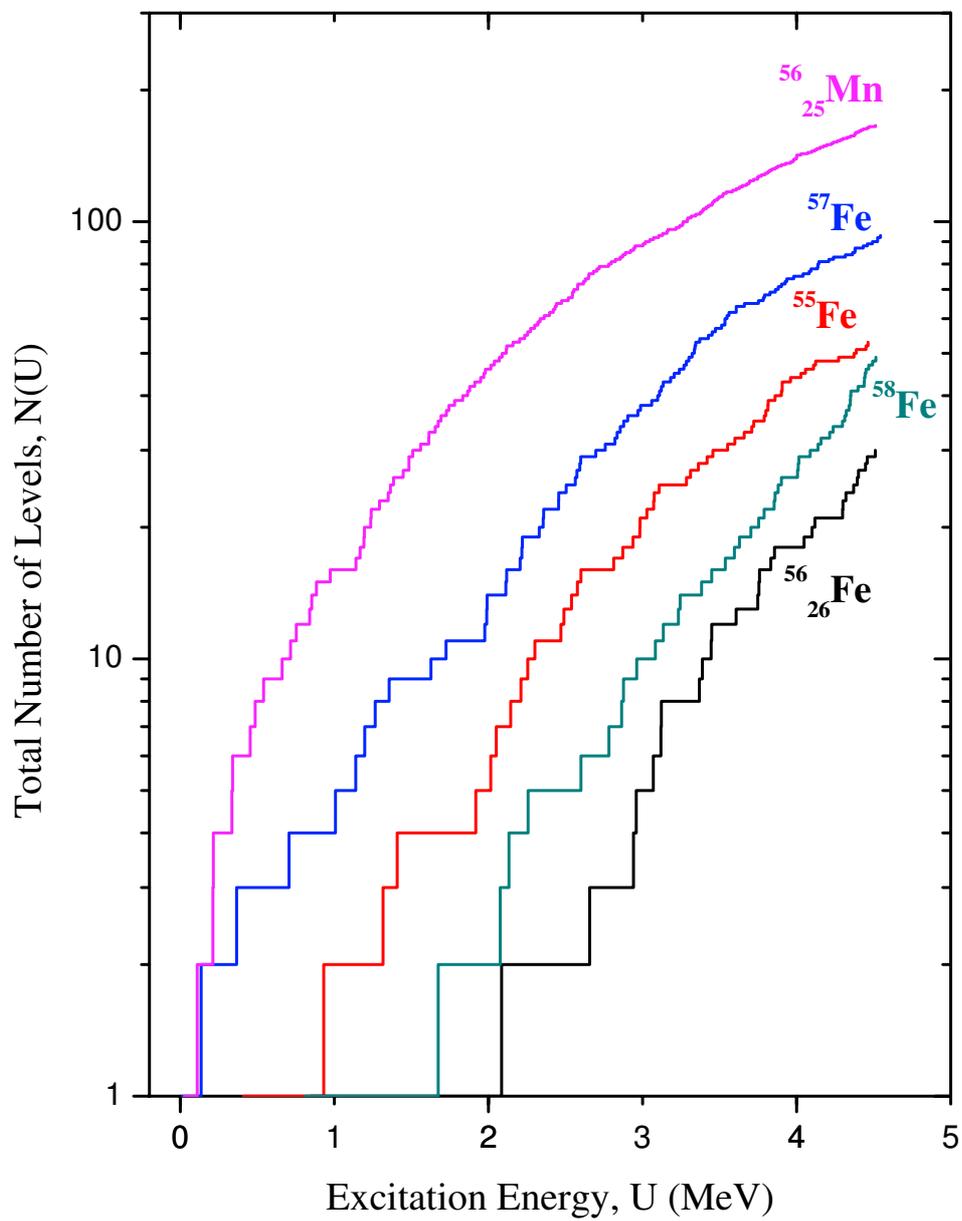


Figure 1.4: The total number of levels as a function of U for ^{56}Mn , ^{55}Fe , ^{56}Fe , ^{57}Fe and ^{58}Fe .

This odd-even effect is related to the nuclear energy gap, due to the pairing correlations in the nucleus, observed in the case of even-even nuclei at low excitation energies (of the order of one MeV). While odd-odd nuclei, even at very low excitation energies, have a number of levels which may be described as single particle excitations and are identified with the shell model configurations, the neighboring even-even nuclei have, at low energy, a far smaller number of excited levels and the few observed are associated with collective excitations, rotations, and vibrations. At energies exceeding a few MeV, the spectra of even nuclei also rapidly becomes complicated, showing the presence of single-particle excitations. This behavior may be described, to a first approximation, by assuming that some energy must be spent to break the binding of a pair of nucleons, and so does not appear as excitation energy. Thus the energy appearing in the state density expression should not be the true excitation energy U , but an effective energy

$$U_{eff} = U - \Delta_Z - \Delta_N, \quad (1.10)$$

where Δ_Z and Δ_N are the proton and neutron pairing energies [14-17].

In addition to energy, other constants of motion may be introduced to characterize the state densities. Among these is the projection M of the total angular momentum J on the z -axis. The hypothesis of a random coupling of the angular momenta of the excited particles and holes [18] led to the following expression for the level density

$$\rho(A, U, J) = \frac{(2J + 1)}{24\sqrt{2}\sigma^3} \frac{\exp [2(aU)^{1/2} - \frac{(J+1/2)^2}{2\sigma^2}]}{a^{1/4}U^{5/4}} \quad (1.11)$$

where σ^2 is the spin cut-off factor.

The level density plays a major role in all statistical model formula relating to cross-section and emission widths, and many experiments and analysis of experimental data have been done to determine with greater accuracy its parameters and to achieve accurate predictions of these quantities.

Furthermore, the superconductivity theory and the BCS Hamiltonian [18, 19], the success of which in dealing with the pairing effects of ground state is well recognized [20], have also been applied in the evaluation of level densities [21, 22]. This theory predicts the existence of transition energy, below which the Fermi gas model is invalidated. In fact in this superconducting phase the energy temperature relation is much different from the normal phase. In this way the prediction of low energy behavior of level densities has been much improved [23-26].

In all level density expressions the level density parameter, a , and the spin cut-off factor, σ^2 , are two parameters of importance. There have been some calculations of level density parameter by some authors [1, 27]. More recently a realistic calculation have been carried out which rely on the BCS theory [28]. There have also been some calculations of the spin cut-off parameter on the basis of the Fermi gas model [29, 30], however, so far realistic calculations have never been applied to obtain the spin cut-off factor, which is important in all statistical codes. In the present research work we have extended the more realistic approach to calculate the level density and the spin cut-off parameter for a large number of nuclei. In calculation we have included a balanced number of even-even, odd A and odd-odd, light, medium, heavy weight, spherical and deformed nuclei.

Second chapter begins with a brief definition of nuclear level density. The combinatorial and partition function methods are discussed as a technique for derivation of the level density from single particle spectrum. The Fermi gas description of nuclear level density is discussed briefly in this chapter. Second chapter also contains a brief discussion of a technique for deriving spin distribution of nuclear level density. In the third chapter the details of the BCS Hamiltonian employed in the calculation are discussed. Besides, the complete statistical formalism with the inclusion of pairing and angular momentum is presented. The grand partition function, the first integral of the motion like en-

ergy, particle number and Z-projection of angular momentum are written down explicitly. The gap equation, entropy expression and the partial derivatives necessary for the calculation of the level density are also presented. We consider the neutron and proton components of the nucleus at the same time and thermodynamic quantities, including level density, are evaluated for the whole nucleus. The calculational procedures are presented in the fourth chapter. It consists of calculating the dependence of energy gap parameter Δ , excitation energy and the spin cut-off parameter, state and level density, all within the framework of BCS formalism. Summary and conclusions are given in the fifth chapter.

CHAPTER 2

METHODS AND MODELS FOR CALCULATING NUCLEAR LEVEL DENSITIES

In the preceding chapter we have seen that the variation of level density with energy is typical for a system which has a large number of degrees of freedom. As a consequence the models for the description of the nuclear level densities mostly picture the nucleus as a gas of Fermions with zero interaction between them. Thus the nucleus has been considered as a system of free neutrons and protons confined to the nuclear volume [30-32], as nucleons moving in a shell model potential [33-38] and as nucleons with residual pairing interactions in a deformed well potential [38-41]. In all of these cases it is possible to express these models in terms of elementary excitations of a Fermion system. The philosophy of these approaches is to replace the complicated nucleon-nucleon interactions by an average potential, this is a reasonable procedure, particularly as we are only interested in the average validity of such a picture. In view of this it is necessary to develop general methods for the theoretical study of the level density of such systems.

2.1 The combinatorial method

The combinatorial approach is suggested by the definition of the level density. For a system of noninteracting Fermions, this method amounts to finding the

number of ways in which the nucleons can be distributed among the available single-particle levels for a fixed energy of the system. A simple way to illustrate the combinatorial method is to consider a set of only one kind independent Fermions distributed among the one particle levels which are equally spaced with a spacing d [42]. The excited states of such system always appear at integer multiples of d , sd . At excitation energy 0 system has one state only, the ground state, at energy $1d$ one state is produced by exciting the Fermion in the highest energy level to the next higher energy level. The other excited states are all degenerate. At energy $2d$, for example, there are two states, one produced by exciting the particle in the highest energy two steps and one by producing a hole by exciting the particle in the next highest level two steps, at energy $7d$ there are fifteen states and so on. In Figure 2.1 we show a typical configuration of such a system at the excitation of $7d$ in which two Fermions are excited and two hole have been created. The number of states at excitation sd as a function of s is shown in Figure 2.2. The exact solution of this problem was obtained and tabulated by Euler [43]. A few authors have used this method in limited calculations [44-46]. A very extended calculation has been performed by Hillman and Grover [47]. In their calculation, all the possible configurations are obtained by means of a simple method of enumeration and classification. The configurations are generated by cycling the occupation number of each of the single particle levels over all its allowable values. The levels are then sorted out in terms of particle number, energy, and angular momentum (and possibly other quantum numbers). The pairing interaction is taken into account.

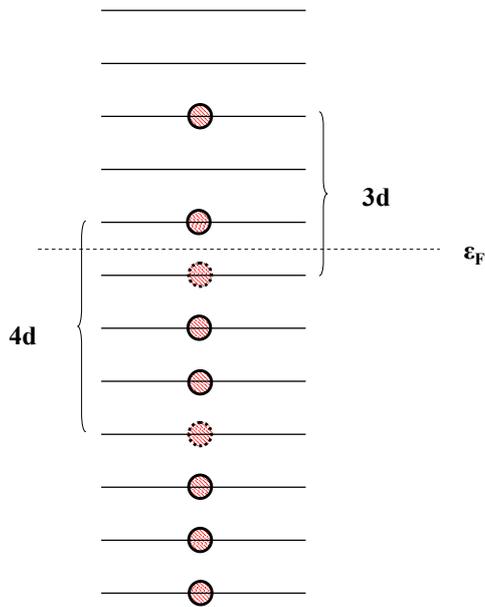


Figure 2.1: Typical excited configuration for an equidistantly spaced Fermi system of one kind of particles. At the excitation energy of $7d$, two particles are excited and two hole have been created.

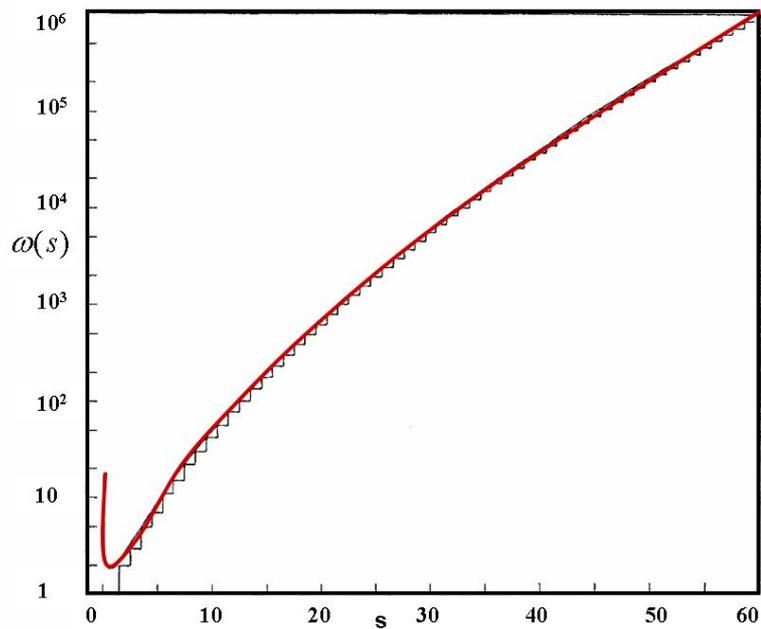


Figure 2.2: The exact state density per unit single particle spacing $\omega(s)$ for a Fermi system of one kind of particle with equidistant single particle levels vs. excitation energy s in units of spacing, d .

Such a procedure has the advantage of performing an exact counting of the levels. Furthermore, it allows one to obtain detailed distributions in various quantities such as angular momentum, parity, gap parameter, etc. Typically, in a heavy nucleus far from a closed shell, the level density may be of the order of 10^6 levels/MeV at the neutron binding energy.

2.2 The partition function method

This very powerful method has become a classical tool in statistical mechanics because of its generality and flexibility. Let the nucleus be defined by its neutron and proton numbers N and Z and by its energy E . The statistical properties of the system are contained in the grand partition function:

$$Z(\alpha_N, \alpha_Z, \beta) = \sum_{N,Z,E} \exp(\alpha_N N + \alpha_Z Z - \beta E) \quad (2.1)$$

where α_N , α_Z , and β are Lagrange multipliers associated with the particle numbers and energy. Of particular significance is the quantity $t = 1/\beta$ which is commonly known as the statistical temperature.

The summation is over all nuclei with N neutrons and Z protons, and over all energy eigenvalues E of each nucleus. The sum over the energy eigenstates can be substituted by an integral:

$$Z(\alpha_N, \alpha_Z, \beta) = \sum_{N,Z} \int \omega(E, N, Z) \exp(\alpha_N N + \alpha_Z Z - \beta E) dE \quad (2.2)$$

The quantity $\omega(E, N, Z)$ represents the state density. The above equation also shows that the grand partition function can be considered a Laplace transform of the state density. A very elegant method for the inversion of Eqn. (2.2) in the case of a system of noninteracting Fermions has been described by Williams [48]. This method uses recursion relations for the calculation of the coefficients of a finite order partition function and yields the exact state density. The method can be generalized to account for quantum numbers which can be expressed in

terms of sums over single particle levels. A more general method yielding the state density makes use of the inverse Laplace transform of Eqn. (2.2):

$$\omega(E, N, Z) = \frac{1}{(2\pi i)^3} \oint d\alpha_N \oint d\alpha_Z \oint d\beta e^S \quad (2.3)$$

where $S = \ln Z(\alpha_N, \alpha_Z, \beta) - \alpha_N N - \alpha_Z Z + \beta E$. The above contour integrals are also known as the Darwin-Fowler integrals. So far the only approximation introduced into the calculation is the continuous approximation whereby the state density is considered a continuous function. However, the generality of the method arises from a remarkable approximation which allows one to evaluate the integrals in Eqn. (2.3).

It can be shown that the integrand has a saddle point whose location is defined by the equations:

$$\frac{\partial S}{\partial \alpha_N} = 0; \quad \frac{\partial S}{\partial \alpha_Z} = 0; \quad \frac{\partial S}{\partial \beta} = 0 \quad (2.4)$$

or

$$\frac{\partial[\ln Z(\alpha_N, \alpha_Z, \beta)]}{\partial \alpha_N} = N; \quad \frac{\partial[\ln Z(\alpha_N, \alpha_Z, \beta)]}{\partial \alpha_Z} = Z; \quad \frac{\partial[\ln Z(\alpha_N, \alpha_Z, \beta)]}{\partial \beta} = -E \quad (2.5)$$

The path of integration can be chosen to pass through this point. By expanding the exponent S in a Taylor series about the saddle point and retaining only the quadratic terms, the integrals in Eqn. (2.3) yield the following result:

$$\omega(E, N, Z) = \frac{\exp S}{(2\pi)^{3/2} D^{1/2}} \quad (2.6)$$

where D is a 3×3 determinant of the second derivatives of $\ln Z(\alpha_N, \alpha_Z, \beta)$ with respect to the Lagrange multipliers α_N , α_Z , and β . All of the quantities contained in Eqn. (2.6) must be evaluated at the saddle point.

Such an approximation corresponds to the Stirling approximation for the evaluation of factorials and its accuracy depends upon the magnitude of the state density itself. The agreement of results based upon the saddle point approximation with the exact results is good even at low excitation energies [42,

49]. The elegance of the method is also quite apparent in the way in which the boundary conditions of the problem are introduced. They appear in a very simple way in Eqn. (2.5) where the saddle point is defined.

2.3 The Equidistant Model

In this model the same system which it is used previously in the combinatorial method is also employed in the partition function method [42], generates

$$\omega(U) = \frac{\exp\{2(\frac{\pi^2}{6}g_0U)^{1/2}\}}{\sqrt{48U}} \quad (2.7)$$

where $g_0 = d^{-1}$ is the single particle level density. The expression (2-7) which gives the solid smooth curve in Figure 2.2 represents a remarkably good approximation to the exact state density that is obtained by the recursion formula of Euler [43]. The explicit dependence of the state density upon excitation energy arises from the simple relation between excitation energy and statistical temperature as given as

$$U = \frac{\pi^2}{6}g_0t^2 \quad (2.8)$$

More realistic expression for level density is obtained in the case of two Fermion system. If the equidistant spacings are d_n and d_p , for neutrons and protons, respectively, the average total Fermion level density $g_0 = d_n^{-1} + d_p^{-1} = g_n + g_p$ and the total state density for a system composed of two kinds of particles (neutron and proton) is given approximately in analytical form by

$$\omega(U) = g_0 \left(\frac{g_0^2}{4g_n g_p}\right)^{1/2} \frac{(6)^{1/4}}{12} \frac{\exp[2(\frac{\pi^2 g_0 U}{6})^{1/2}]}{(g_0 U)^{5/4}} \quad (2.9)$$

If the difference between neutron and proton single particle level density is neglected, $g_n \simeq g_p$, the state density is given by Eqn (1.5).

In this approximation the equidistant spacing model gives a remarkably simple expression for the state density. At high excitation the exponential factor in Eqn. (1.5) is dominating. This has led to the commonly found statement

that level density should vary with energy as $\exp 2(aU)^{1/2}$, where $a = \frac{\pi^2 g_0}{6}$ is a constant. According to the above it must be emphasized that this statement is valid only for high excitations and for a model similar to the one considered, i.e. with a fairly well defined average single Fermion spacing near Fermi levels.

2.4 Fermi Gas Model

The simplest system which does not have equidistant levels is the Fermi gas system, where the single particle level density increases with the square root of the kinetic energy of the particles. This model which historically has had the largest impact on the interpretation of experiments was used by Bethe [50] and Oppenheimer [51] separately.

In Fermi gas model the nucleons are treated as freely moving non-interacting Fermions in a spherical potential well whose size corresponds to that of the nucleus, and its depth adjusted so that the Fermi energy raises the highest nucleons up to the observed binding energy usually near 8 MeV. In this model the difference between neutron and proton single particle spacing is neglected and the particles are supposed to occur with equal probability.

The nucleus is considered as a free Fermi gas of neutrons and protons of both spins confined to move in a nuclear volume $V = (4\pi/3)R^3$, R being the nuclear radius. The Fermi energy is thus given by the phase space occupied in the ground state

$$\frac{V}{h^3} 4 \int_0^{\varepsilon_F} 4\pi p^2 \frac{dp}{d\varepsilon} d\varepsilon = A \quad (2.10)$$

The Fermi energy is then

$$\varepsilon_F = \left(\frac{\pi}{3}\right)^{2/3} \frac{9}{4} \frac{\hbar^2}{2m_n r_0^2} \quad (2.11)$$

where m_n is the nucleon mass and r_0 the nucleon radius. The density of single particle levels at the Fermi level is

$$g_0 = \frac{3}{2} \frac{A}{\varepsilon_F} \quad (2.12)$$

Here, again the state density given by Eqn. (1.5) is obtained if the difference between neutron and proton single particle level density is neglected. The level density parameter, a , is related to mass number, A , and Fermi energy, ε_F , by

$$a = \frac{\pi^2 A}{4\varepsilon_F} \quad (2.13)$$

Therefore, the only difference between the equidistant and Fermi gas model expressions given with the Eqn. (1.5) is the value of the level density parameter a .

To eliminate the singularity at $U = 0$ Lang and Le Couter [41] replaced the equation of state Eqn. (1.7) by

$$U = at^2 - t \quad (2.14)$$

and Eqn. (1.5) becomes

$$\omega(A, U) \simeq \frac{\sqrt{\pi} \exp(2(aU)^{1/2})}{12a^{1/4}(U + t)^{5/4}} \quad (2.15)$$

2.5 Spin Dependence

Suppose the projection of angular momentum J in some space fixed axis is denoted by M . Each level with spin equal to or greater than J will give one projection of magnitude J on the space fixed axis. Each level with spin equal to or greater than $J+1$ will give one projection of magnitude $J+1$ on the space fixed axis. Therefore the difference between the number of projections on the space fixed axis of magnitude J and $J+1$ will give the number of levels of spin J .

$$\rho(U, N, Z, J) = P(U, N, Z, M = J) - P(U, N, Z, M = J + 1) \quad (2.16)$$

The number of cases of angular momentum projection M along the space fixed axis is given in first approximation by a Gaussian law [32, 42, 49].

$$P(U, N, Z, M = J) = P(U, N, Z, M = 0) \exp\left\{-\frac{M^2}{2\sigma^2}\right\} \quad (2.17)$$

Substitution Eqn (2.17) into Eqn (2.16) and using the value J and $J + 1$ for M gives

$$\rho(U, N, Z, J) = P(U, N, Z, M = 0) \left\{ \exp\left(-\frac{J^2}{2\sigma^2}\right) - \exp\left(-\frac{(J+1)^2}{2\sigma^2}\right) \right\} \quad (2.18)$$

Since each level has exactly one projection on the space fixed axis of magnitude $M = 0$, the quantity $P(U, N, Z, M = 0)$ is identical to the total level density $\rho(U, N, Z)$, Eqn. (2.18) can be written as

$$\rho(U, N, Z, J) = \rho(U, N, Z) \left\{ \exp\left(-\frac{J^2}{2\sigma^2}\right) - \exp\left(-\frac{(J+1)^2}{2\sigma^2}\right) \right\} \quad (2.19)$$

Eqn (2.19) is in convenient form for most computer applications. However, for a number of applications an approximate form of this equation is useful which can be easily obtain as

$$\rho(U, N, Z, J) = \rho(U, N, Z) \frac{2J+1}{2\sigma^2} \exp\left\{-\frac{(J+1/2)^2}{2\sigma^2}\right\} \quad (2.20)$$

The level density $\rho(U, N, Z)$ is related to the state density $\omega(U, N, Z)$ by the relationship

$$\rho(U, N, Z) = \omega(U, N, Z) / \bar{N} \quad (2.21)$$

\bar{N} is the average number of states per level

$$\bar{N} = \frac{\int_0^\infty (2J+1)(2J+1) e^{-(J+1/2)^2/2\sigma^2} dJ}{\int_0^\infty (2J+1) e^{-(J+1/2)^2/2\sigma^2} dJ} \quad (2.22)$$

Let $x = (J + 1/2)^2$ then $dx = 2(J + 1/2)dJ$

$$\bar{N} = \frac{2 \int_0^\infty x^{1/2} e^{-x/2\sigma^2} dx}{\int_0^\infty e^{-x/2\sigma^2} dx} = \frac{\pi^{1/2} (2\sigma^2)^{3/2}}{2\sigma^2} \quad (2.23)$$

The average number of state per level = $(2\pi\sigma^2)^{1/2}$. So the level density of a given nucleus at a given excitation energy is related to its state density by

$$\rho(U, N, Z) = \omega(U, N, Z)/(2\pi\sigma^2)^{1/2} \quad (2.24)$$

then the level density in Eqn. (2.20) can be expressed in terms of state density by

$$\rho(U, N, Z, J) = \frac{\omega(U, N, Z)}{(2\pi\sigma^2)^{1/2}} \frac{(2J+1)}{2\sigma^2} \exp \left\{ -\frac{(J+1/2)^2}{2\sigma^2} \right\} \quad (2.25)$$

2.6 Spin Cut-off Factor

In the present study, the spin cut-off parameters calculated with the microscopic theory are compared with their corresponding values in the macroscopic model. There are two commonly used paths to obtain spin cut-off parameters. The spin cut-off parameter is given by [42]

$$\sigma^2 = g \langle m^2 \rangle t \quad (2.26)$$

where g is the density of single particle levels, $\langle m^2 \rangle$ is the average square of the spin projection for the single particle levels near the Fermi energy and t is the thermodynamic temperature. The quantity of $g \langle m^2 \rangle$ for a Fermi gas of nucleus can be shown to be related to rigid body moment of inertia of the nucleus, \mathfrak{S} , by

$$g \langle m^2 \rangle = \frac{\mathfrak{S}}{\hbar^2} \quad (2.27)$$

The rigid body moment of inertia for a spherical nucleus is given by

$$\mathfrak{S} = \frac{2}{5} m_n A R^2 \quad (2.28)$$

where A is the mass number of the nucleus, m_n is the nucleon mass and R is the nucleus radius. If R is taken as $1.20A^{1/3} fm$ then

$$\sigma_{rigid}^2 = 0.0138A^{5/3}t \quad (2.29)$$

The thermodynamic temperature, t , and excitation energy, U are related by the expression

$$U = at^2 - t \quad (2.30)$$

An alternative method of determining σ^2 is to relate single particle level density, g , to the level density parameter, a through the equation

$$a = \frac{\pi^2}{6}g \quad (2.31)$$

Jensen and Luttinger [52] estimated from the shell model energy levels

$$\langle m^2 \rangle = 0.146A^{2/3} \quad (2.32)$$

with some fluctuations due to shell effects. Putting the above equations together we obtain

$$\sigma_{GC}^2 = 0.0888A^{2/3}\sqrt{a(U - E_0)} \quad (2.33)$$

where E_0 is the back shift energy.

2.7 Residual Interaction

The previous treatment was based on the approximation of the noninteracting nucleons. However, we know that there are residual interaction between nucleons and these may alter the energy dependence of the level density, especially at low energy. The most obvious of these interactions is the pairing interaction which as discussed in the introduction, reduces the state density by forbidding, states near the Fermi energy to be occupied by unpaired nucleons [1, 49]. We simply note that the comparison of level densities of neighboring even-even, even-odd, and odd-odd nuclei suggests, as first proposed by Hurwitz and Bethe [62], that,

to first order approximation, pairing effects might be accounted for by using excitation energies $U - \Delta_Z - \Delta_N$ instead of true energies U in the state and level densities expressions. Δ_Z and Δ_N , loosely speaking, are the energies necessary to break a proton or a neutron pair and are related to the energy gap associated with the pairing correlation in the ground state. Δ_Z and Δ_N are positive and different from zero, and they can be deduced from the comparison of the ground state masses of neighbouring even-even, even-odd, and odd-odd nuclei. Tables of pairing energies, widely used in the literature are given by Cameron [14], Nemirovski and Adamchuck [15], Cameron and Elkin [53] and Truran *et al.* [17].

More refined calculations [54] suggest that this simple procedure to account for pairing effect should apply only above a critical temperature T_c . Also, angular momentum reduces the pairing correlation, which vanishes above a critical value M_c . Thereafter, in this case also, the usual procedure to account for the pairing interaction remains valid.

2.8 Shell Model

Comparing the spacing of the nuclear levels observed in neutron resonances, one notices that the level density is strongly influenced by nuclear shell structure. The density of resonances for magic or nearly magic nuclei is one to three order of magnitude smaller than mid-shell nuclei at the same excitation energy [12, 42, 55]. It has been pointed out that this effect is related to the larger single particle spacing in the magic nuclei near the ground state rather than to a shift of the entire energy scale of excited nuclei [14, 37, 42, 56].

The importance of the shell effects was first emphasized by Bloch [35], who developed general methods to deal with the mathematical problem. His shell model was succeeded by Rosenzweig, paying attention to a marked effect in the level density [37, 57], usually named after him. It is an effect depending on to

what extent the last shell is filled in the ground state. Rosenzweig has shown that this effect is describable as a simple shift of the excitation energy. Though the effect should be taken into account at least in highly degenerate shells, there are some reasons, to believe that it is smaller than what might be first thought [42].

Newson has derived phenomenological description [58] of the neutron resonance spacing by considering only the pair excitation within the partially filled major shells. The success of his model seems to be a rather general consequence of the shell model and may be rather independent of the special model used. This indicates the desirability of the introduction of a more realistic single fermion level structure into the calculation of the level density.

The main difficulty in obtaining numerical results lies in the evaluation of the grand partition function with such a realistic single particle level structure. This could well be done by use of the microscopic theory which will be discussed in the next section.

2.9 Deformed Nuclei

The sequence of single particle levels depend on the shape of the nuclear potential acting upon the nucleons. Discontinuities in the level density sequence, such as large gaps, may occur for neutron and proton numbers different from the magic values of spherical nuclei depending on the deformation of the nucleus. Consideration of nuclear deformation is of particular importance for understanding of many aspects of nuclear properties. The fact that the sequence of single particle level dependence on the deformation has obviously greater importance in the evaluation of the state and level density of a deformed nucleus as discussed in previous sections. Deformation is characteristic of nuclei with $150 < A < 250$ (in particular with $160 < A < 190$ and $230 < A < 250$) at rather low excitation energies. Calculations by Moretto [54] and Mosel *et al.* [59] indicate that, by

increasing the excitation energy, the effect of deformation on level density tends to disappear.

CHAPTER 3

BCS MODEL

3.1 Basic Formulas

Consider a system of nucleons interacting with the pairing force. For a spherically symmetric nuclei, in addition to being characterized by energy ε_k , the single fermion states also characterized by the projection of the angular momentum on the z-axis, m_k . In the superconducting theory, the nucleons having angular momentum $(m_k, -m_k)$ couple so as to form a quasi bound particle.

The state density of such an N nucleon system of energy E is related to the logarithm of grand partition function [60],

$$\ln Z(\alpha, \beta) = -\beta \sum_k (\varepsilon_k - \lambda - E_k) + 2 \sum_k \ln[1 + \exp(-\beta E_k)] - \beta \frac{\Delta^2}{G} \quad (3.1)$$

where α and β are two Lagrangian multipliers associated with the nucleon number and $E_k = [(\varepsilon_k - \lambda)^2 + \Delta^2]^{1/2}$ is the quasiparticle energy and Δ is the pairing parameter. $\lambda = \frac{\alpha}{\beta}$ is the chemical potential and G is the strength of pairing. Eq. (3.1) is valid only if the quantities Δ , λ and β satisfy the following gap equation:

$$\frac{2}{G} = \sum_k \frac{1}{E_k} \tanh \frac{\beta E_k}{2} \quad (3.2)$$

The state density is the inverse Laplace transform of the grand partition function,

$$\omega(N, E) = \left[\frac{1}{2\pi i} \right]^2 \oint d\alpha \oint d\beta Z(\alpha, \beta) \exp(-\alpha N + \beta E) \quad (3.3)$$

The above contour integrals can be evaluated by the method outlined previously [31], the result is:

$$\omega(N, U) = \frac{\exp(S)}{2\pi D^{1/2}} \quad (3.4)$$

here the entropy S can be written as:

$$S = 2 \sum_k \ln[1 + \exp(-\beta E_k)] + 2\beta \sum_k \frac{E_k}{1 + \exp(\beta E_k)} \quad (3.5)$$

and "D" is a 2×2 determinant with its elements given in terms of the second derivations of the grand partition function.

$$D = \begin{vmatrix} \frac{1}{\beta^2} \frac{\partial^2 \ln Z}{\partial \lambda^2} & \frac{\partial}{\partial \beta} \left[\frac{1}{\beta} \frac{\partial \ln Z}{\partial \lambda} \right] \\ \frac{\partial}{\partial \beta} \left[\frac{1}{\beta} \frac{\partial \ln Z}{\partial \lambda} \right] & \frac{\partial^2 \ln Z}{\partial \beta^2} \end{vmatrix} \quad (3.6)$$

The second derivatives of the grand partition function are:

$$\frac{1}{\beta^2} \frac{\partial^2 \ln Z}{\partial \lambda^2} = \sum_k a_k E_k^2 - \Delta^2 \sum_k (a_k - b_k) - \Delta \frac{\partial \Delta}{\partial \lambda} \sum_k (\varepsilon_k - \lambda)(a_k - b_k) \quad (3.7)$$

$$\frac{\partial}{\partial \beta} \left[\frac{1}{\beta} \frac{\partial \ln Z}{\partial \lambda} \right] = -\beta \Delta \frac{\partial \Delta}{\partial \beta} \sum_k (\varepsilon_k - \lambda)(a_k - b_k) - \sum_k (\varepsilon_k - \lambda) E_k^2 a_k \quad (3.8)$$

$$\frac{\partial^2 \ln Z}{\partial \beta^2} = \sum_k a_k E_k^2 [E_k^2 + \beta \Delta \frac{\partial \Delta}{\partial \beta}] \quad (3.9)$$

where

$$a_k = \frac{1}{2E_k^2} \operatorname{sech}^2 \left[\frac{1}{2} \beta E_k \right], b_k = \frac{1}{\beta E_k^3} \tanh \left[\frac{1}{2} \beta E_k \right] \quad (3.10)$$

and

$$\frac{\partial \Delta}{\partial \lambda} = \frac{\sum_k (\varepsilon_k - \lambda)(a_k - b_k)}{\Delta \sum_k (a_k - b_k)}, \quad \frac{\partial \Delta}{\partial \beta} = -\frac{\sum_k E_k^2 a_k}{\beta \Delta \sum_k (a_k - b_k)} \quad (3.11)$$

In addition, the nucleon number N and energy E are given by

$$N = \frac{1}{\beta} \frac{\partial \ln Z}{\partial \lambda} = \sum_k n_k \quad (3.12)$$

$$E = \frac{-\partial \ln Z}{\partial \beta} = \sum_k \varepsilon_k n_k - \frac{\Delta^2}{G} \quad (3.13)$$

where the occupation probability, n_k is given by

$$n_k = 1 - \frac{\varepsilon_k - \lambda}{E_k} \tanh \frac{\beta E_k}{2} \quad (3.14)$$

The statistical properties of a nucleus is defined in terms of its neutron and proton numbers N and Z and the total energy E . Since the neutron -proton superfluids are independent, their correlation can be neglected. Then the above derivation can be extended to include a nuclear system. For a nucleus of N neutrons of energies $\varepsilon_k^{(n)}$ with magnetic quantum numbers $m_k^{(n)}$ and Z protons of energies $\varepsilon_k^{(p)}$ with magnetic quantum numbers $m_k^{(p)}$, the constants of motion are then neutron and proton numbers given by Eqn. (3.12) and the total energy given by Eqn. (3.13).

The total state density for a system of N neutrons and Z protons at an excitation energy $U = U_n + U_p$ is given as Eqn. (2.6)

$$\omega(N, Z, U) = \frac{\exp(S)}{(2\pi)^{3/2} D^{1/2}} \quad (3.15)$$

here $S = S_n + S_p$ is the total entropy and " D " is now a 3×3 determinant defined by

$$D = \left(\frac{1}{\beta^2} \frac{\partial^2 \ln Z}{\partial \lambda_p^2} \right) D_n + \left(\frac{1}{\beta^2} \frac{\partial^2 \ln Z}{\partial \lambda_n^2} \right) D_p \quad (3.16)$$

where D_n and D_p are 2×2 determinant similar to relation (3.6).

Since the level density $\rho(U, N, Z)$ is related to the state density $\omega(U, N, Z)$ by the relationship

$$\rho(U, N, Z) = \omega(U, N, Z)/(\text{Average number of state per level})$$

Since the average number of state per level = $(2\pi\sigma^2)^{1/2}$, hence the total level density for a nuclear system at excitation energy $U = E - E_g$ is given by

$$\rho(N, Z, U) = \frac{\omega(N, Z, U)}{(2\pi\sigma^2)^{1/2}} \quad (3.17)$$

where σ^2 is the total spin cut-off parameter defined as:

$$\sigma^2 = \sigma_n^2 + \sigma_p^2 \quad (3.18)$$

with

$$\sigma_n^2 = \frac{1}{2} \sum_k m_k^{n^2} \text{sech}^2\left[\frac{1}{2}\beta E_k^n\right] \quad (3.19)$$

Similar relation can be given for σ_p^2 case.

3.2 Energy Gap and Critical Temperature

In view of the importance of pairing energy in nuclear level density, we have calculated its dependence on nuclear temperature. For a nuclear system characterized by its single particle energies ε_k and magnetic quantum numbers m_k , calculations are done in the following way.

1. At zero temperature Eqs.(3.2) and (3.12) are solved for $\lambda(0)$ and the pairing strength G for known particle number N and pairing energy parameter Δ . The initial values of Δ for neutron and for proton were computed using the following relations [15]

$$\Delta_n = 11.56N^{-0.552} \quad (3.20)$$

$$\Delta_p = 11.40Z^{-0.567} \quad (3.21)$$

2. The critical temperature, T_c and the corresponding chemical potential λ_c are evaluated by setting $\Delta = 0$ and solving the same equations for specified nucleon number, N and pairing strength, G obtained from step 1.
3. The quantities $\lambda(T)$ and $\Delta(T)$ are then evaluated for a given value of T by solving Eqns. (3.2) and (3.12) with the values of N and G from (1).
4. These values of $\lambda(T)$ and $\Delta(T)$ are used to compute other thermodynamic quantities which will be discussed in the next sections.

It is worth noting that the pairing strength G depends on the number of single particle levels which are included in the calculation. The number of single particle levels as long as sufficient levels are included so that the levels of largest 'k' have very small occupational probabilities. Temperature dependence of the energy gap parameters for both the neutron and proton system for ^{243}Cm and ^{244}Am are shown in Figures 3.1 and 3.2.

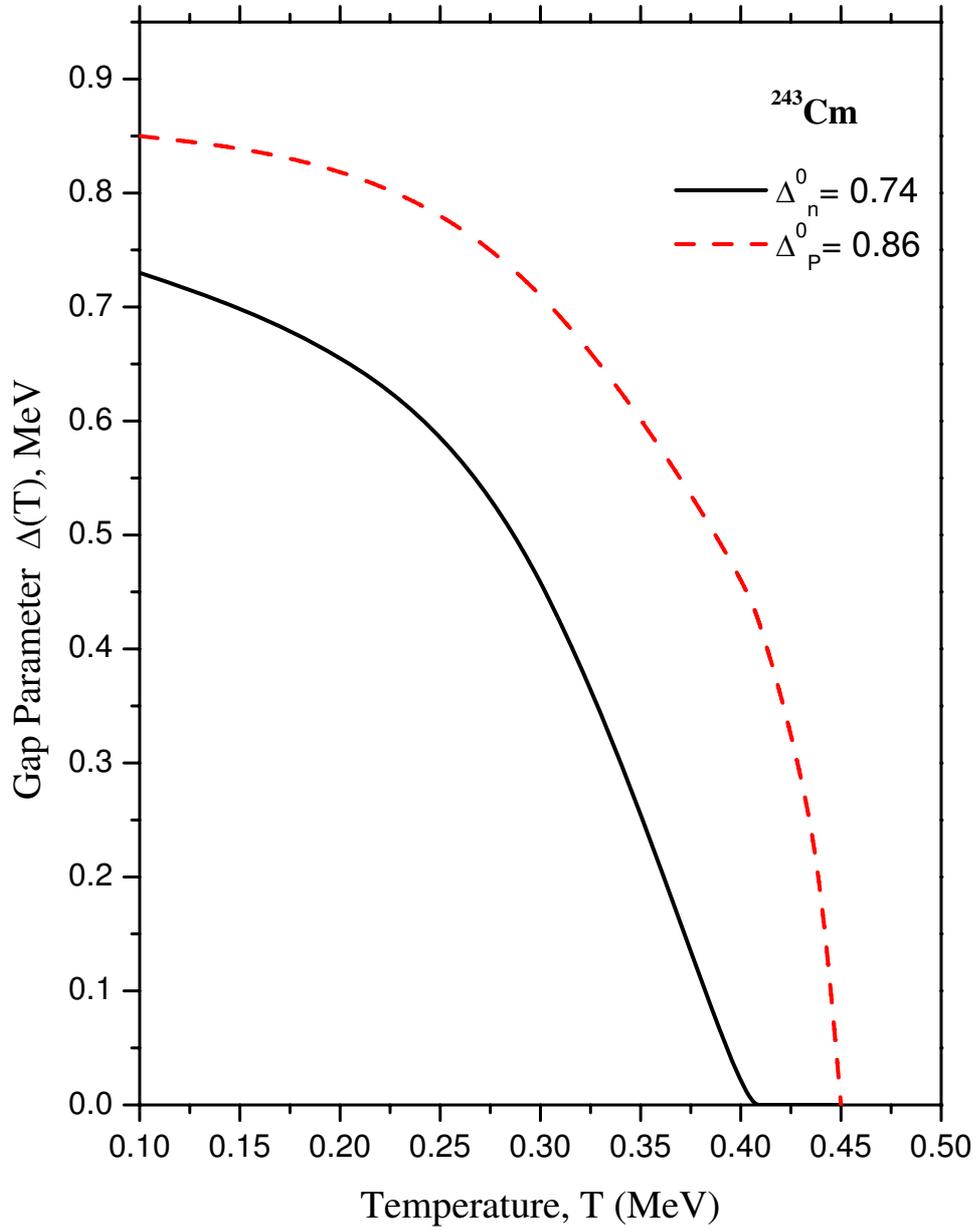


Figure 3.1: Temperature dependence of the neutron and proton gap parameters for ^{243}Cm .

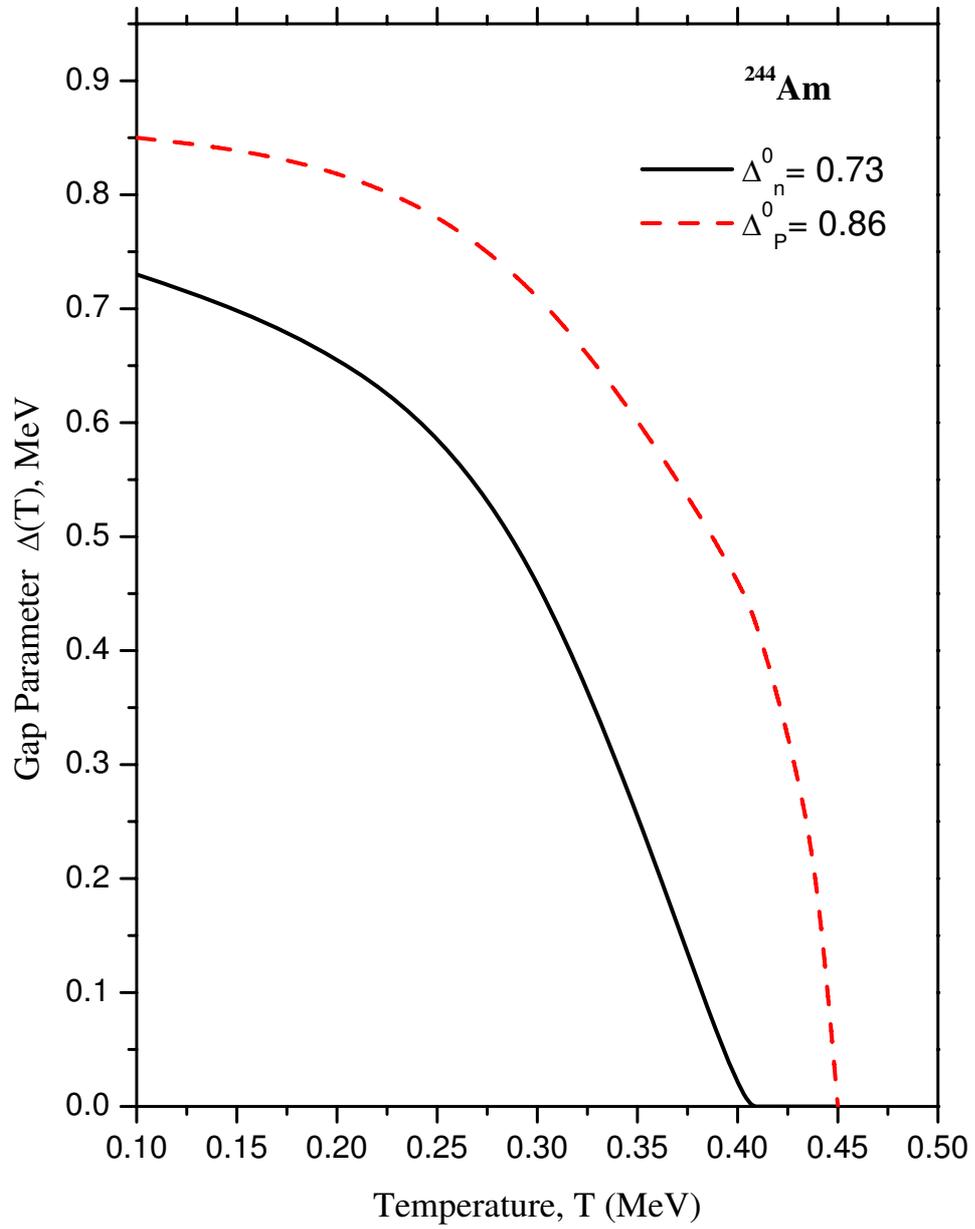


Figure 3.2: Temperature dependence of the neutron and proton gap parameters for ^{244}Am .

3.3 Excitation Energy and Entropy

Dependence of the excitation energy of the nuclear system with temperature can be evaluated as follows :

1. The intrinsic energy of the ground state, $E_n(0)$ is obtained from (3-13) for known values of $\lambda(0)$ and G obtained in section 3.2.
2. In the same way, the intrinsic energy $E_n(T)$ is obtained from known values of $\lambda(T)$ and $\Delta(T)$ obtained again in section (3-2). Thus the excitation energy of the neutron system at temperature T is given by $U_n = E_n(T) - E_n(0)$. The excitation energy of the proton system is obtained in the same way, $U_p = E_p(T) - E_p(0)$, Thus the total excitation energy at temperature T is $U = U_n + U_p$. The excitation energy for neutron and proton system for ^{243}Cm and ^{244}Am nuclei are plotted as a function of temperature in Figures 3.3 and 3.4. The arrows indicate the energies of the phase transition for neutrons and protons from the superconducting state to the normal state.
3. The entropy of the neutron and proton system is evaluated from Eqn. (3.5) at temperature T from the values of $\lambda(T)$ and $\Delta(T)$ obtained in section 3.2. From the additivity property of entropy, the total entropy is obtained as, $S = S_n + S_p$. The entropies are plotted as a function of temperature in Figures 3.5 and 3.6 for ^{243}Cm and ^{244}Am . Again the arrows indicate the phase transition from superconducting state to the normal state.

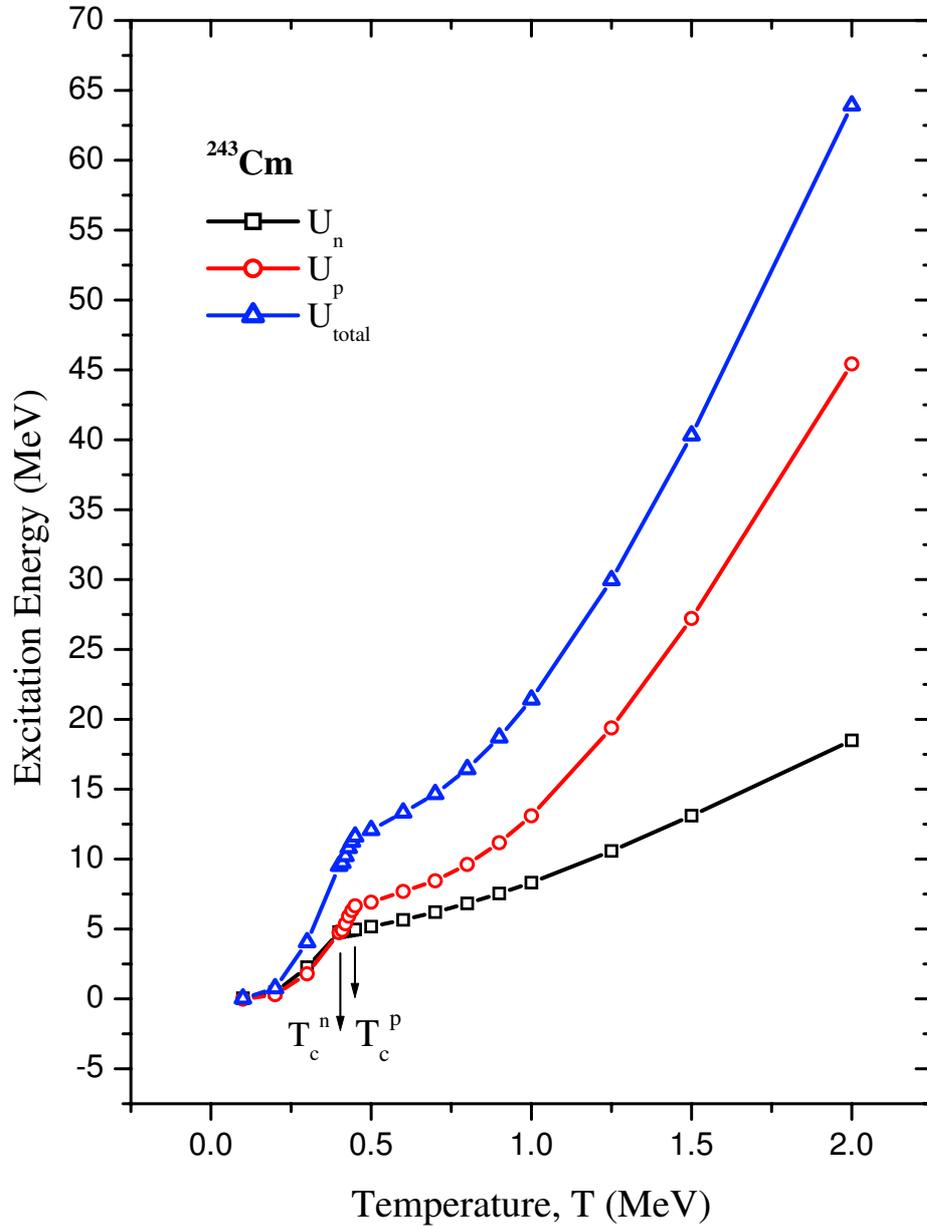


Figure 3.3: Excitation energy for ^{243}Cm as a function of temperature. The neutron and proton components are shown separately.

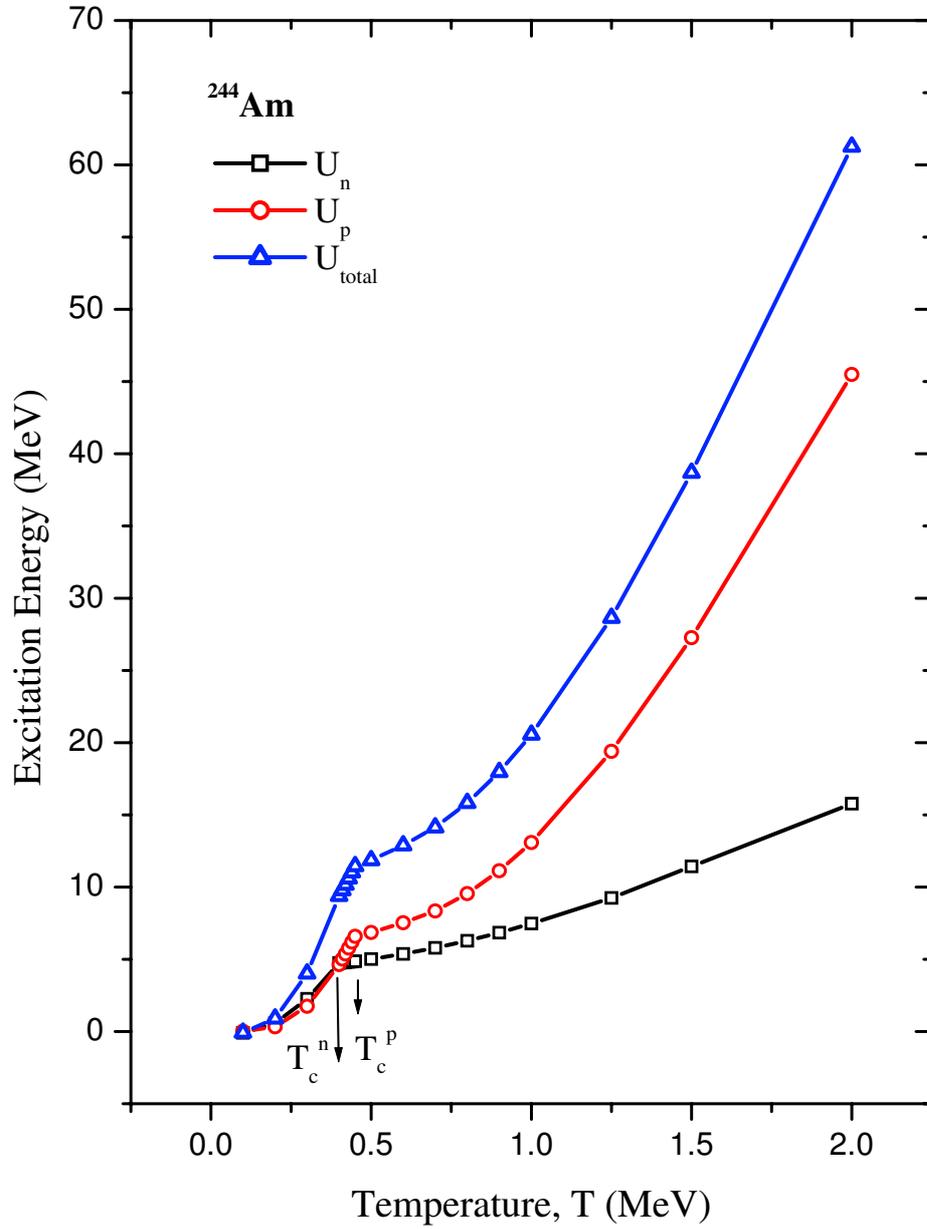


Figure 3.4: Excitation energy for ^{244}Am as a function of temperature. The neutron and proton components are shown separately.

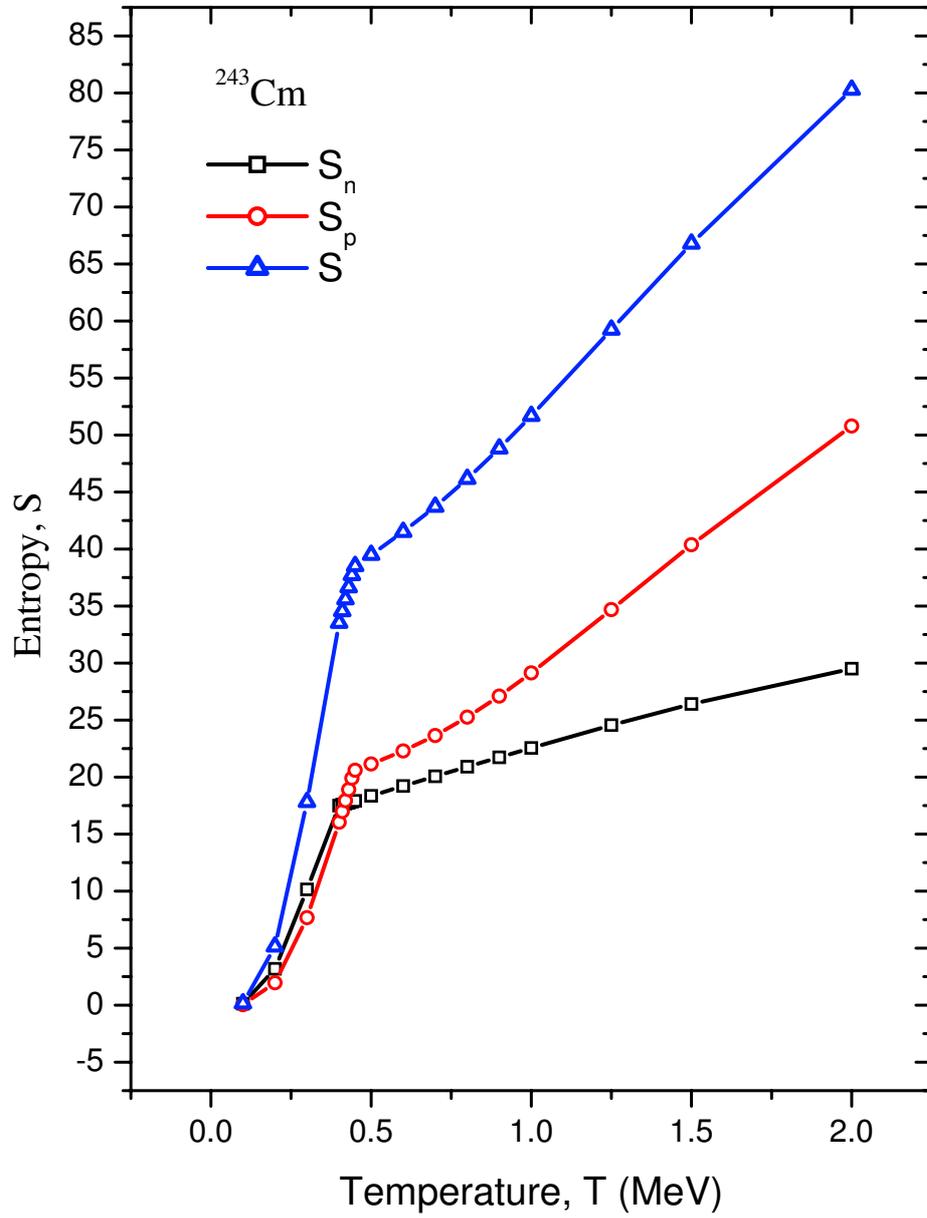


Figure 3.5: Relation between the entropy, S and temperature, T for ^{243}Cm .

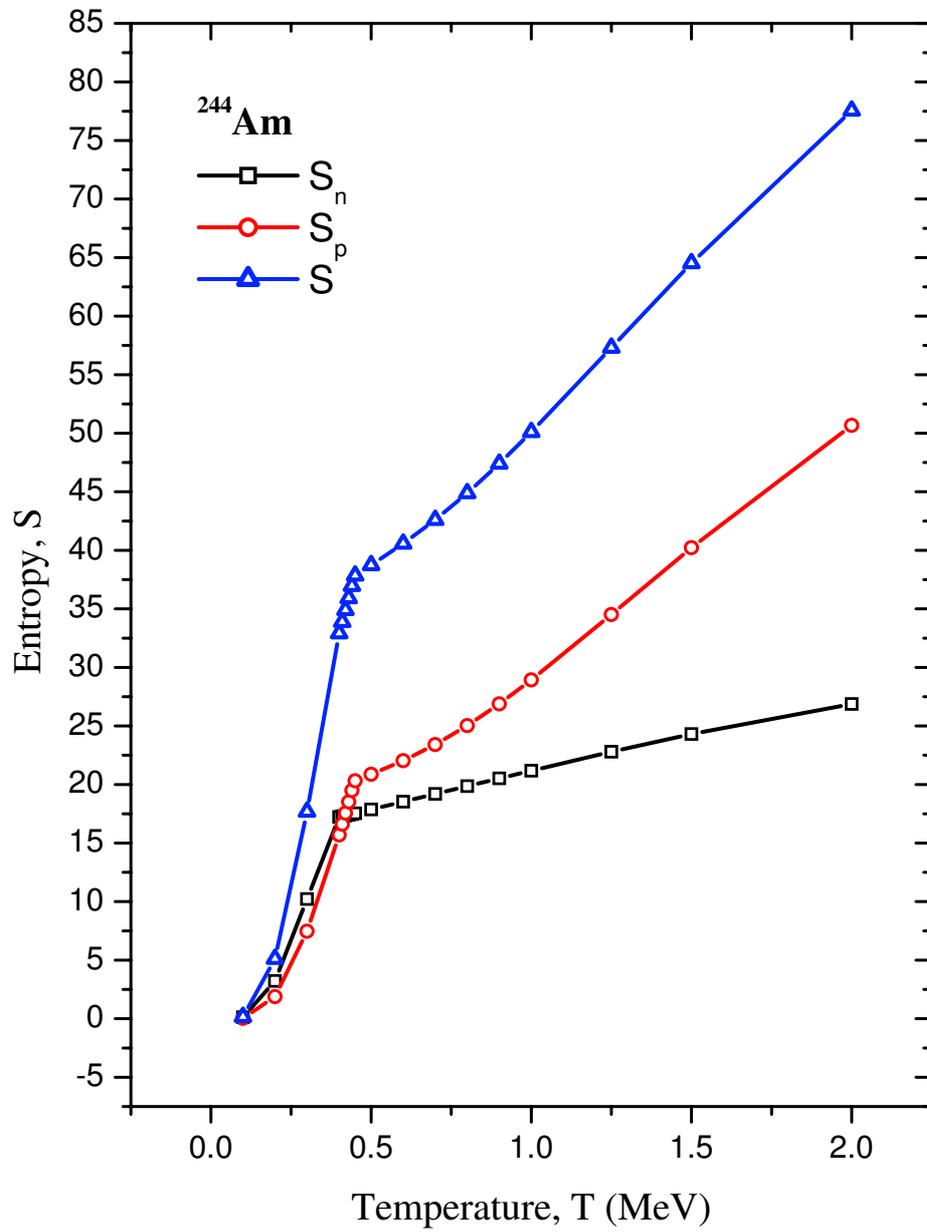


Figure 3.6: Relation between the entropy, S and temperature, T for ^{244}Am .

3.4 Odd Particle System

For an odd particle system, blocking is important and must be included. When a level near the Fermi surface is occupied by an odd particle, the effect of the pairing correlation is reduced. The reduction necessary depends on which level is occupied. The change in Δ between the even and odd case due to the blocking of one level by the odd particle is estimated as [61].

$$\Delta^{odd} \cong \Delta^{even}(0) - \frac{1}{(\Delta^{even}(0))^2} \left[\sum_{k \neq k'} \frac{1}{E_k^3} \right]^{-1} \quad (3.22)$$

where k' indicates a state occupied by the odd particle. The actual calculation, in which the blocking effect has been included exactly indicates a difference between even and odd system of the order of 20 percent. These results are roughly in agreement with Eqn. (3.22). We have investigated the blocking effect by two different methods.

- i) By reducing the strength of pairing parameter Δ . The change in Δ leads to a change in the particle occupational probabilities. After a proper reduction in Δ , the odd particle system is treated in a way analogous to the even particle system.
- ii) By adjusting the ground state for nuclear pairing. The statistical functions here were calculated from the adjacent doubly even nucleus and then the energy scale was shifted by an energy equivalent to that required to produce one quasi-particle. It turns out that the results of both procedures give generally identical level densities especially at higher excitation energies. The occupation probabilities for neutrons and protons for ^{244}Am is shown in Figures 3.7. The effect of pairing interaction is apparent near the Fermi energy

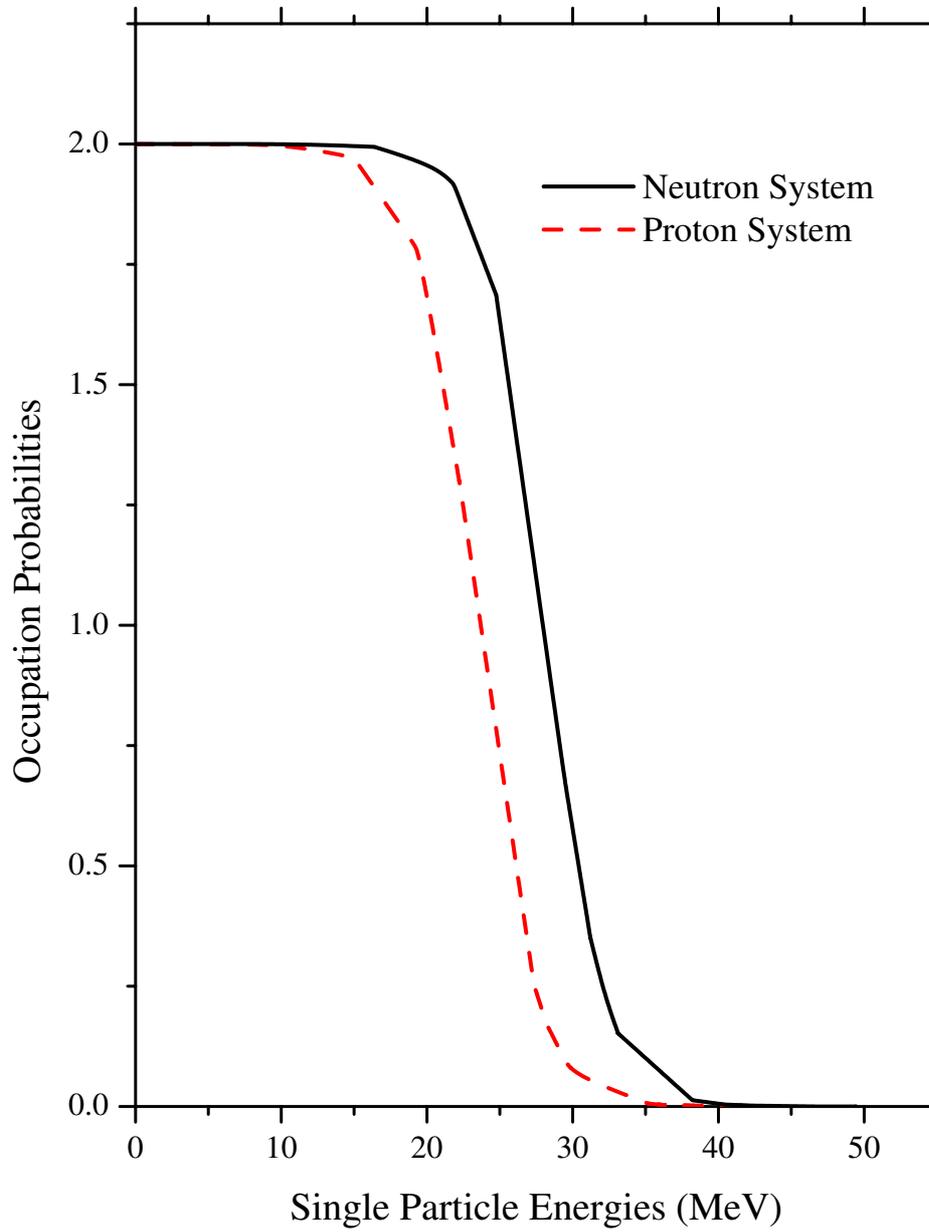


Figure 3.7: Occupation probabilities of double degenerate single particle levels at excitation energy of 2.0 MeV, for ^{244}Am .

3.5 Nuclear State and Level Density

In performing calculation of state and level density the energies and spins of the single particle levels were first obtained from Seeger potential [62]. The relative energies and spins for ^{244}Am is given in Table 3.1. Some of the energies up to 30 MeV together with their spins are displayed in Figure 3.8 for neutrons and protons separately. Note that the Fermi energies are indicated for neutron and proton components. In actual calculation however, many more single-particle levels were introduced. Next the values of E_n , S_n and $\omega(N, U_n)$ were calculated from Eqns. (3.13), (3.5) and (3.4) using the values of λ_T and Δ_T obtained in section (3-2). The spin cut - off factor σ_n^2 is calculated using Eqn. (3.18) from the known valued of eigenvalues $\varepsilon_k^{(n)}$ and their corresponding magnetic quantum numbers $m_k^{(n)}$. Then the calculation are repeated for proton component. Finally, the quantities σ^2 , $\omega(N, Z, U)$ and $\rho(N, Z, U)$ are calculated with Eqns. (3.19), (3.15) and (3.17), the total excitation energy $U = U_n + U_p$.

In Figures 3.9 and 3.10 the logarithm of the state density is plotted as a function of excitation energy for ^{243}Cm and ^{244}Am nucleus.

It should be noted that the initial values of Δ_n^0 and Δ_p^0 used in our analysis in order to calculate the gap parameters G_n and G_p were determined using equations (3-20) and (3-21) respectively [15]. Since Δ_n^0 and Δ_p^0 are deduced from mass differences, they also include shell effects.

Table 3.1: Energies of single particle levels with their spins for ^{244}Am nucleus.

k	Energies of Proton	Spin	Energies of Neutron	Spin
1	0.00	1/2	0.00	1/2
2	5.16	3/2	5.20	3/2
3	5.76	1/2	5.77	1/2
4	7.44	1/2	7.40	1/2
5	10.09	5/2	10.19	5/2
6	11.09	3/2	11.15	3/2
7	11.32	1/2	11.36	1/2
8	12.84	3/2	12.77	3/2
9	13.11	1/2	13.05	1/2
10	14.78	7/2	14.93	1/2
11	15.01	1/2	14.97	7/2
12	15.99	5/2	16.16	5/2
13	16.50	3/2	16.63	3/2
14	16.84	1/2	16.97	1/2
15	18.18	5/2	18.10	5/2
16	18.57	3/2	18.50	3/2
17	19.13	1/2	18.99	1/2
18	19.25	9/2	19.54	9/2
19	20.25	3/2	20.17	3/2
20	20.51	1/2	20.43	1/2
21	20.57	7/2	20.85	7/2
22	21.32	5/2	21.55	5/2
23	21.86	3/2	22.09	3/2
24	22.10	1/2	22.32	1/2
25	22.87	1/2	22.72	1/2

Table 3.1: Continue.

k	Energies of Proton	Spin	Energies of Neutron	Spin
26	23.40	7/2	23.32	7/2
27	23.48	11/2	23.77	5/2
28	23.82	5/2	23.90	11/2
29	24.87	9/2	24.85	3/2
30	25.02	3/2	24.99	1/2
31	25.16	1/2	25.27	9/2
32	25.37	5/2	25.30	5/2
33	25.79	3/2	25.73	3/2
34	25.79	7/2	26.08	1/2
35	26.18	1/2	26.16	7/2
36	26.48	5/2	26.85	5/2
37	26.92	3/2	27.27	3/2
38	27.14	1/2	27.48	1/2
39	27.48	13/2	27.95	3/2
40	28.12	3/2	28.04	13/2
41	28.34	1/2	28.18	1/2
42	28.43	9/2	28.39	9/2
43	28.88	7/2	28.87	7/2
44	28.91	11/2	29.46	11/2
45	29.96	9/2	30.29	7/2
46	30.32	7/2	30.46	5/2
47	30.61	5/2	30.48	9/2
48	30.77	7/2	30.73	1/2
49	30.87	5/2	30.73	3/2
50	30.88	3/2	30.84	5/2

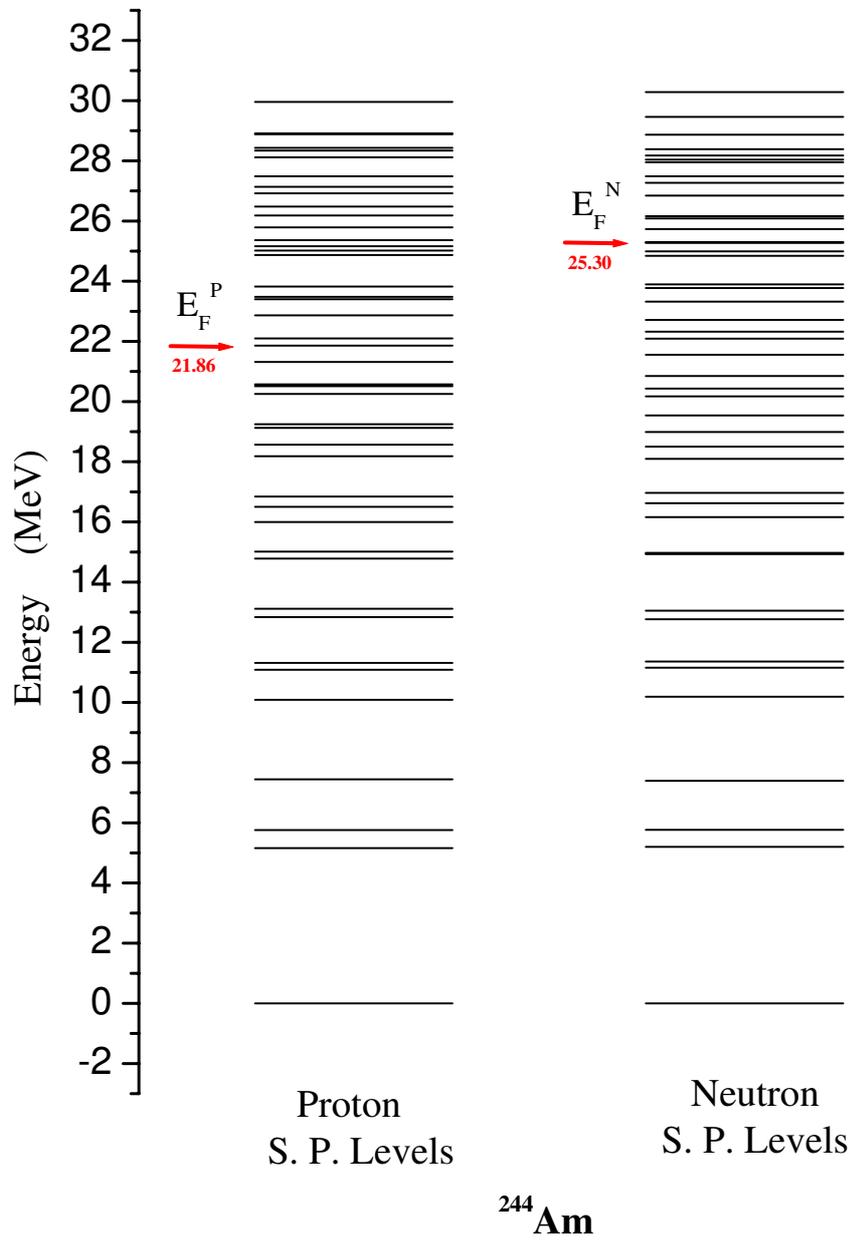


Figure 3.8: The single particle energy levels of ^{244}Am .

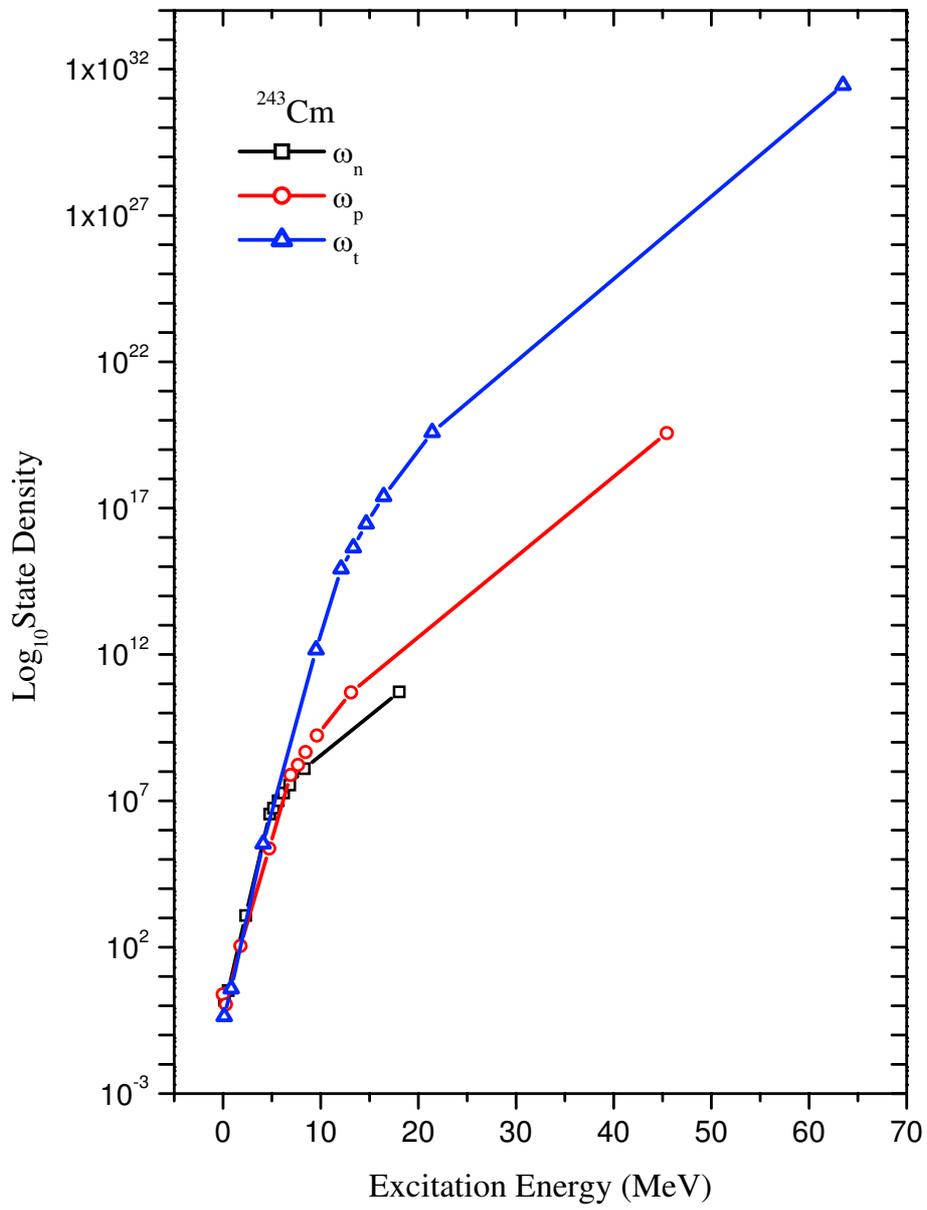


Figure 3.9: Relation between the state density, ω and excitation energy for ^{243}Cm .

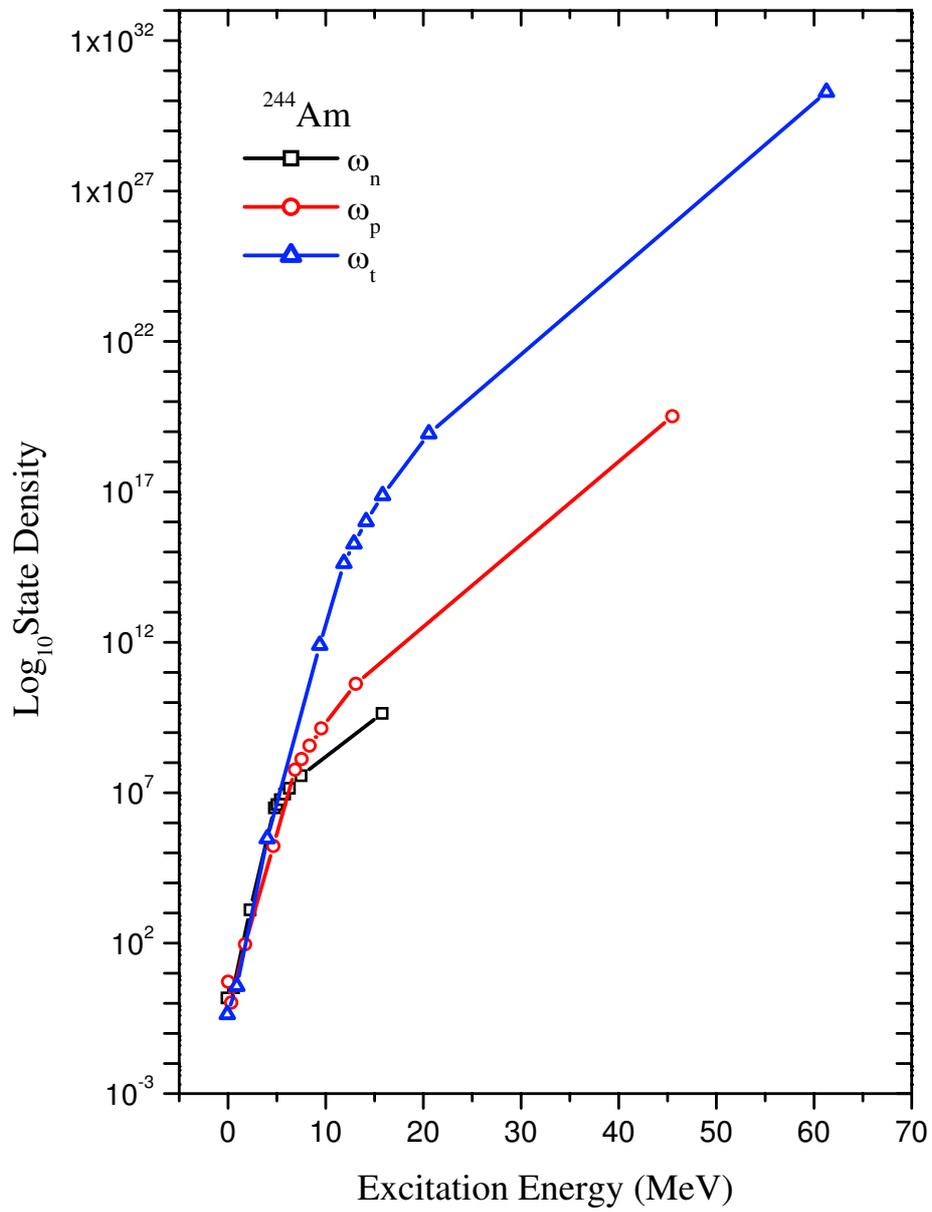


Figure 3.10: Relation between the state density, ω and excitation energy for ^{244}Am .

3.6 Spin Cut-off Factor

The spin cut-off parameter which is an important parameter in all statistical model codes is usually determined by counting levels with given spins and by fitting the spin distribution with

$$f(J) = \exp\left(\frac{-J^2}{2\sigma^2}\right) - \exp\left(\frac{-(J+1)^2}{2\sigma^2}\right) \quad (3.23)$$

where σ^2 is the variance of the distribution. This formula has been applied for measured spin distribution of ^{20}F nucleus. The parameter σ^2 , has been deduced by fitting the data using least square method. The fitted distribution for the best value of σ^2 is plotted in Figure 3.11.

The spin cut-off parameter can also be determined from the knowledge of the single particle energies and their corresponding magnetic quantum numbers. This is done using:

$$\sigma^2(E) = \frac{1}{2} \sum_k m_{n_k}^2 \operatorname{sech}^2\left(\frac{1}{2}\beta E_k\right) + \frac{1}{2} \sum_k m_{p_k}^2 \operatorname{sech}^2\left(\frac{1}{2}\beta E_k\right) \quad (3.24)$$

which is made up of the sum of the neutron and proton components. This is shown in Figures 3.12 and 3.13 where σ_n^2 and σ_p^2 as well as $\sigma^2 = \sigma_n^2 + \sigma_p^2$ are plotted as a function of excitation energy for ^{243}Cm and ^{244}Am nuclei.

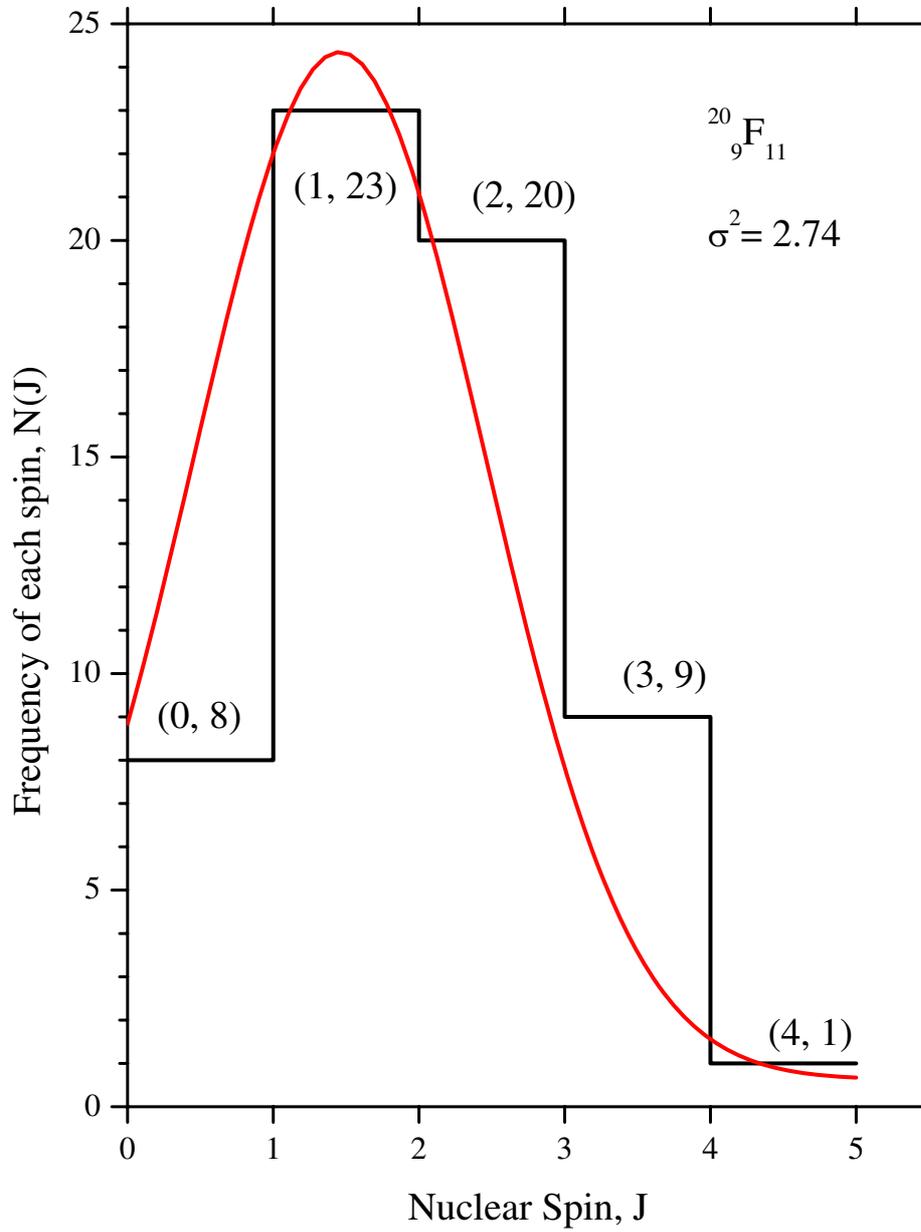


Figure 3.11: The spin distribution for ${}^{20}\text{F}$. The histogram showing the experimental spin distribution and the solid curve is a fit.

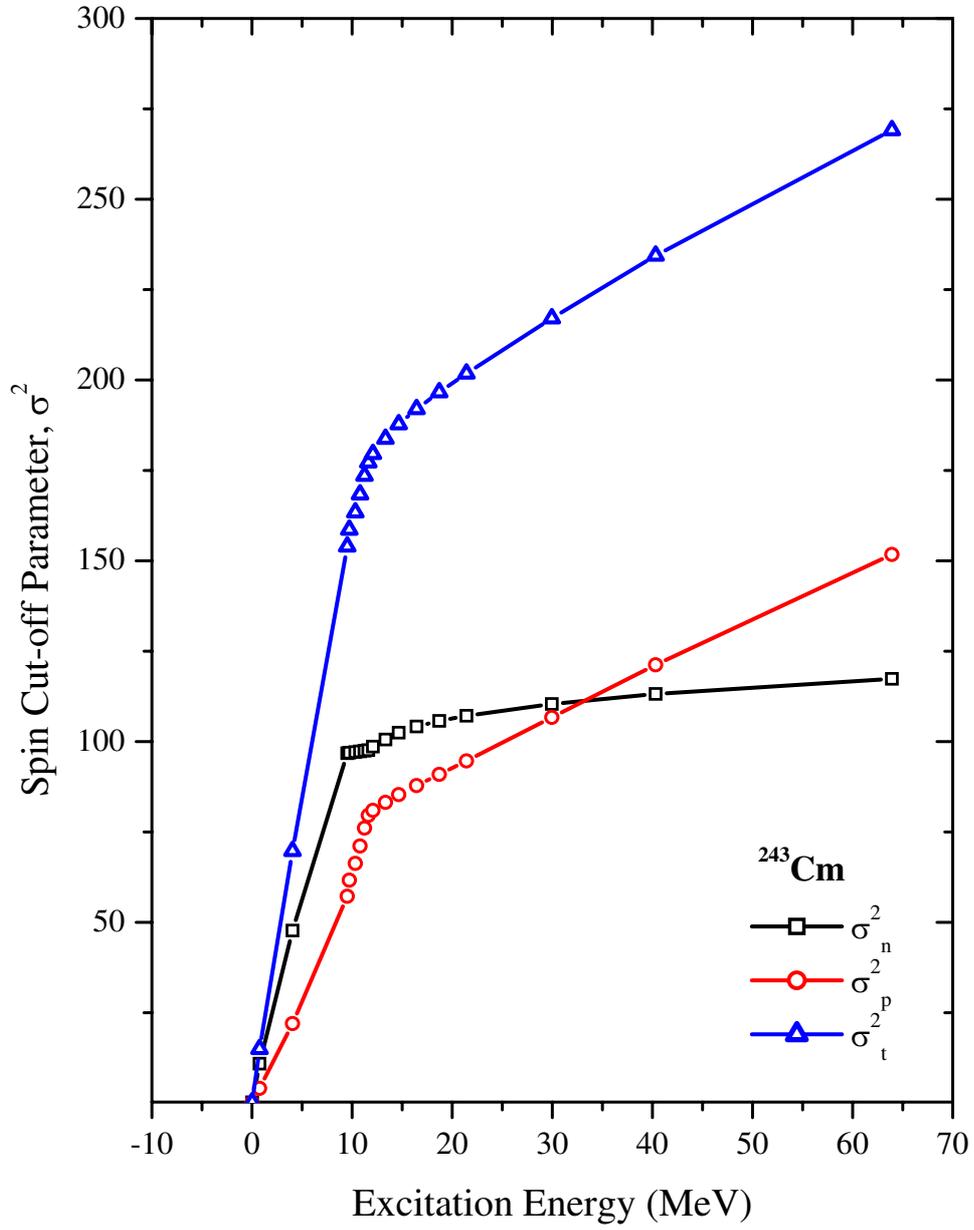


Figure 3.12: The Spin Cut-off parameter from microscopic theory. The individual contributions of neutron and proton are shown for ^{243}Cm .

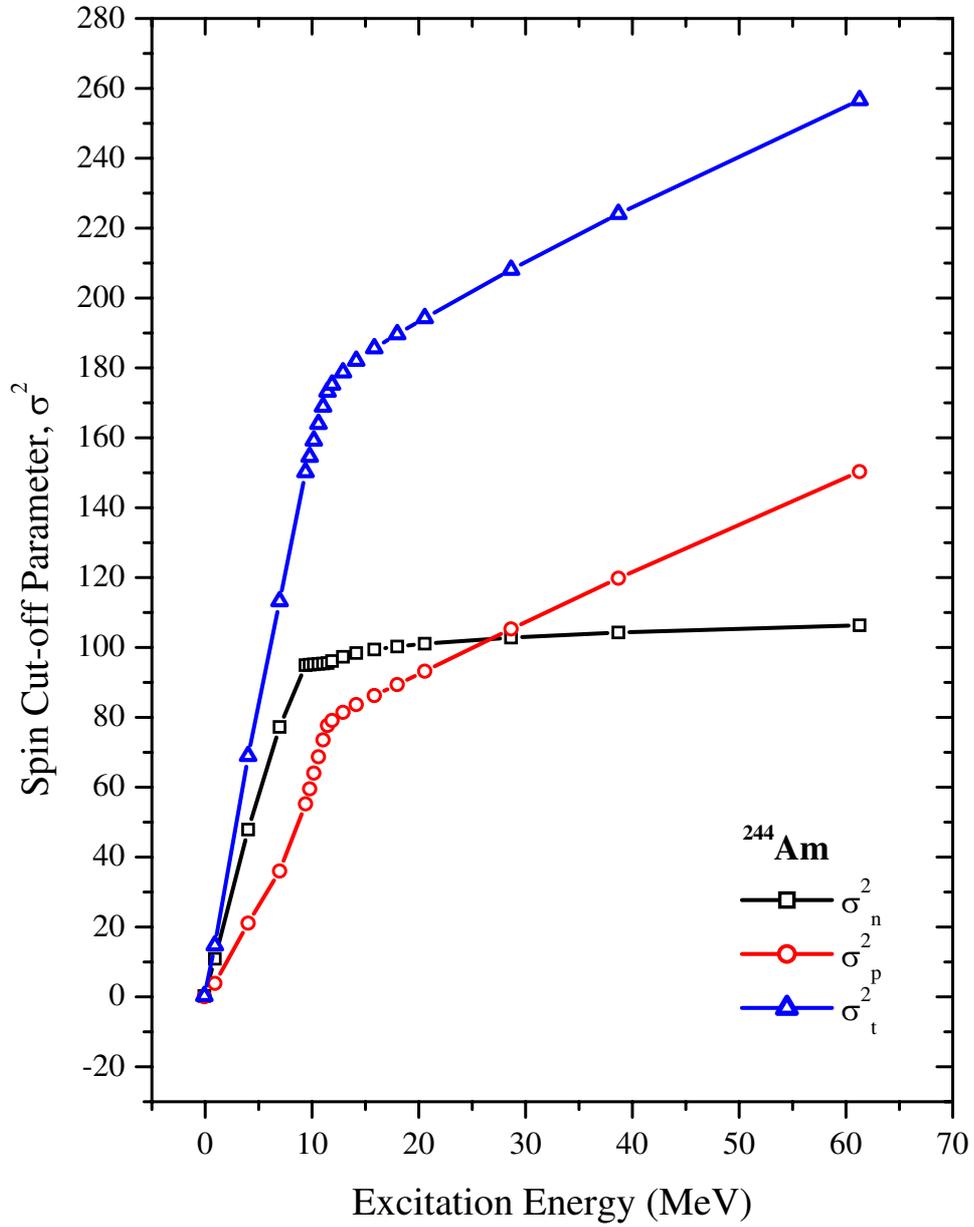


Figure 3.13: The Spin Cut-off parameter from microscopic theory. The individual contributions of neutron and proton are shown for ^{244}Am .

3.7 Nuclear Isospin

Consider a single nucleon, either neutron or proton. Introduce a quantum number I_z which we call isospin projection. By definition it is given a value of $1/2$ for proton and $-1/2$ for neutron. The word projection means that there is a total isospin and an axis which has a projection. We will define total isospin below and the axis is entirely fictitious.

The total isospin projection of a system with N , neutrons and Z , protons is

$$I_z = 1/2(Z - N) \quad (3.25)$$

then we consider the proton and neutron as different quantum states of the same particle, the nucleon. So, in any system with more than one nucleon, the total isospin projection I_z measures the proton excess of the system.

By introducing $N = A - Z$, equation (1) becomes

$$I_z = 1/2(Z - A + Z) \Rightarrow I_z = Z - 1/2A \Rightarrow Z = I_z + A/2 \quad (3.26)$$

Since in any nuclear reaction the total charge Z and the total nucleon number A , are conserved then the total isospin projection, I_z must also be conserved.

There is no fundamental importance attached to the isospin projection number I_z beyond what we already discussed. It sometimes offers a convenient way of writing the total wave function. For a single nucleon the two possible values of I_z reminds us of the ordinary spin projection m_s for a single nucleon.

In the spin formalism, total spin quantum number $S = 1/2$ for a single particle, $S = 0$ or 1 for two particles etc. It is possible and convenient to use such a formalism to express the symmetry of the total wave functions. Lets first consider the ordinary spin state of two nucleons. The total spin quantum number S are either $S = 0$ or $S = 1$, in the former case $m_s = 0$ in the later case $m_s = -1, 0$ and $+1$.

Table 3.2: Symmetries of the two nucleon system.

	I	I_z	Particle	Symmetry		
				Isospin	Space spin	Total
Singlet	0	0	np	Antisym.	Sym.	Antisym.
Triplet	1	1, 0, -1	pp, np, nn	Sym.	Antisym.	Antisym.

The total spin quantum number S is associated with magnitude of angular momentum,

$$P_s^2 = S(S + 1)\hbar^2 \quad (3.27)$$

So there is a concrete physical quantity associated with S . In contrast, now an abstract quantum number isospin, I , is introduced which is equal to $1/2$ for a single nucleon. A total isospin quantum number I is either 0 or 1 for two nucleons.

Considering two nucleons the isospin quantum number then is $I = 0$ isospin singlet, and projection I_z must be zero. According to Eqn (3.25) this means that $Z = N = 1$; that is system consists of a proton and a neutron.

For $I = 1$ we have an isospin triplet, and the projection can be either -1, 0 or 1 representing two neutrons, a neutron and a proton or two protons. Figure 3.14 shows an energy diagram of the three possible two body systems, the dineutron, the deuteron and the diproton. Only the $J = 1^+$ state of the deuteron is a bound state, the others are virtual states.

In the case of deuteron ground state, both particles are in the symmetric space-spin states which is possible due to the antisymmetry in isospin part of the wavefunction. However, two protons or two neutrons can not occupy this state because of their symmetric isospin wavefunctions. Table 3.2 summarizes the results for two nucleons.

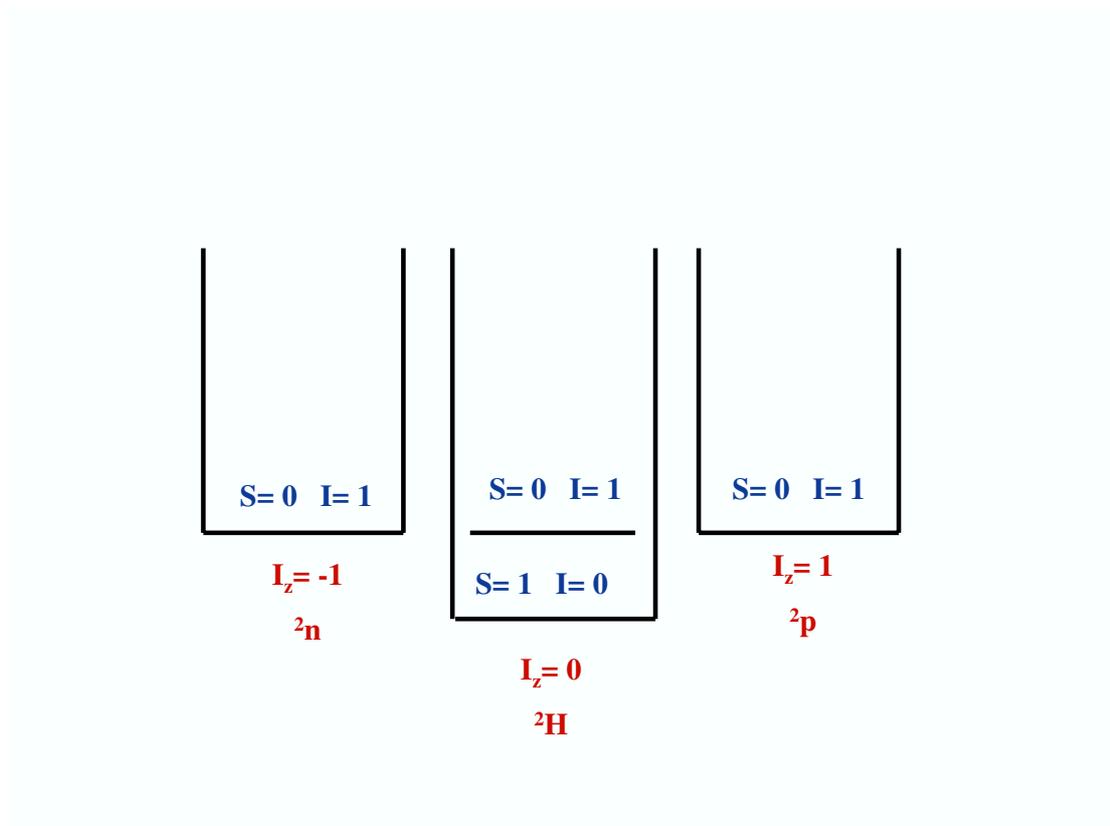


Figure 3.14: The lowest levels of the three possible two nucleon systems. None of the $S=0$, $I=1$ levels are stable.

In the isospin formalism, the total wave function is written as a product of a (*Spacepart*) \times (*SpinPart*) \times (*IsospinPart*). The form of spin part is identical to the form of isospin part.

3.8 Isospin Dependent Nuclear Level Density

As described above by considering the proton and neutron as different quantum states of the same particle, the total isospin projection of a system with N neutrons and Z protons is, I_z .

It has been pointed out for some time that the isospin quantum number is a good quantum number even for states of high excitation energies [61]. We have studied the influence of the isospin on the nuclear level densities and the spin cut-off parameter on the basis of spin formalism. The isospin dependent nuclear level density is

$$\rho(U, I) = \rho(U)f(I) \quad (3.28)$$

with spin distribution as

$$f(I) = \frac{2I + 1}{2\sigma_{I_z}^2} \exp\left[-\frac{(I + 1/2)^2}{2\sigma_{I_z}^2}\right] \quad (3.29)$$

where $\sigma_{I_z}^2 = 1/4gt$, g is the density of single particle levels.

The spin cut-off parameter is given by the relation [35]

$$\sigma_{I_z}^2 = g \langle m_i^2 \rangle t \quad (3.30)$$

where $\langle m_i^2 \rangle$ is the average squared of the nucleon isospin projections. Due to isospin, for light nuclei, the neutron and proton single particle levels coincide. So, the energy levels require a further two fold degeneracy, since they can be occupied by a neutron or by a proton. This arise because of the nucleon isospin projections ($\pm 1/2$). So, the average of the square of the isospin projections

$\langle m_i^2 \rangle = 1/4$, thus the isospin cut-off parameter [1]

$$\sigma_{I_z}^2 = 1/4gt \quad (3.31)$$

where the nuclear temperature at neutron binding energy is

$$t = \frac{1 + \sqrt{1 + 4a(B_n - E_0)}}{2a} \quad (3.32)$$

a , is the level density parameter in MeV^{-1} and E_0 is the back shift energy in MeV. Combining Eqns. (3.31) and (3.32) together with the value of g in terms of a gives

$$\sigma_{I_z}^2 = \frac{3(1 + \sqrt{1 + 4a(B_n - E_0)})}{4\pi^2} \quad (3.33)$$

CHAPTER 4

CALCULATIONS AND RESULTS

4.1 Introduction

Nuclear level densities are important in all statistical model calculations. Analytical expressions which contain free parameters adjusted on scarce experimental data are the Bethe and Constant Temperature formula. They mainly differ in the low excitation energy region where pairing corrections play an important role.[4, 9].

Sophisticated theoretical approaches have been developed to study level densities. In particular is the microscopic approach based on the BCS Hamiltonian [18]. In all level density expressions, two parameters are of importance, namely, the level density parameter a and the spin cut off factor, σ^2 . There have been some calculations of the level density parameter by some authors [63, 64]. More recently a realistic calculation of the level density parameter was performed which relies on the BCS theory [28]. There have also been some calculations of the spin cut-off parameter on the basis of the Fermi gas model[65, 67]. However, so far realistic calculations have never been applied to obtain the spin cut off factor which is important in all statistical model codes. Having seen a good agreement of the BCS results with experimental data [68, 69] for the level density $\rho(U)$ and for the level density parameter $a(E)$ [28, 70], in the present work we have extended the more realistic approach to calculate the level density and

spin cut-off parameter for a large number of nuclei.

4.2 Method of calculations

In the present study nuclear level density and spin cut-off factor have been determined at neutron binding energies for 295 nuclei between ^{20}F and ^{253}Cf using microscopic theory. The steps necessary to calculate level density $\rho(U)$ and the relevant spin cut-off parameter $\sigma(U)$ as outlined above are as follows: For a set of single particle levels and particular choice of temperature, T , the parameter λ and Δ are estimated and a set of occupational probabilities is calculated using Eqn. (3.14). Next, the stationary point conditions are checked for a given nucleon number using Eqn. (3.12). If the conditions are not met, the values of λ and Δ are adjusted and the procedure is repeated until the saddle point conditions are satisfied. Once the proper set of n_k values are computed, the entropy S_k is calculated using Eqn. (3.5). The energy E_n is calculated by applying Eqns. (3.13) and (3.14) at particular temperature, T . The excitation energy U_n is then determined by subtracting the energy at $T=0$. The quantities σ_n , $\omega(N, U_n)$ are then calculated using Eqns. (3.19) and (3.4). A similar set of calculations are used to calculate U_p and S_p for proton system. The total level density and spin cut-off factor are then calculated from Eqns. (3.17) and (3.18).

4.3 Calculations of the spin cut-off parameter

4.3.1 Calculations of σ^2 , Using Microscopic Model

A systematic study of the behavior of level density and of the spin cut off parameter across a large mass region has been performed using the microscopic model. The results for even- even nuclei are shown in Table 4.1. Their corresponding rigid body values, $\sigma_{rigid}^2 = 0.0138A^{5/3}[\frac{1+\sqrt{1+4aU}}{2a}]$, as well as their values obtained from the Gilbert and Cameron expression, $\sigma_{GC}^2 = 0.0888A^{2/3}\sqrt{a(U - E_0)}$, where

a is the level density parameter, U is the excitation energy and E_0 is the back shift energy [69] are also given in Table 4.1. These results are plotted in Figure 4.1 for comparison. Similar results for odd-odd nuclei are listed in Table 4.2 and are plotted in Figure 4.2. The same results for odd-A nuclei are listed in Table 4.3 and are plotted in Figure 4.3. Examination of these figures reveals that the values of the spin cut off factor deduced from the BCS theory do not increase smoothly with A , as expected on the basis of macroscopic theory with rigid body moment of inertia, instead the values of $\sigma^2(U)$ show structure reflecting the angular momentum of shell model orbitals near the Fermi energy.

We have found it worth while to compare our results with those obtained using the analytic expression, $\sigma_{BSFG}^2 = 0.0146A^{5/3} \frac{1 + \sqrt{1 + 4a(U - E_0)}}{2a}$, introduced recently [67]. The σ^2 values computed from this for all nuclei under study at neutron binding energy ($U = B_n$) of Ref. [70] are plotted in Figure 4.4. The corresponding values of σ^2 from microscopic theory are also shown in Figure 4.4 for comparison. Examination of this figure reveals that although the results from both methods are in general agreement, they differ for nuclei near major shells; in particular, this difference is very large for nuclei near the doubly magic nuclei $A \simeq 208$. This may be accounted for by the fact that in microscopic theory the realistic single particle orbitals are used which is ignored in the empirical expression above.

Table 4.1: Comparison of Spin Cut-off Parameter, σ^2 from different methods for even-even nuclei.

Z	A	Element	B_n	a	E_0	$\sigma^2(B_n)$			
						a)	b)	c)	d)
12	26	Mg	11.09	4.50	0.41	5.41	5.30	5.51	6.77
14	30	Si	10.61	3.32	-3.89	5.95	7.77	9.50	5.33
16	34	S	11.42	4.66	-0.12	6.83	8.26	8.78	7.15
20	44	Ca	11.13	7.36	-0.07	10.05	9.84	10.44	17.31
22	48	Ti	11.63	6.92	-1.23	11.06	11.99	13.30	17.86
22	50	Ti	10.94	6.69	0.99	9.83	12.69	12.84	14.27
24	54	Cr	9.720	7.05	-0.62	10.83	13.28	14.47	14.86
26	58	Fe	10.04	7.61	-1.02	12.21	14.59	16.15	15.17
28	60	Ni	11.39	7.29	-0.85	12.86	16.75	18.34	13.94
28	62	Ni	10.60	7.82	-0.57	13.00	16.48	17.88	15.53
30	68	Zn	10.20	9.74	-0.19	14.88	16.82	17.96	20.58
32	74	Ge	10.20	12.04	-0.29	17.59	17.33	18.59	28.15
34	78	Se	10.50	11.98	-0.35	18.48	19.23	20.67	31.92
36	84	Kr	10.52	10.26	0.13	17.58	23.63	24.85	26.28
38	88	Sr	11.11	9.320	1.00	17.05	27.55	27.87	27.70
40	92	Zr	8.63	11.46	0.32	17.67	23.62	24.54	24.40
40	94	Zr	8.22	13.87	0.66	18.79	21.63	21.99	24.40
42	96	Mo	9.15	12.95	-0.04	20.32	24.45	25.93	28.50
42	98	Mo	8.64	14.26	-0.14	21.12	23.41	24.95	28.60
44	100	Ru	9.67	14.13	-0.18	22.58	25.67	27.40	33.10
44	102	Ru	9.22	15.35	0.18	22.84	24.84	26.03	33.70
46	106	Pd	9.56	15.60	0.13	24.12	26.73	28.09	38.23
46	108	Pd	9.22	16.13	0.34	24.10	26.63	27.67	40.87

- a) : Calculated with Gilbert and Cameron Expression.
b) : Calculated with Rigid Body approximation.
c) : Calculated with Back Shift Fermi Gas (BSFG) Expression.
d) : Calculated with Microscopic Theory.

Table 4.1: Continue.

Z	A	Element	B_n	a	E_0	$\sigma^2(B_n)$			
						a)	b)	c)	d)
48	112	Cd	9.40	16.33	-0.1	25.70	28.36	30.16	45.50
48	114	Cd	9.04	16.70	0.28	25.25	28.35	29.54	45.60
50	118	Sn	9.33	15.10	0.68	24.41	32.11	32.76	48.60
50	120	Sn	9.11	14.80	0.70	24.10	32.99	33.58	47.20
52	124	Te	9.43	16.68	0.19	27.41	33.29	34.88	50.23
52	126	Te	9.11	16.10	0.23	26.68	34.27	35.80	46.40
54	130	Xe	9.25	15.91	0.34	27.14	36.59	38.03	45.66
54	132	Xe	8.94	15.20	0.40	26.22	37.80	39.13	38.35
56	136	Ba	9.11	15.24	0.14	27.45	40.03	42.02	38.75
56	138	Ba	8.61	13.47	0.78	24.37	42.59	43.08	34.34
58	142	Ce	7.17	17.83	0.88	25.59	35.35	35.12	33.05
60	144	Nd	7.82	17.29	0.53	27.39	38.32	39.21	39.27
60	146	Nd	7.56	19.19	0.19	29.30	36.56	38.22	40.61
60	148	Nd	7.33	23.23	0.25	31.86	33.36	34.70	39.41
62	148	Sm	8.14	19.80	0.21	31.13	38.12	39.82	46.62
62	150	Sm	7.99	21.83	0.07	32.96	36.71	38.68	46.72
62	152	Sm	8.26	22.66	-0.13	34.86	37.40	39.87	50.32
64	156	Gd	8.54	21.64	-0.27	35.53	40.65	43.66	58.12
64	158	Gd	7.94	21.41	-0.38	34.63	40.32	43.61	58.44
66	162	Dy	8.20	21.42	-0.46	35.92	42.68	46.34	66.95
66	164	Dy	7.66	21.07	-0.07	33.95	42.53	45.19	70.93
68	168	Er	7.77	21.30	-0.40	35.66	44.32	48.03	77.65
70	170	Yb	8.47	21.13	-0.32	37.13	47.32	50.96	84.19
70	172	Yb	8.02	22.21	-0.25	37.22	45.79	49.18	84.09
70	174	Yb	7.46	21.47	0.04	34.94	45.90	48.43	77.57

- a) : Calculated with Gilbert and Cameron Expression.
b) : Calculated with Rigid Body approximation.
c) : Calculated with Back Shift Fermi Gas (BSFG) Expression.
d) : Calculated with Microscopic Theory.

Table 4.1: Continue.

Z	A	Element	B_n	a	E_0	$\sigma^2(B_n)$			
						a)	b)	c)	d)
72	178	Hf	7.63	22.87	-0.21	37.61	46.61	49.97	77.87
72	180	Hf	7.39	22.18	-0.3	36.96	47.52	51.24	75.22
74	184	W	7.41	22.82	-0.12	37.65	48.65	51.86	66.70
76	188	Os	7.99	23.15	0.07	39.46	51.89	54.67	62.61
76	190	Os	7.79	22.84	0.01	39.13	52.55	55.57	56.87
78	196	Pt	7.92	20.72	0.00	38.39	58.67	62.07	36.97
80	200	Hg	8.03	18.00	0.001	36.50	65.72	69.52	31.07
80	202	Hg	7.75	17.36	-0.24	36.02	66.96	71.89	28.16
90	230	Th	6.79	29.74	-0.28	48.37	58.98	63.65	89.21
92	234	U	6.84	29.81	-0.26	49.08	60.85	65.55	101.59
92	236	U	6.54	31.35	-0.28	49.62	58.85	63.54	107.58
92	238	U	6.15	31.32	-0.36	48.69	57.96	63.01	–
93	239	Np	6.22	30.20	-1.07	50.72	59.77	68.25	104.1
94	240	Pu	6.53	30.50	-0.43	49.99	61.33	66.93	108.24
94	242	Pu	6.31	31.87	-0.40	50.44	59.78	65.17	106.88
96	244	Cm	6.80	29.39	-0.08	49.30	65.51	69.69	116.09
96	246	Cm	6.46	29.22	-0.20	48.63	64.97	69.78	109.86
96	248	Cm	6.21	29.94	0.06	47.57	63.83	67.23	100.03
98	250	Cf	6.62	29.57	0.06	49.09	67.15	70.74	108.55

- a) : Calculated with Gilbert and Cameron Expression.
b) : Calculated with Rigid Body approximation.
c) : Calculated with Back Shift Fermi Gas (BSFG) Expression.
d) : Calculated with Microscopic Theory.

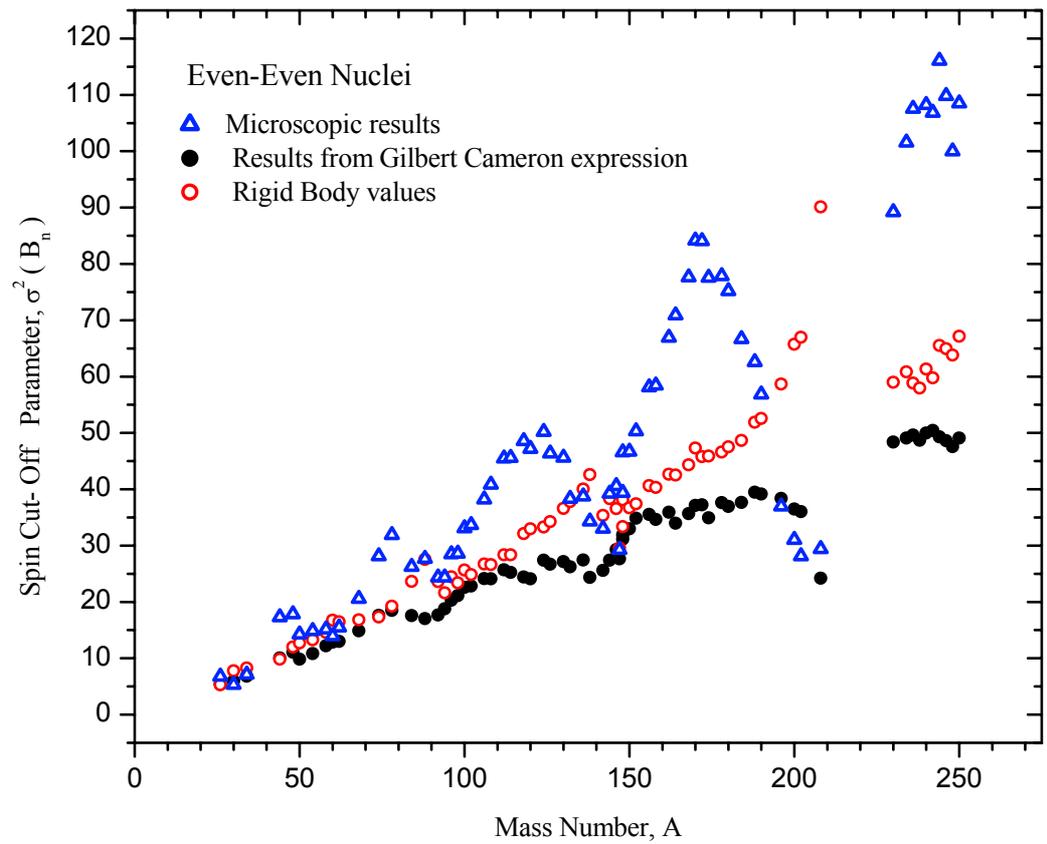


Figure 4.1: Comparison of Spin Cut-off Parameter, σ^2 from different methods for even-even nuclei.

Table 4.2: Comparison of Spin Cut-off Parameter, σ^2 from different methods for odd-odd nuclei.

Z	A	Element	B_n	a	E_0	$\sigma^2(B_n)$			
						a)	b)	c)	d)
9	20	F	6.60	3.12	-4.78	3.90	3.3	4.47	4.34
11	24	Na	6.96	3.42	-4.87	4.70	4.35	5.86	5.10
13	28	Al	7.72	3.93	-2.29	5.14	5.47	6.51	4.27
17	36	Cl	8.58	4.38	-1.88	6.55	8.22	9.53	6.30
17	38	Cl	6.11	5.95	0.91	5.58	6.52	6.41	6.27
19	40	K	7.80	5.15	-2.47	7.55	8.6	10.34	8.75
19	42	K	7.53	5.35	-4.97	8.77	8.99	12.04	8.45
21	46	Sc	8.76	6.83	-2.85	10.15	9.84	11.89	15.76
23	52	V	7.31	6.88	-1.53	9.65	11.06	12.79	11.33
25	56	Mn	7.27	7.54	-2.85	11.35	11.88	14.68	11.72
27	60	Co	7.49	8.1	-2.2	12.05	13.02	15.54	10.91
29	64	Cu	7.92	8.38	-2.62	13.35	14.6	17.67	12.65
29	66	Cu	7.07	8.84	-1.7	12.77	14.17	16.59	13.79
31	70	Ga	7.65	9.84	-1.93	14.65	15.33	18.03	13.34
31	72	Ga	6.52	11.06	-2.49	15.34	14.01	17.27	17.52
33	76	As	7.33	12.17	-2.53	17.45	15.39	18.75	22.36
35	80	Br	7.89	12.22	-2.33	18.42	17.33	20.74	25.70
35	82	Br	7.59	11.68	-2.16	17.89	18.16	21.64	22.58
37	86	Rb	8.65	9.90	-1.91	17.69	22.82	26.54	22.90
37	88	Rb	6.08	10.25	-1.44	15.42	19.71	23.05	14.75
39	90	Y	6.86	9.35	-0.82	15.11	22.73	25.35	19.10
41	94	Nb	7.23	12.35	-1.51	19.07	21.63	25.04	21.80
43	100	Tc	6.76	15.88	-1.61	22.06	20.36	23.85	23.90

- a) : Calculated with Gilbert and Cameron Expression.
b) : Calculated with Rigid Body approximation.
c) : Calculated with Back Shift Fermi Gas (BSFG) Expression.
d) : Calculated with Microscopic Theory.

Table (4.2): Continue.

Z	A	Element	B_n	a	E_0	$\sigma^2(B_n)$			
						a)	b)	c)	d)
45	104	Rh	7.00	15.62	-2.01	23.29	22.28	26.59	26.90
47	108	Ag	7.27	15.82	-1.8	24.13	24	28.23	30.50
47	110	Ag	6.81	17.29	-1.54	24.49	22.9	26.71	32.40
49	114	In	7.27	15.14	-0.97	23.32	26.89	30.19	37.50
49	116	In	6.78	16.54	-1.1	24.12	25.56	29.05	37.30
51	122	Sb	6.81	16.47	-1.41	25.41	27.91	32.30	38.00
51	124	Sb	6.47	16.02	-1.64	25.16	28.4	33.47	36.50
53	128	I	6.83	16.39	-1.7	26.66	30.36	35.72	37.04
53	130	I	6.46	15.84	-1.55	25.67	30.9	36.21	35.16
55	134	Cs	6.89	15.66	-2.04	27.5	33.71	40.36	29.04
55	136	Cs	6.83	14.54	-2.01	26.63	35.76	42.79	25.75
57	140	La	5.16	15.65	-1.37	24.2	31.62	37.39	23.52
59	142	Pr	5.84	15.63	-0.87	24.76	34.36	38.83	28.27
61	148	Pm	5.89	20.50	-0.97	29.48	32.06	36.49	31.72
63	152	Eu	6.31	23.32	-1.86	34.91	32.37	38.79	38.42
63	154	Eu	6.44	22.24	-1.86	34.66	34.26	40.94	41.65
63	156	Eu	6.34	20.18	-1.3	31.95	36.55	42.28	44.95
65	160	Tb	6.38	20.80	-1.33	33.13	37.62	43.58	51.52
67	166	Ho	6.24	20.37	-1.29	33.23	40.05	46.36	60.39
69	170	Tm	6.59	20.42	-1.34	34.69	42.71	49.39	69.90
71	176	Lu	6.29	21.05	-1.24	35.12	43.57	50.24	65.92
73	182	Ta	6.06	21.21	-1.2	35.39	45.07	51.98	56.73
75	186	Re	6.18	21.90	-1.15	36.66	46.37	53.25	52.38
75	188	Re	5.87	22.33	-1.28	36.82	45.6	53.02	45.12
77	192	Ir	6.20	23.02	-1.26	38.73	47.72	55.19	39.47
77	194	Ir	6.07	21.56	-1.35	37.64	49.71	57.93	30.58

- a) : Calculated with Gilbert and Cameron Expression.
b) : Calculated with Rigid Body approximation.
c) : Calculated with Back Shift Fermi Gas (BSFG) Expression.
d) : Calculated with Microscopic Theory.

Table (4.2): Continue.

Z	A	Element	B_n	a	E_0	$\sigma^2(B_n)$			
						a)	b)	c)	d)
79	198	Au	6.51	19.03	-1.44	37.11	56.79	66.10	20.97
81	204	Tl	6.66	15.51	-1.28	34.15	67.13	77.25	23.38
81	206	Tl	6.50	11.72	-0.94	28.92	78.22	88.18	22.80
83	210	Bi	4.60	13.32	-1.69	28.71	64.17	78.61	22.49
91	232	Pa	5.57	29.72	-0.61	45.42	54.4	60.49	79.66
91	234	Pa	5.22	30.69	-0.64	45.24	52.62	58.86	84.71
93	238	Np	5.49	28.88	-1.2	47.39	57.21	66.56	91.19
95	242	Am	5.54	28.71	-1.34	48.48	59.26	69.6	94.08
95	244	Am	5.36	29.00	-1.22	47.89	58.85	68.69	105.59
97	250	Bk	4.96	29.52	-1.04	46.91	58.5	67.82	70.70

- a) : Calculated with Gilbert and Cameron Expression.
b) : Calculated with Rigid Body approximation.
c) : Calculated with Back Shift Fermi Gas (BSFG) Expression.
d) : Calculated with Microscopic Theory.

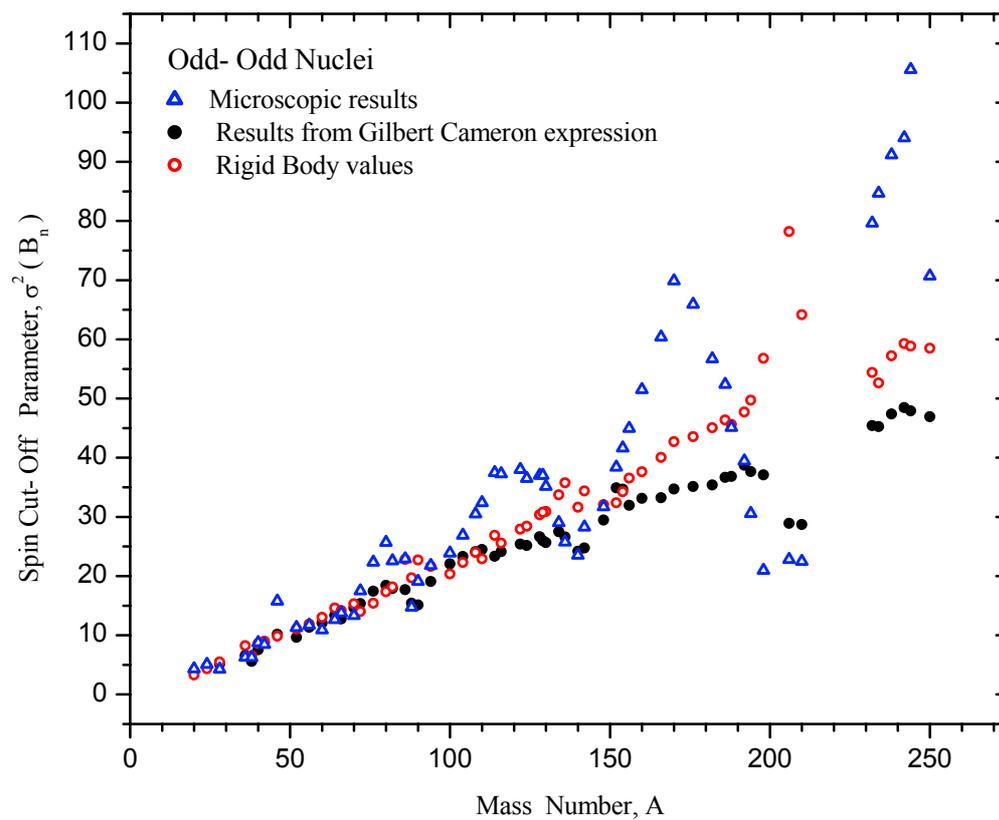


Figure 4.2: Comparison of Spin Cut-off Parameter, σ^2 from different methods for odd-odd nuclei.

Table 4.3: Comparison of Spin Cut-off Parameter, σ^2 from different methods for odd-A nuclei.

Z	A	Element	B_n	a	E_0	$\sigma^2(B_n)$			
						a)	b)	c)	d)
12	25	Mg	7.33	3.63	-4.57	4.99	4.62	6.1	5.39
12	27	Mg	6.45	4.65	-0.84	4.65	4.33	4.84	3.96
14	29	Si	8.47	4.08	0.58	4.76	5.93	6.07	4.13
14	31	Si	6.59	4.59	0.40	4.67	5.54	5.7	3.62
15	33	P	7.94	4.78	0.63	5.40	6.55	6.67	4.78
16	33	S	8.64	4.42	-1.26	6.05	7.10	8.00	4.61
16	35	S	6.99	5.04	0.08	5.61	6.61	6.96	4.16
18	41	Ar	6.10	7.10	-0.54	7.25	6.73	7.40	8.89
20	43	Ca	7.93	7.00	-1.77	8.98	8.29	9.64	12.46
20	45	Ca	7.41	7.30	-1.03	8.82	8.48	9.53	12.47
22	47	Ti	8.88	6.33	-3.22	10.12	10.69	13.08	15.91
22	49	Ti	8.14	7.17	-0.56	9.39	10.30	11.24	13.24
22	51	Ti	6.37	6.64	1.90	6.66	10.24	9.21	8.06
23	51	V	11.05	6.65	-1.54	11.18	13.22	14.87	16.02
24	51	Cr	9.26	6.79	-2.25	10.80	12.04	14.10	16.65
24	53	Cr	7.94	6.62	-1.18	9.74	12.11	13.66	13.05
24	55	Cr	6.25	7.72	-0.93	9.56	10.61	11.98	10.19
26	55	Fe	9.30	6.64	-1.38	10.81	13.85	15.63	13.04
26	57	Fe	7.65	7.51	-2.23	11.33	12.56	14.98	11.48
26	59	Fe	6.58	8.59	-1.19	10.99	11.55	13.20	10.86
28	59	Ni	9.00	7.21	-2.00	11.98	14.67	17.06	10.34
28	61	Ni	7.82	8.13	-1.31	11.86	13.62	15.50	10.61
28	63	Ni	6.84	9.00	-0.47	11.40	12.78	13.95	11.18

- a) : Calculated with Gilbert and Cameron Expression.
b) : Calculated with Rigid Body approximation.
c) : Calculated with Back Shift Fermi Gas (BSFG) Expression.
d) : Calculated with Microscopic Theory.

Table (4.3): Continue.

Z	A	Element	B_n	a	E_0	$\sigma^2(B_n)$			
						a)	b)	c)	d)
28	65	Ni	6.10	9.74	-0.02	11.08	12.24	12.98	12.15
30	65	Zn	7.98	9.60	-1.63	13.78	14.00	16.17	12.44
30	67	Zn	7.05	10.43	-1.54	13.87	13.29	15.44	13.57
30	69	Zn	6.48	11.05	-0.97	13.56	13.02	14.71	15.16
30	71	Zn	5.83	11.81	0.06	12.58	12.54	13.20	16.39
32	71	Ge	7.42	12.23	-1.76	16.13	13.79	16.14	16.61
32	73	Ge	6.78	12.56	-1.95	16.25	13.65	16.28	17.82
32	75	Ge	6.51	12.09	-1.56	15.59	14.29	16.73	19.81
32	77	Ge	6.07	12.30	-1.12	15.12	14.32	16.41	20.36
34	75	Se	8.03	12.75	-1.91	17.78	15.34	17.97	21.56
34	77	Se	7.42	12.85	-1.62	17.32	15.38	17.88	22.30
34	79	Se	6.96	12.06	-1.93	16.93	16.11	19.13	22.31
34	83	Se	5.82	12.82	-1.15	15.96	15.56	17.92	13.42
36	79	Kr	8.37	12.79	-1.75	18.60	17.04	19.74	26.28
36	81	Kr	7.87	13.42	-1.53	18.67	16.83	19.38	26.25
36	85	Kr	7.12	12.96	-1.13	17.75	17.70	20.08	18.23
38	85	Sr	8.53	12.44	-1.83	19.49	19.71	22.89	28.09
38	87	Sr	8.43	10.12	-1.08	17.10	22.71	25.44	23.53
38	89	Sr	6.37	9.88	-0.06	14.10	20.94	22.25	16.50
40	91	Zr	7.19	10.63	-0.20	15.92	22.13	23.72	20.80
40	93	Zr	6.73	12.04	-0.17	16.61	20.83	22.29	19.75
40	95	Zr	6.46	12.67	0.29	16.35	20.60	21.33	19.10
40	97	Zr	5.58	12.20	0.76	14.37	20.31	20.05	17.80
42	93	Mo	8.07	10.61	-0.64	17.52	24.25	26.59	26.60
42	95	Mo	7.37	12.47	-0.88	18.74	22.11	24.67	23.10
42	97	Mo	6.82	13.73	-1.05	19.50	20.97	23.75	22.70

- a) : Calculated with Gilbert and Cameron Expression.
b) : Calculated with Rigid Body approximation.
c) : Calculated with Back Shift Fermi Gas (BSFG) Expression.
d) : Calculated with Microscopic Theory.

Table (4.3): Continue.

Z	A	Element	B_n	a	E_0	$\sigma^2(B_n)$			
						a)	b)	c)	d)
42	99	Mo	5.92	15.73	-1.26	20.20	18.90	21.91	20.80
42	101	Mo	5.40	17.63	-1.44	21.15	17.61	20.85	20.00
44	103	Ru	6.23	16.13	-1.73	22.11	20.40	24.26	24.40
44	105	Ru	5.91	18.10	-1.30	22.58	19.34	22.51	24.90
46	105	Pd	7.09	15.66	-1.35	22.72	22.76	26.16	26.30
46	107	Pd	6.54	16.72	-1.07	22.58	21.83	24.83	27.70
46	109	Pd	6.15	18.45	-1.34	23.82	20.78	24.15	29.60
46	111	Pd	5.76	20.06	-0.94	23.77	19.85	22.57	30.20
48	107	Cd	7.93	15.04	-0.93	23.09	25.30	28.21	27.60
48	109	Cd	7.33	16.37	-0.72	23.25	24.03	26.58	24.50
48	111	Cd	6.97	16.75	-1.11	23.87	23.91	27.14	33.30
48	113	Cd	6.54	17.47	-0.92	23.69	23.37	26.33	33.40
48	115	Cd	6.14	18.17	-0.61	23.25	22.87	25.31	34.90
48	117	Cd	5.77	18.35	-0.96	23.59	22.73	25.88	33.60
50	113	Sn	7.74	15.28	-0.26	22.95	27.17	29.21	36.60
50	115	Sn	7.54	14.80	0.25	21.83	28.09	29.25	38.80
50	117	Sn	6.94	15.55	-0.06	22.16	27.09	28.76	38.70
50	119	Sn	6.49	16.19	-0.18	22.31	26.40	28.29	38.60
50	121	Sn	6.17	15.18	0.06	20.92	27.43	28.88	37.40
50	123	Sn	5.95	15.74	-0.56	22.23	27.17	30.01	34.60
50	125	Sn	5.73	14.14	-0.46	20.78	29.02	31.85	31.80
52	123	Te	6.94	17.39	-0.77	25.43	27.74	30.87	40.66
52	125	Te	6.57	17.69	-0.75	25.25	27.53	30.66	37.90
52	127	Te	6.29	16.60	-0.77	24.29	28.62	31.99	33.90
52	129	Te	6.09	16.64	-0.87	24.39	28.89	32.57	29.50
52	131	Te	5.93	15.85	-0.54	23.20	30.03	33.12	22.90

- a) : Calculated with Gilbert and Cameron Expression.
b) : Calculated with Rigid Body approximation.
c) : Calculated with Back Shift Fermi Gas (BSFG) Expression.
d) : Calculated with Microscopic Theory.

Table (4.3): Continue.

Z	A	Element	B_n	a	E_0	$\sigma^2(B_n)$			
						a)	b)	c)	d)
54	129	Xe	6.91	16.55	-1.03	25.98	30.77	34.78	37.02
54	131	Xe	6.62	17.39	-0.86	26.13	30.14	33.81	31.08
54	133	Xe	6.44	15.88	-0.7	24.64	31.99	35.55	27.03
54	135	Xe	6.38	14.83	-0.06	22.85	33.86	35.99	21.73
55	135	Cs	8.83	14.51	-0.25	26.81	39.97	42.85	35.35
56	131	Ba	7.49	17.67	-1.00	28.06	31.71	35.62	41.74
56	133	Ba	7.19	17.35	-1.04	27.65	32.20	36.33	37.42
56	135	Ba	6.97	15.93	-0.88	26.13	34.02	38.08	32.21
56	137	Ba	6.90	14.31	0.01	23.43	36.69	38.78	28.13
56	139	Ba	4.72	14.59	-0.19	20.18	31.10	33.53	19.73
57	139	La	8.78	13.64	-0.19	26.36	43.23	46.21	37.03
58	137	Ce	7.48	18.06	-0.76	28.8	33.76	37.41	37.01
58	141	Ce	5.43	16.05	0.12	22.20	32.34	33.84	27.20
58	143	Ce	5.14	18.92	-0.09	24.16	29.61	31.57	24.88
60	143	Nd	6.12	16.60	0.26	23.95	34.44	35.68	32.02
60	145	Nd	5.75	18.79	-0.34	26.23	32.07	34.87	30.46
60	147	Nd	5.29	21.25	-0.59	27.66	29.56	32.89	29.27
60	149	Nd	5.04	23.71	-1.01	29.89	27.89	32.20	28.39
60	151	Nd	5.33	22.39	-0.98	29.94	30.19	34.63	30.63
62	145	Sm	6.76	15.64	0.20	24.82	38.13	39.76	37.74
62	149	Sm	5.87	21.44	-0.73	29.69	31.62	35.39	34.07
62	150	Sm	7.99	21.83	0.07	32.96	36.71	38.68	46.72
62	151	Sm	5.60	24.11	-1.43	32.77	29.72	35.06	33.99
62	153	Sm	5.87	23.03	-1.42	32.90	31.82	37.35	36.87
62	155	Sm	5.81	21.52	-0.85	30.68	33.53	37.87	41.46
63	153	Eu	8.55	20.36	-1.48	36.29	40.66	46.44	51.80

- a) : Calculated with Gilbert and Cameron Expression.
b) : Calculated with Rigid Body approximation.
c) : Calculated with Back Shift Fermi Gas (BSFG) Expression.
d) : Calculated with Microscopic Theory.

Table (4.3): Continue.

Z	A	Element	B_n	a	E_0	$\sigma^2(B_n)$			
						a)	b)	c)	d)
63	155	Eu	8.15	20.49	-0.87	34.84	40.47	44.97	54.22
64	153	Gd	6.25	24.20	-1.37	34.49	31.96	37.21	39.22
64	155	Gd	6.43	23.51	-1.33	34.61	33.63	38.93	42.66
64	157	Gd	6.36	22.37	-1.24	33.70	35.06	40.40	49.36
64	159	Gd	5.94	21.81	-1.05	32.18	35.12	40.16	45.36
64	161	Gd	5.63	21.11	-0.75	30.52	35.57	39.95	50.54
66	157	Dy	6.97	23.95	-1.21	36.17	35.35	40.40	46.53
66	159	Dy	6.83	21.55	-1.21	34.31	37.78	43.23	50.30
66	161	Dy	6.45	22.36	-1.29	34.58	36.83	42.53	51.04
66	163	Dy	6.27	21.38	-1.28	33.67	37.96	43.91	57.77
66	165	Dy	5.72	21.50	-1.02	32.14	36.95	42.28	55.57
68	163	Er	6.90	23.31	-1.18	36.36	37.99	43.36	55.85
68	165	Er	6.65	22.31	-1.26	35.48	38.97	44.80	59.17
68	167	Er	6.44	21.88	-1.08	34.53	39.54	45.06	62.79
68	169	Er	6.00	21.42	-0.88	32.96	39.44	44.55	62.18
68	171	Er	5.68	21.78	-0.83	32.59	38.84	43.87	60.93
69	171	Tm	7.49	21.17	-0.71	36.03	44.98	49.70	76.5
70	169	Yb	6.87	23.54	-1.00	36.93	40.05	45.22	66.55
70	171	Yb	6.62	21.68	-0.95	35.02	41.87	47.24	69.19
70	173	Yb	6.37	21.05	-0.89	34.07	42.57	47.94	67.86
70	175	Yb	5.82	21.19	-0.70	32.65	41.43	46.27	61.24
70	177	Yb	5.57	21.84	-0.70	32.76	40.68	45.56	56.92
71	177	Lu	7.07	21.30	-0.80	36.24	46.21	51.46	72.47
72	175	Hf	6.71	22.61	-0.95	36.56	42.86	48.33	68.96
72	177	Hf	6.38	22.70	-0.90	35.98	42.55	47.95	65.88
72	179	Hf	6.10	22.41	-0.90	35.32	42.72	48.28	62.38

- a) : Calculated with Gilbert and Cameron Expression.
b) : Calculated with Rigid Body approximation.
c) : Calculated with Back Shift Fermi Gas (BSFG) Expression.
d) : Calculated with Microscopic Theory.

Table (4.3): Continue.

Z	A	Element	B_n	a	E_0	$\sigma^2(B_n)$			
						a)	b)	c)	d)
72	181	Hf	5.70	22.85	-0.22	33.04	41.69	44.92	54.49
73	181	Ta	7.58	23.18	-0.03	37.72	47.45	50.29	71.88
73	183	Ta	6.93	21.77	-0.43	36.25	47.84	52.11	62.23
74	181	W	6.68	22.61	-0.73	36.78	45.25	50.31	66.18
74	183	W	6.19	22.09	-0.77	35.49	44.98	50.33	56.95
74	185	W	5.75	23.32	-0.80	35.66	42.99	48.42	47.56
74	187	W	5.47	24.07	-0.75	35.52	42.01	47.26	43.25
76	187	Os	6.29	23.25	-1.00	37.82	45.75	51.96	52.86
76	189	Os	5.92	23.61	-0.96	37.29	44.87	51.04	42.95
76	191	Os	5.76	23.43	-1.12	37.38	45.24	52.11	36.26
76	193	Os	5.58	23.07	-0.78	35.93	45.73	51.50	29.29
77	192	Ir	6.20	23.02	-1.26	38.73	47.72	55.19	39.47
77	193	Ir	7.77	22.18	-0.91	41.14	54.69	61.02	42.87
78	193	Pt	6.25	24.05	-1.12	39.50	47.25	54.11	37.34
78	195	Pt	6.11	20.27	-1.23	36.40	51.95	59.99	31.22
78	197	Pt	5.85	20.02	-1.04	35.31	52.09	59.60	25.89
78	199	Pt	5.57	21.00	-0.42	33.94	50.49	55.29	21.19
80	199	Hg	6.66	19.93	-0.93	37.23	56.52	63.65	27.48
80	201	Hg	6.23	17.90	-0.21	32.71	58.88	63.27	24.16
82	205	Pb	6.73	15.03	-0.71	32.65	69.17	76.75	25.19
82	207	Pb	6.74	11.15	0.97	24.92	82.30	80.93	25.25
82	209	Pb	3.94	12.36	0.21	21.22	61.59	63.50	15.74
88	227	Ra	4.56	32.06	-0.84	43.47	45.82	52.56	55.33
90	229	Th	5.24	32.77	-0.99	47.49	49.14	56.50	63.04
90	231	Th	5.12	31.82	-0.8	45.86	50.05	56.76	71.77
90	233	Th	4.79	32.43	-0.81	45.29	48.69	55.53	71.55

- a) : Calculated with Gilbert and Cameron Expression.
b) : Calculated with Rigid Body approximation.
c) : Calculated with Back Shift Fermi Gas (BSFG) Expression.
d) : Calculated with Microscopic Theory.

Table (4.3): Continue.

Z	A	Element	B_n	a	E_0	$\sigma^2(B_n)$			
						a)	b)	c)	d)
92	233	U	5.74	30.33	-0.72	47.09	55.02	61.63	85.40
92	235	U	5.30	30.32	-0.93	46.48	53.69	61.42	81.65
92	237	U	5.13	30.74	-0.88	46.20	53.22	60.77	86.22
92	239	U	4.81	31.80	-0.82	45.74	51.42	58.68	82.94
93	239	Np	6.22	30.20	-1.07	50.72	59.77	68.25	104.10
94	239	Pu	5.65	29.31	-0.89	47.33	57.96	65.78	94.37
94	241	Pu	5.24	30.65	-1.02	47.63	55.41	63.84	90.55
94	243	Pu	5.03	31.64	-0.90	47.38	54.18	62.05	82.27
94	245	Pu	4.70	32.85	-0.62	45.97	52.12	58.54	79.74
95	243	Am	6.37	28.38	-1.07	50.23	64.20	73.19	104.45
96	243	Cm	5.69	28.13	-0.40	45.26	61.11	66.78	96.84
96	245	Cm	5.52	29.38	-0.98	48.05	59.69	68.30	97.53
96	247	Cm	5.16	29.00	-0.82	46.04	58.95	66.97	86.75
98	251	Cf	5.11	31.64	-0.75	48.10	57.60	65.08	72.85

- a) : Calculated with Gilbert and Cameron Expression.
b) : Calculated with Rigid Body approximation.
c) : Calculated with Back Shift Fermi Gas (BSFG) Expression.
d) : Calculated with Microscopic Theory.

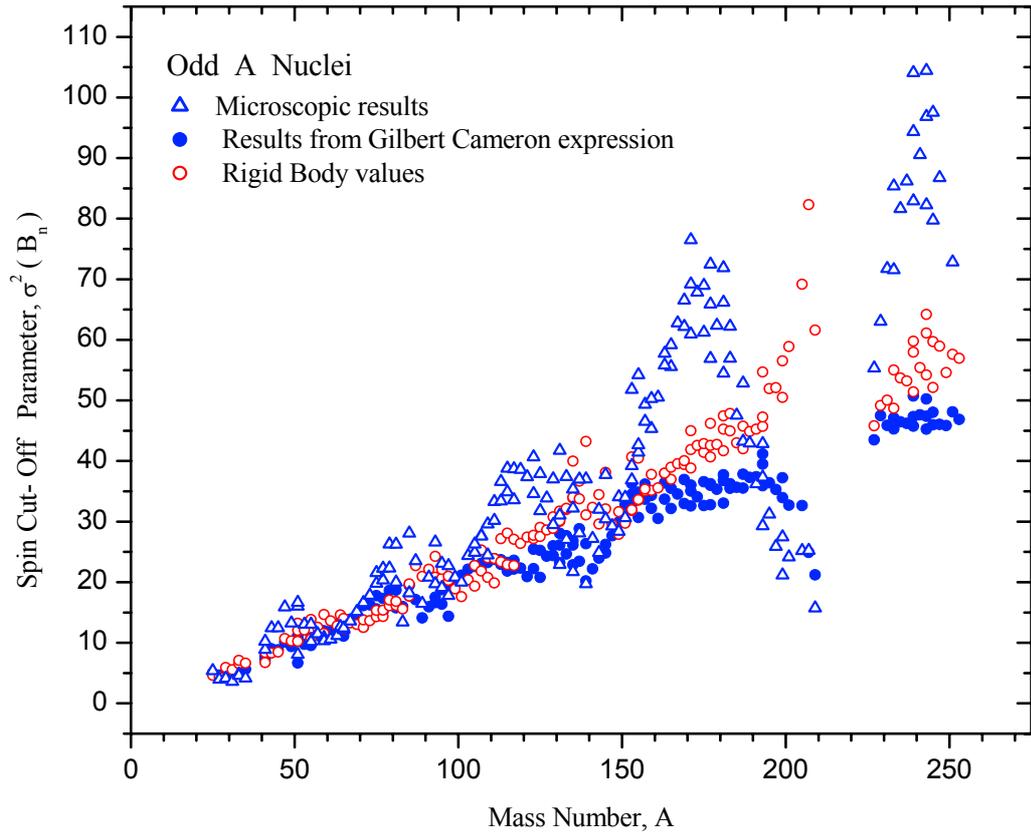


Figure 4.3: Comparison of Spin Cut-off Parameter, σ^2 from different methods for odd-A nuclei.

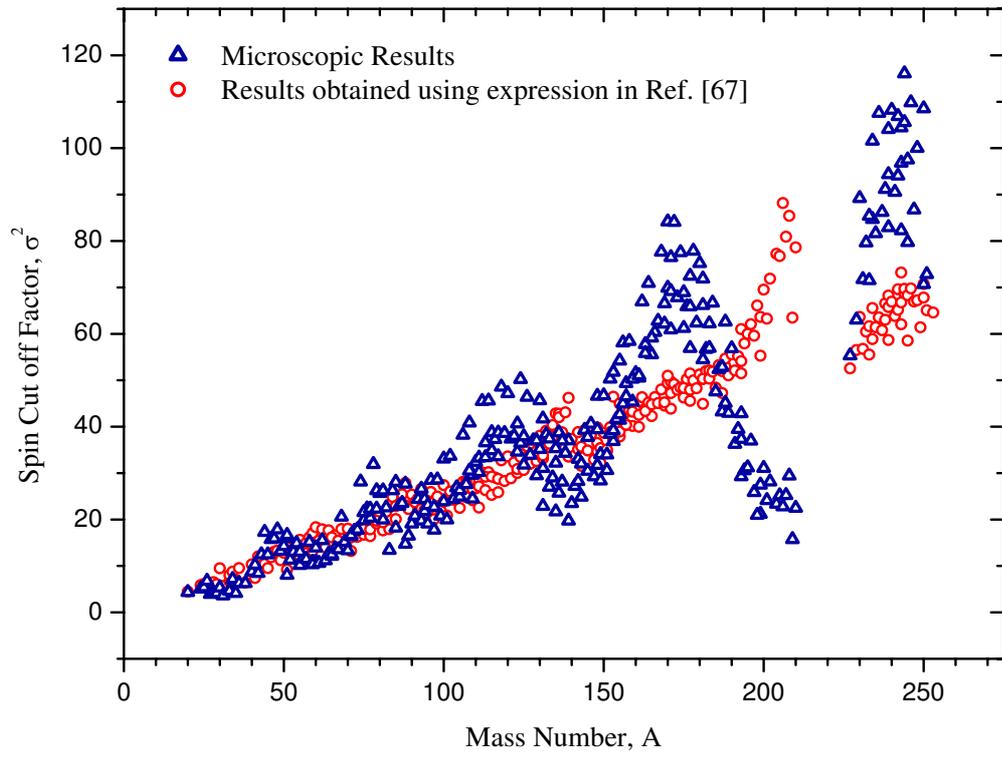


Figure 4.4: Comparison of Spin Cut-off Parameter, σ^2 at Neutron Binding Energy.

4.3.2 Calculations of σ^2 , from the Level Spacing Information

We have also computed the spin cut-off parameter for all nuclei under study from the knowledge of the nuclear level density at neutron binding energy, B_n and the average s-wave neutron spacing $\langle D_{1/2^+} \rangle$ which is [27]

$$\sigma^2 = \rho(B_n) \langle D_{1/2^+} \rangle / 2 \quad (4.1)$$

To do this, we have first computed nuclear level density around neutron binding energy from microscopic theory. The values of the average s-wave neutron spacing $\langle D_{1/2^+} \rangle$ were taken from compilation of Ignatyuck et. al [71, 72]. The deduced values of $\sigma^2(E)$ from Eqn. (3.22) together with their corresponding level densities obtained from the BCS approach and the average resonance spacing for selected odd A nuclei are listed in Table 4.4. Study of this table reveals that the $\sigma^2(E)$ values obtained from microscopic theory are much larger than their values obtained from the knowledge of the average spacing. However, if the values of the spin cut off factor deduced from Eqn. (4.1) are multiplied by a factor of $F = 0.25Z(\frac{Z}{N} + 1)$ the agreement between the two sets of results becomes very satisfactory. The corrected values of the spin cut off factors are also listed in Table 4.4 and are plotted in Figure 4.5.

Table 4.4: The Spin Cut-off Parameter, σ^2 at neutron binding energy for odd-A Spherical Nuclei.

N	Z	A	Element	$\rho(B_n)$	D_{exp}	Spin Cut-off Parameter, σ^2		
						a	b	c
13	12	25	Mg	2	1000000	5.39	1.00	5.77
17	16	33	S	10	87000	4.61	0.44	3.38
23	18	41	Ar	5	286000	8.89	0.72	5.74
21	20	41	Ca	25	74000	10.24	0.93	9.03
23	20	43	Ca	27	59000	12.46	0.80	7.45
25	20	45	Ca	20	148000	12.47	1.48	13.32
25	22	47	Ti	89	45000	15.91	2.00	20.71
27	22	49	Ti	34	200000	13.24	3.40	33.94
29	22	51	Ti	7	380000	8.06	1.33	12.86
27	24	51	Cr	147	76000	16.65	5.59	63.31
29	24	53	Cr	31	47000	13.05	0.73	7.99
31	24	55	Cr	13	95000	10.19	0.62	6.57
29	26	55	Fe	93	25000	13.04	1.16	14.33
31	26	57	Fe	45	62000	11.48	1.40	16.67
31	28	59	Ni	77	27000	10.34	1.04	13.85
33	28	61	Ni	63	39000	10.61	1.23	15.9
35	28	63	Ni	41	39000	11.18	0.80	10.07
37	28	65	Ni	29	64000	12.15	0.93	11.41
35	30	65	Zn	147	9000	12.44	0.66	9.21
37	30	67	Zn	100	6200	13.57	0.31	4.21
39	30	69	Zn	72	27000	15.16	0.97	12.9
39	32	71	Ge	346	4000	16.61	0.69	10.08
41	32	73	Ge	184	10000	17.82	0.92	13.1

a) : σ^2 , Calculated with Microscopic Model.

b) : $\sigma^2 = \frac{1}{2}\rho(B_n) \langle D_{1/2}^+ \rangle$.

c) : $\sigma^2 = \frac{1}{2}\rho(B_n) \langle D_{1/2}^+ \rangle \times [0.25Z(\frac{Z}{N} + 1)]$ (Modified Formula).

Table (4.4): Continue.

N	Z	A	Element	$\rho(B_n)$	D_{exp}	Spin Cut-off Parameter, σ^2		
						a	b	c
43	32	75	Ge	149	14000	19.81	1.04	14.55
45	32	77	Ge	104	43000	20.36	2.24	30.61
41	34	75	Se	1571	370	21.56	0.29	4.52
43	34	77	Se	750	1800	22.30	0.68	10.27
45	34	79	Se	415	4500	22.31	0.93	13.93
47	34	81	Se	206	10000	19.98	1.03	15.09
49	34	83	Se	41	69000	13.42	1.41	20.37
45	36	81	Kr	2400	1100	26.25	1.32	21.38
47	38	85	Sr	4127	950	28.09	1.96	33.68
49	38	87	Sr	2380	1000	23.53	1.19	20.07
51	38	89	Sr	137	12000	16.50	0.82	13.63
51	40	91	Zr	408	5000	20.80	1.02	18.20
53	40	93	Zr	467	4200	19.75	0.98	17.21
55	40	95	Zr	389	7500	19.10	1.46	25.20
51	42	93	Mo	2064	900	26.60	0.93	17.78
53	42	95	Mo	1027	670	23.10	0.34	6.48
55	42	97	Mo	913	1400	22.70	0.64	11.83
65	48	113	Cd	3948	200	33.40	0.39	8.24
67	48	115	Cd	3404	560	34.90	0.95	19.63
63	50	113	Sn	11937	330	36.60	1.97	44.16
65	50	115	Sn	14942	230	38.80	1.72	38.00
67	50	117	Sn	7562	350	38.70	1.32	28.89
69	50	119	Sn	5431	730	38.60	1.98	42.73
71	50	121	Sn	3356	1700	37.40	2.85	60.77

a) : σ^2 , Calculated with Microscopic Model.

b) : $\sigma^2 = \frac{1}{2}\rho(B_n) < D_{1/2}^+ >$.

c) : $\sigma^2 = \frac{1}{2}\rho(B_n) < D_{1/2}^+ > \times [0.25Z(\frac{Z}{N} + 1)]$ (Modified Formula).

Table (4.4): Continue.

N	Z	A	Element	$\rho(B_n)$	D_{exp}	Spin Cut-off Parameter, σ^2		
						a	b	c
73	50	123	Sn	1582	2500	34.60	1.98	41.65
75	56	131	Ba	80111	55	41.74	2.20	53.87
79	56	135	Ba	8003	380	32.21	1.52	36.38
81	56	137	Ba	2624	1850	28.13	2.43	57.47
83	56	139	Ba	84	18000	19.73	0.76	17.73
79	58	137	Ce	33837	63	37.01	1.07	26.80
83	58	141	Ce	491	5500	27.20	1.35	33.26
85	58	143	Ce	397	8900	24.88	1.77	43.10
83	60	143	Nd	3031	1700	32.02	2.58	66.58
109	72	181	Hf	41371	100	54.49	2.07	61.83
107	74	181	W	380889	8	66.18	1.52	47.68
109	74	183	W	77096	55	56.95	2.12	65.85
111	74	185	W	16343	140	47.56	1.14	35.27
113	74	187	W	15190	150	43.25	1.14	34.88
111	76	187	Os	83876	33	52.86	1.38	44.30
119	80	199	Hg	26866	90	27.48	1.21	40.43
123	82	205	Pb	15344	530	25.19	4.07	138.93

a) : σ^2 , Calculated with Microscopic Model.

b) : $\sigma^2 = \frac{1}{2}\rho(B_n) < D_{1/2}^+ >$.

c) : $\sigma^2 = \frac{1}{2}\rho(B_n) < D_{1/2}^+ > \times [0.25Z(\frac{Z}{N} + 1)]$ (Modified Formula).

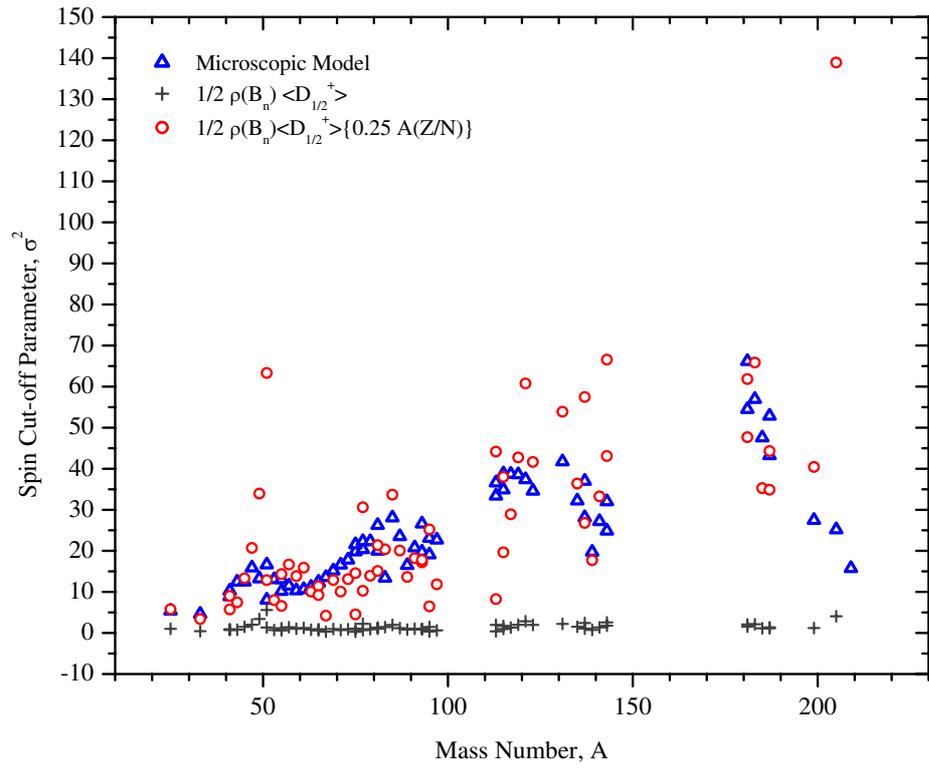


Figure 4.5: The Spin Cut-off Parameter, σ^2 at Neutron Binding Energy for Odd-A Spherical Nuclei.

4.4 Isospin Dependent Nuclear Level Density

The isospin dependent level density for ^{30}P and ^{32}S nuclei as a function of excitation energy for various isospins using Eqns. (3.28) and (3.29) was computed. First nuclear level density $\rho(E)$ were calculated as a function of energy as outlined in the previous chapter. The isospin dependent level density were then calculated by combining Equations (3.28) and (3.29). The results are given in Tables 4.5 and 4.6 and are displayed in Figures 4.6 and 4.7. Examination of these figures show that different isospin components of the level density sums up to total nuclear level density, $\rho(E)$.

Table 4.5: Calculated Level Density for ^{30}P for various isospin.

Energy	$\rho(U)_{BCS}$	$\rho(U, 0)$	$\rho(U, 1)$	$\rho(U, 2)$	$\rho(U, 3)$	$\rho(U, I_{all})$
2.47	0.14391	0.10138	0.05262	0.00262	1.87083E-5	0.15664
2.65	0.25915	0.16931	0.10307	0.00707	8.2928E-5	0.27953
5.12	0.57656	0.35107	0.2441	0.02186	3.8053E-4	0.61741
6.90	1.5446	0.88045	0.68508	0.07677	0.00187	1.64416
8.95	4.9102	2.63933	2.25388	0.30645	0.01002	5.20967
11.39	18.098	9.14401	8.51764	1.36857	0.05737	19.0876
13.71	80.631	38.54323	38.62547	7.18342	0.37493	84.72705
15.44	250.64	113.67777	121.50777	25.70814	1.62916	262.52284
16.92	484.58	209.06235	236.64949	56.15313	4.22554	506.09051
18.50	938.42	386.01907	459.96656	120.93419	10.60415	977.52396

Table 4.6: Calculated Level Density for ^{32}S for various isospin.

Energy	$\rho(U)_{BCS}$	$\rho(U, 0)$	$\rho(U, 1)$	$\rho(U, 2)$	$\rho(U, 3)$	$\rho(U, I_{all})$
3.43	0.31909	0.10138	0.12374	0.00769	7.65816E-5	0.34515
4.85	0.78079	0.16931	0.32568	0.02728	4.29435E-4	0.83761
6.73	2.3745	0.35107	1.04454	0.11227	0.00256	2.53041
8.88	8.8439	0.88045	4.04334	0.53665	0.01689	9.37312
11.39	38.965	2.63933	18.31238	2.91185	0.12001	41.10652
13.34	231.08	9.14401	110.69656	20.58692	1.0699	242.81424
14.62	420.86	38.54323	204.15498	43.54638	2.7903	440.72038
15.99	784.98	113.67777	383.61973	92.3372	7.09622	819.52697
17.46	1489.1	209.06235	730.13551	195.69752	17.67562	1550.40625
19.002	2858.3	386.01907	1401.5388	413.56743	43.13175	2968.51605

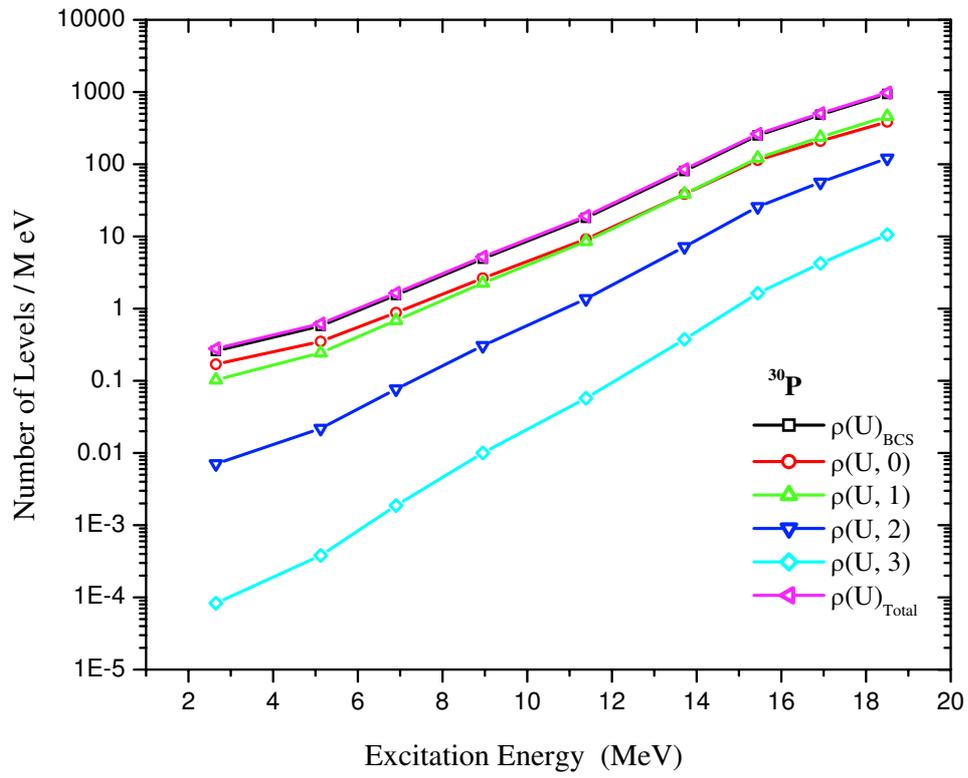


Figure 4.6: Level density of ^{30}P as a function of energy and isospin.

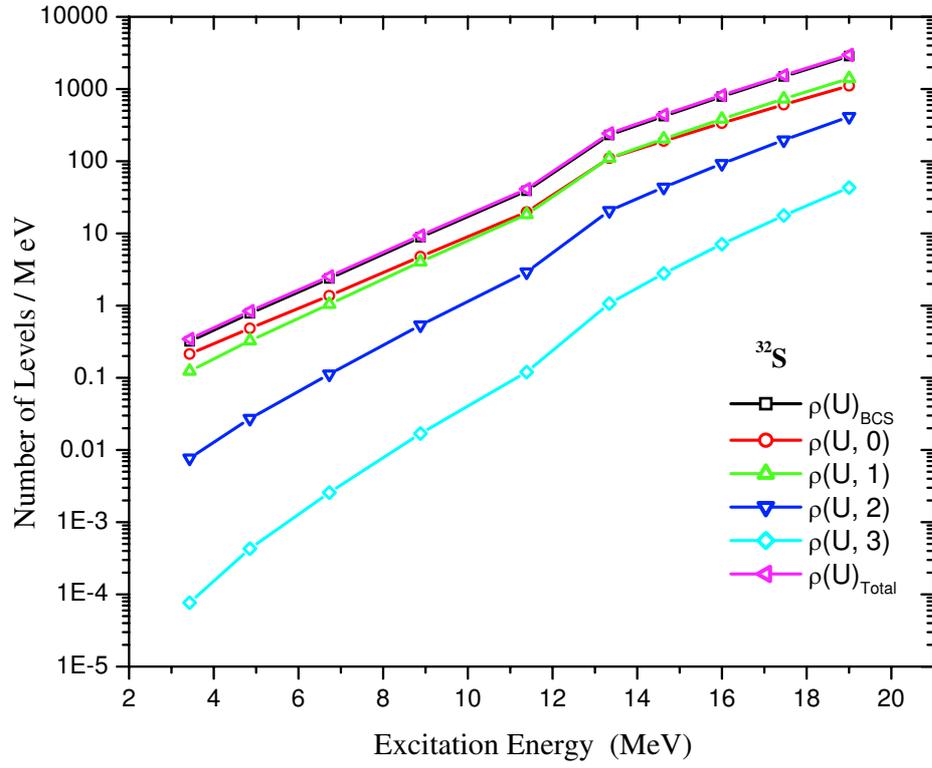


Figure 4.7: Level density of ^{32}S as a function of energy and isospin.

4.5 Isospin Cut-off Parameter

We have made study of isospin cut-off parameter (GC) for a large range of nuclei from ^{19}F to ^{253}Cf using the known values of a , E_0 , and B_n taken from Ref. [71]. The results are listed in Table 4.7 and are displayed in Figure 4.8, where isospin cut-off parameter is plotted in terms of mass number. Examination of this figure shows interesting results namely, that it shows structure in certain mass regions. The isospin cut-off parameter (BSFG) is also computed using different sets of parameters of a , E_0 , and B_n taken from Ref. [72]. The results are listed in Table 4.7 and are plotted in Figure 4.9. It is clear that the isospin cut-off parameters show the similar structure at certain mass regions. The isospin cut-off parameters calculated using two different sets of a , E_0 , and B_n values are plotted in Figure 4.10 for comparison.

The results of isospin cut-off parameter (GC) are compared with the spin cut-off parameter deduced from the BCS theory in Figure 4.11. In order to allow easy comparison the values of the isospin cut-off parameter are multiplied by a , level density parameter. We note that the position of the peaks coincide with that predicted from the BCS theory.

Table 4.7: The Isospin Cut-off parameters calculated using a , E_0 , and B_n values from Ref [71] and Ref [72].

Mass Number	Element	Isospin Cut-off Parameter, $\sigma_{I_z}^2$	
		a)	b)
20	F	0.81	0.99
24	Na	0.88	1.05
25	Mg	0.82	1.08
26	Mg	0.95	1.13
27	Mg	0.80	0.96
28	Al	0.94	1.03
29	Si	0.86	0.94
30	Si	0.88	1.13
31	Si	0.80	0.89
33	P	0.90	0.98
33	S	0.96	1.09
34	S	1.01	1.19
35	S	0.88	0.98
36	Cl	1.01	1.11
38	Cl	0.95	0.93
41	Ar	0.94	1.12
40	K	1.05	1.18
42	K	1.08	1.32
41	Ca	1.05	1.19
43	Ca	1.10	1.33
44	Ca	1.24	1.46
45	Ca	1.08	1.27
46	Sc	1.27	1.43

- a) : Calculated using the values of a , E_0 , and B_n from Ref[72].
b) : Calculated with parameters of a , E_{bs} , and B_n from Ref[71].

Table 4.7: Continue.

Mass Number	Element	Isospin Cut-off Parameter, $\sigma_{I_z}^2$	
		a)	b)
47	Ti	1.14	1.41
48	Ti	1.25	1.51
49	Ti	1.11	1.28
50	Ti	1.17	1.32
51	Ti	0.90	0.91
51	V	1.34	1.47
52	V	1.16	1.26
51	Cr	1.19	1.42
53	Cr	1.08	1.26
54	Cr	1.14	1.38
55	Cr	1.02	1.21
56	Mn	1.21	1.41
55	Fe	1.17	1.36
57	Fe	1.14	1.39
58	Fe	1.21	1.47
59	Fe	1.11	1.32
60	Co	1.27	1.43
59	Ni	1.20	1.43
60	Ni	1.27	1.52
61	Ni	1.18	1.39
62	Ni	1.26	1.50
63	Ni	1.14	1.31
65	Ni	1.10	1.25

a) : Calculated using the values of a , E_0 , and B_n from Ref[72].

b) : Calculated with parameters of a , E_{bs} , and B_n from Ref[71].

Table 4.7: Continue.

Mass Number	Element	Isospin Cut-off Parameter, $\sigma_{I_z}^2$	
		a)	b)
64	Cu	1.31	1.51
66	Cu	1.27	1.42
65	Zn	1.29	1.54
67	Zn	1.26	1.52
68	Zn	1.37	1.61
69	Zn	1.23	1.46
71	Zn	1.17	1.34
70	Ga	1.38	1.56
72	Ga	1.37	1.60
71	Ge	1.39	1.69
73	Ge	1.35	1.67
74	Ge	1.53	1.79
75	Ge	1.30	1.58
77	Ge	1.26	1.51
76	As	1.50	1.74
75	Se	1.48	1.79
77	Se	1.42	1.72
78	Se	1.53	1.81
79	Se	1.35	1.65
81	Se	1.30	1.52
83	Se	1.25	1.52
80	Br	1.55	1.78
82	Br	1.48	1.70

- a) : Calculated using the values of a , E_0 , and B_n from Ref[72].
b) : Calculated with parameters of a , E_{bs} , and B_n from Ref[71].

Table 4.7: Continue.

Mass Number	Element	Isospin Cut-off Parameter, $\sigma_{I_z}^2$	
		a)	b)
79	Kr	1.52	1.81
81	Kr	1.49	1.79
84	Kr	1.45	1.65
85	Kr	1.37	1.65
86	Rb	1.45	1.63
88	Rb	1.25	1.41
85	Sr	1.50	1.80
87	Sr	1.34	1.57
88	Sr	1.42	1.55
89	Sr	1.12	1.29
90	Y	1.25	1.37
91	Zr	1.26	1.43
92	Zr	1.35	1.56
93	Zr	1.29	1.46
94	Zr	1.43	1.64
95	Zr	1.29	1.42
97	Zr	1.17	1.24
94	Nb	1.51	1.66
93	Mo	1.35	1.54
95	Mo	1.40	1.62
96	Mo	1.49	1.74
97	Mo	1.41	1.66
98	Mo	1.51	1.78

a) : Calculated using the values of a , E_0 , and B_n from Ref[72].
b) : Calculated with parameters of a , E_{bs} , and B_n from Ref[71].

Table 4.7: Continue.

Mass Number	Element	Isospin Cut-off Parameter, $\sigma_{I_z}^2$	
		a)	b)
99	Mo	1.4	1.70
101	Mo	1.41	1.75
100	Tc	1.65	1.83
100	Ru	1.61	1.87
102	Ru	1.63	1.87
103	Ru	1.47	1.80
105	Ru	1.50	1.82
104	Rh	1.64	1.88
105	Pd	1.54	1.83
106	Pd	1.68	1.92
107	Pd	1.52	1.79
108	Pd	1.67	1.90
109	Pd	1.54	1.87
111	Pd	1.54	1.84
108	Ag	1.68	1.90
110	Ag	1.69	1.91
107	Cd	1.59	1.83
109	Cd	1.59	1.82
111	Cd	1.57	1.85
112	Cd	1.69	1.97
113	Cd	1.55	1.81
114	Cd	1.68	1.92
115	Cd	1.52	1.76

a) : Calculated using the values of a , E_0 , and B_n from Ref[72].

b) : Calculated with parameters of a , E_{bs} , and B_n from Ref[71].

Table 4.7: Continue.

Mass Number	Element	Isospin Cut-off Parameter, $\sigma_{I_z}^2$	
		a)	b)
117	Cd	1.49	1.77
114	In	1.65	1.78
116	In	1.67	1.81
113	Sn	1.58	1.76
115	Sn	1.52	1.66
117	Sn	1.50	1.66
118	Sn	1.62	1.82
119	Sn	1.47	1.66
120	Sn	1.59	1.77
121	Sn	1.39	1.54
123	Sn	1.40	1.62
125	Sn	1.32	1.50
122	Sb	1.66	1.85
124	Sb	1.61	1.81
123	Te	1.60	1.84
124	Te	1.72	1.97
125	Te	1.56	1.81
126	Te	1.66	1.90
127	Te	1.48	1.72
129	Te	1.47	1.71
131	Te	1.41	1.62
128	I	1.66	1.88
130	I	1.60	1.79

a) : Calculated using the values of a , E_0 , and B_n from Ref[72].

b) : Calculated with parameters of a , E_{bs} , and B_n from Ref[71].

Table 4.7: Continue.

Mass Number	Element	Isospin Cut-off Parameter, $\sigma_{I_z}^2$	
		a)	b)
129	Xe	1.56	1.82
130	Xe	1.67	1.89
131	Xe	1.56	1.81
132	Xe	1.60	1.81
133	Xe	1.48	1.70
135	Xe	1.39	1.57
134	Cs	1.64	1.88
135	Cs	1.68	1.82
136	Cs	1.58	1.80
131	Ba	1.68	1.94
133	Ba	1.63	1.90
135	Ba	1.54	1.78
136	Ba	1.63	1.86
137	Ba	1.43	1.59
138	Ba	1.48	1.64
139	Ba	1.19	1.37
139	La	1.62	1.76
140	La	1.42	1.62
137	Ce	1.68	1.93
141	Ce	1.33	1.48
142	Ce	1.52	1.69
143	Ce	1.40	1.59
142	Pr	1.50	1.64

a) : Calculated using the values of a , E_0 , and B_n from Ref[72].
b) : Calculated with parameters of a , E_{bs} , and B_n from Ref[71].

Table 4.7: Continue.

Mass Number	Element	Isospin Cut-off Parameter, $\sigma_{I_z}^2$	
		a)	b)
143	Nd	1.44	1.58
144	Nd	1.59	1.79
145	Nd	1.50	1.71
146	Nd	1.65	1.89
147	Nd	1.53	1.78
148	Nd	1.76	2.03
149	Nd	1.58	1.90
151	Nd	1.58	1.89
148	Pm	1.72	1.88
145	Sm	1.49	1.62
148	Sm	1.74	1.98
149	Sm	1.62	1.89
150	Sm	1.81	2.08
151	Sm	1.69	2.06
152	Sm	1.88	2.17
153	Sm	1.70	2.05
155	Sm	1.63	1.90
152	Eu	1.90	2.18
153	Eu	1.95	2.25
154	Eu	1.87	2.14
155	Eu	1.90	2.15
156	Eu	1.77	1.97
153	Gd	1.79	2.14

a) : Calculated using the values of a , E_0 , and B_n from Ref[72].

b) : Calculated with parameters of a , E_{bs} , and B_n from Ref[71].

Table 4.7: Continue.

Mass Number	Element	Isospin Cut-off Parameter, $\sigma_{I_z}^2$	
		a)	b)
155	Gd	1.79	2.13
156	Gd	1.88	2.18
157	Gd	1.74	2.06
158	Gd	1.80	2.11
159	Gd	1.66	1.96
161	Gd	1.59	1.84
160	Tb	1.80	2.00
157	Dy	1.89	2.21
159	Dy	1.78	2.08
161	Dy	1.76	2.08
162	Dy	1.83	2.15
163	Dy	1.69	2.01
164	Dy	1.74	2.02
165	Dy	1.62	1.91
166	Ho	1.76	1.96
163	Er	1.85	2.17
165	Er	1.78	2.10
167	Er	1.73	2.03
168	Er	1.78	2.08
169	Er	1.65	1.93
171	Er	1.62	1.89
170	Tm	1.80	2.01
171	Tm	1.84	2.08

a) : Calculated using the values of a , E_0 , and B_n from Ref[72].

b) : Calculated with parameters of a , E_{bs} , and B_n from Ref[71].

Table 4.7: Continue.

Mass Number	Element	Isospin Cut-off Parameter, $\sigma_{I_z}^2$	
		a)	b)
169	Yb	1.85	2.15
170	Yb	1.86	2.15
171	Yb	1.75	2.03
172	Yb	1.84	2.14
173	Yb	1.69	1.96
174	Yb	1.73	2.00
175	Yb	1.61	1.87
177	Yb	1.60	1.86
176	Lu	1.79	1.99
177	Lu	1.82	2.05
175	Hf	1.80	2.08
177	Hf	1.75	2.03
178	Hf	1.82	2.11
179	Hf	1.70	1.98
180	Hf	1.77	2.06
181	Hf	1.63	1.85
181	Ta	1.92	2.10
182	Ta	1.77	1.97
183	Ta	1.80	2.00
181	W	1.79	2.05
183	W	1.71	1.96
184	W	1.79	2.07
185	W	1.68	1.96

a) : Calculated using the values of a , E_0 , and B_n from Ref[72].

b) : Calculated with parameters of a , E_{bs} , and B_n from Ref[71].

Table 4.7: Continue.

Mass Number	Element	Isospin Cut-off Parameter, $\sigma_{I_z}^2$	
		a)	b)
187	W	1.66	1.94
186	Re	1.81	2.01
188	Re	1.78	2.00
187	Os	1.77	2.06
188	Os	1.88	2.14
189	Os	1.72	2.02
190	Os	1.84	2.11
191	Os	1.70	2.01
193	Os	1.66	1.92
192	Ir	1.85	2.07
193	Ir	1.94	2.19
194	Ir	1.78	2.00
193	Pt	1.79	2.10
195	Pt	1.64	1.93
196	Pt	1.77	2.03
197	Pt	1.59	1.86
199	Pt	1.55	1.78
198	Au	1.73	1.95
199	Hg	1.70	1.95
200	Hg	1.67	1.91
201	Hg	1.53	1.71
202	Hg	1.62	1.87
204	Tl	1.58	1.77

a) : Calculated using the values of a , E_0 , and B_n from Ref[72].

b) : Calculated with parameters of a , E_{bs} , and B_n from Ref[71].

Table 4.7: Continue.

Mass Number	Element	Isospin Cut-off Parameter, $\sigma_{I_z}^2$	
		a)	b)
206	Tl	1.38	1.50
205	Pb	1.48	1.69
207	Pb	1.23	1.30
208	Pb	1.19	1.26
209	Pb	0.99	1.11
210	Bi	1.25	1.47
227	Ra	1.74	2.08
229	Th	1.90	2.25
230	Th	1.96	2.28
231	Th	1.85	2.16
233	Th	1.79	2.13
232	Pa	1.99	2.14
234	Pa	1.96	2.12
233	U	1.92	2.21
234	U	1.97	2.29
235	U	1.84	2.17
236	U	1.96	2.30
237	U	1.81	2.14
238	U	1.89	2.25
239	U	1.77	2.11
238	Np	1.95	2.19
239	Np	2.00	2.33
239	Pu	1.87	2.18

a) : Calculated using the values of a , E_0 , and B_n from Ref[72].

b) : Calculated with parameters of a , E_{bs} , and B_n from Ref[71].

Table 4.7: Continue.

Mass Number	Element	Isospin Cut-off Parameter, $\sigma_{I_z}^2$	
		a)	b)
240	Pu	1.93	2.30
241	Pu	1.83	2.18
242	Pu	1.94	2.30
243	Pu	1.82	2.16
245	Pu	1.78	2.09
242	Am	1.96	2.22
243	Am	1.98	2.29
244	Am	1.92	2.18
243	Cm	1.82	2.07
244	Cm	1.95	2.24
245	Cm	1.85	2.18
246	Cm	1.88	2.20
247	Cm	1.77	2.08
248	Cm	1.86	2.14
249	Cm	1.76	2.06
250	Bk	1.89	2.10
250	Cf	1.93	2.20
251	Cf	1.85	2.15
253	Cf	1.78	2.08

- a) : Calculated using the values of a , E_0 , and B_n from Ref[72].
b) : Calculated with parameters of a , E_{bs} , and B_n from Ref[71].

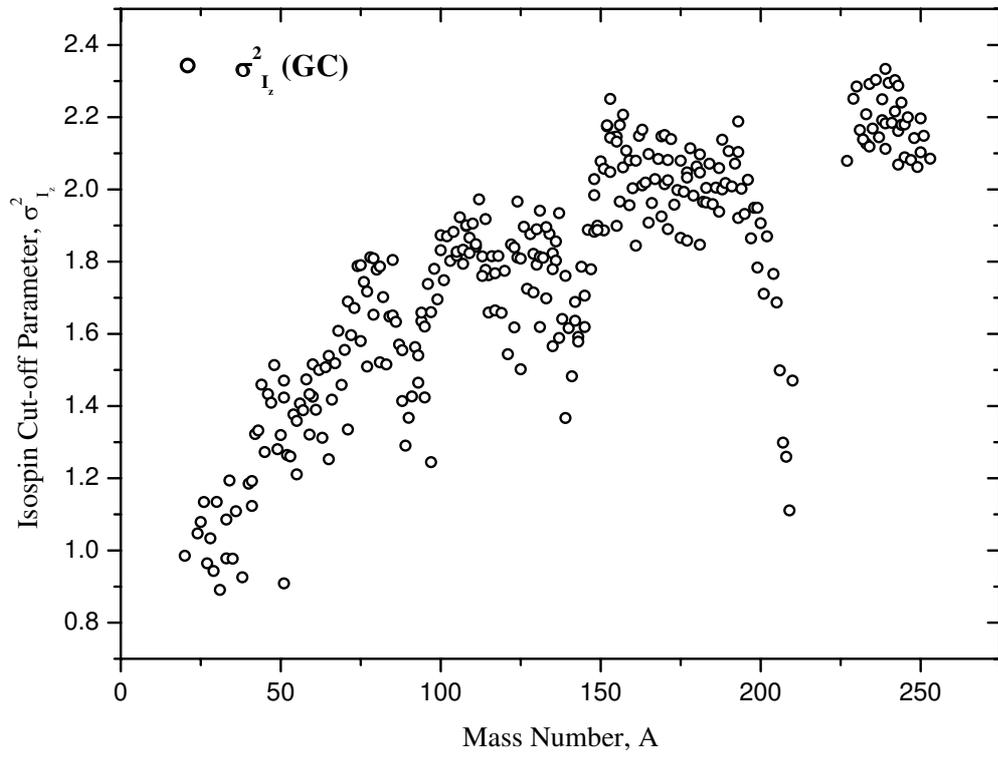


Figure 4.8: The Isospin Cut-off parameter plotted as a function of mass number, A . The parameters of a , E_0 , and B_n are taken from Ref [71].

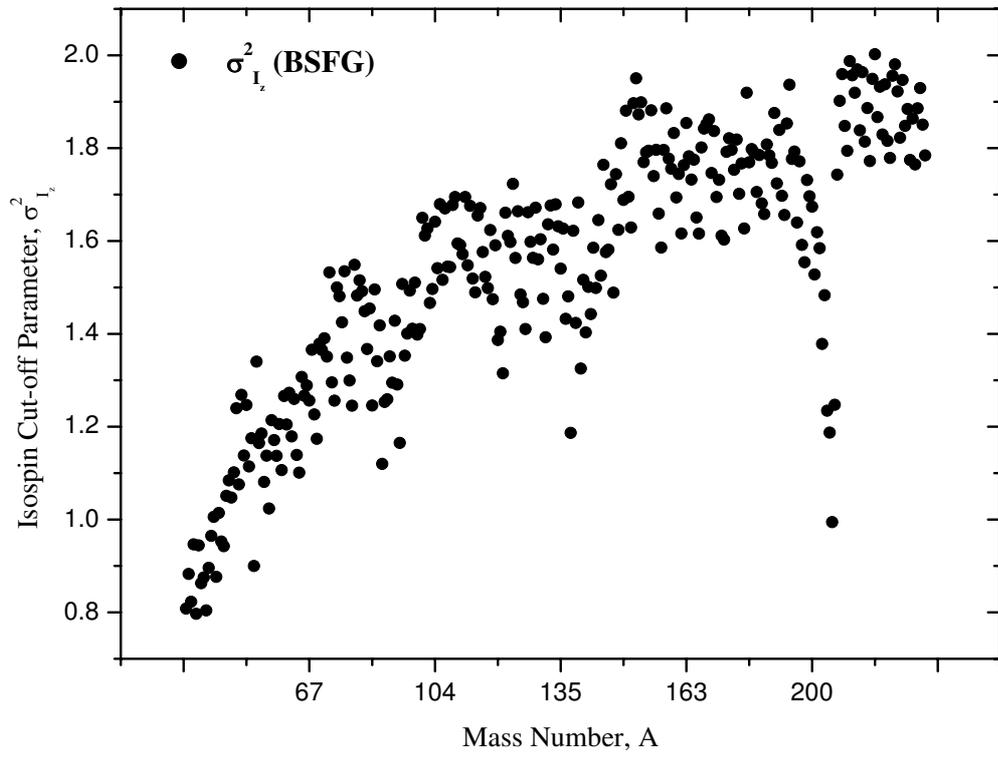


Figure 4.9: The Isospin Cut-off parameter plotted as a function of mass number, A . The parameters of a , E_0 , and B_n are taken from Ref [72].

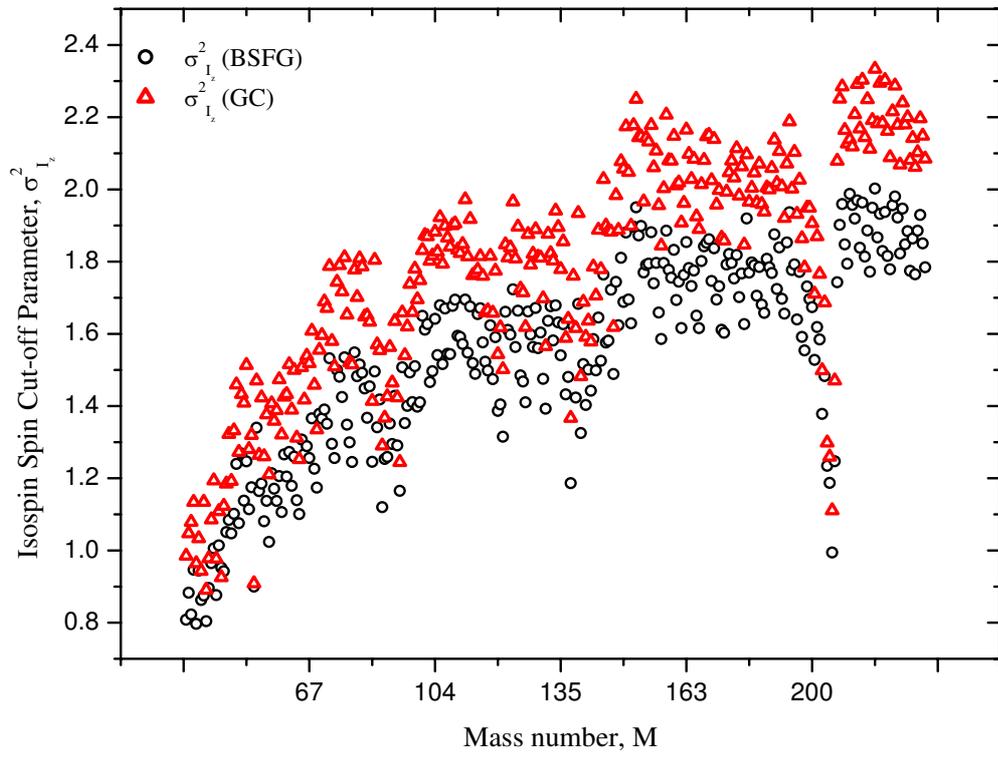


Figure 4.10: Comparison of the Isospin Cut-off parameter for two different sets of parameters a , E_0 , and B_n .

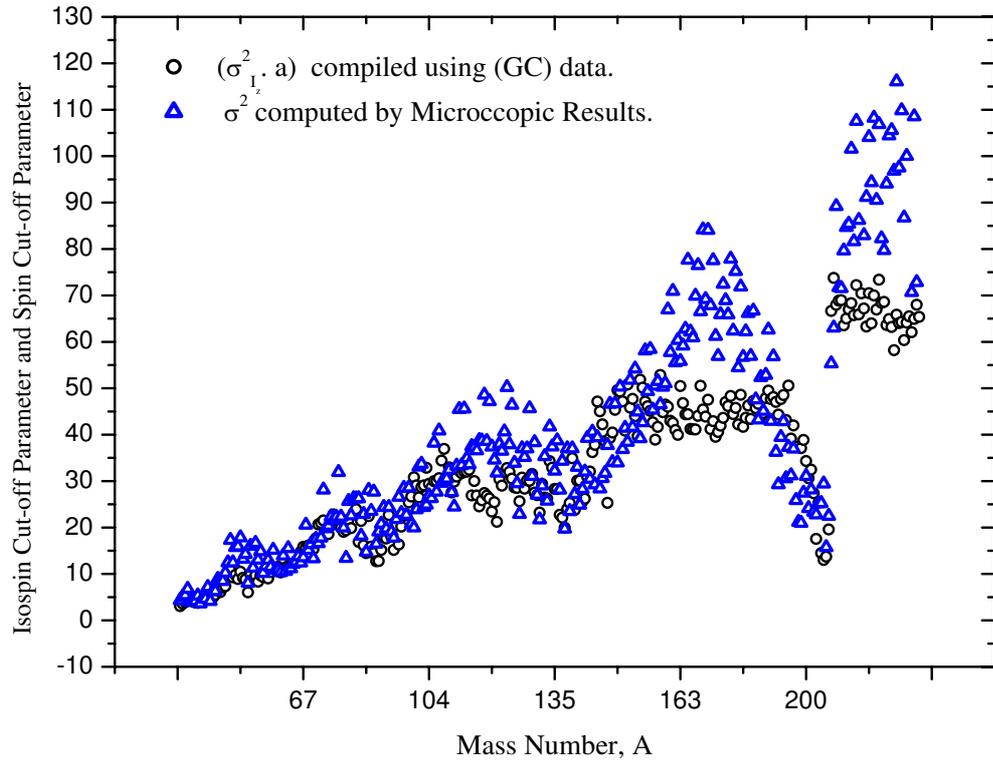


Figure 4.11: Comparison of the Isospin Cut-off parameter multiplied by a using parameters of a , E_0 , and B_n from Ref [71] with that of Spin Cut-off parameter from the BCS theory.

CHAPTER 5

SUMMARY AND CONCLUSIONS

Nuclear level density is an important quantity in the nuclear reaction theory. In this work program we have shown that the microscopic theory provides more precise information on the energy dependence of the nuclear level densities.

The spin cut-off parameter which is an important parameter in all statistical model codes has been computed for the first time using the microscopic approach. The spin cut-off parameter has been computed for a large range of nuclear mass by including a balanced number of even-even, odd A and odd-odd, light, medium weight and heavy and spherical and deformed nuclei. Our results indicate that the spin cut-off parameter, σ^2 values at neutron binding energy, B_n show structure reflecting the angular momentum of the shell model orbitals near the Fermi energy. For example there are four strong peaks in Figure 4.1 where the difference between current and the rigid body calculations are huge. The same results are seen in Figure 4.2 and Figure 4.3. Examination of the single particle level schemes for nuclei in these mass regions indicate that the orbitals with large angular momentum are responsible for these differences. In particular the $1f_{5/2}$, $1g_{7/2}$, $2d_{5/2}$ and $1i_{11/2}$ proton orbitals and $1g_{9/2}$, $1h_{9/2}$, $1h_{11/2}$ and $1i_{13/2}$ neutron orbitals play an important role in the $\sigma^2(B_n)$ values. This finding is no longer consistent with the claims made by some authors [27] that the spin cut-off parameter corresponds to their rigid body values.

In summary, in this work we have presented more realistic calculations of the

spin cut-off parameter for a wide range of mass region and show that the values $\sigma^2(B_n)$ obtained from the macroscopic methods are approximate. They are completely inadequate near magic nuclei; instead, significant shell and pairing effects appear for these nuclei.

The influence of the isospin has also been introduced in the calculations of the nuclear level densities. Such results for ^{30}P and ^{32}Si are reported in section (4-4). The isospin cut-off parameter has also been obtained as outlined in section (4-5). The results are displayed in chapter 4 are interesting in that they show structure similar to that observed in the spin cut-off parameters. This finding confirms the generally reported shell structure.[28, 67, 73]

Finally, we have presented a method of computing the isospin dependent nuclear level density, in particular the isospin cut-off parameter.

REFERENCES

1. J. R. Huizenga and L. G. Moretto, *Ann. Rev. Nucl. Sci.*, **22**, 427(1972).
2. A. N. Behkami and M. N. Nasrabadi, *Comm. Theo. Phys.*, **37**, 457(2002).
3. T. von Egidy, A. N. Behkami, and H. H. Schmidt, *Nucl. Phys.*, **A454**, 109(1986).
4. <http://www.nndc.bnl.gov/chart/chartNuc.jsp>, Last observed on July. 5, (2007).
5. J. M. Blatt and V. F. Weisskopf, *Theoretical Nuclear Physics*, p367, Wiley, (1960).
6. F. C. Jr. Williams, G. Chang, and J. R. Huizenga, *Nucl. Phys.*, **A187**, 225(1972).
7. A. Gilbert and A. G. W. Cameron, *Can. J. Phys.*, **43**, 1248(1965).
8. R. Fischer, G. Traxler, M. Uhl, and H. Vonach, *Phys. Rev.*, **C30**, 72(1984).
9. T. von Egidy, H. H. Schmidt, and A. N. Behkami, *Nucl. Phys.* **A481**, 189(1988).
10. C. H. Holbrow and H. H. Barschall, *Nucl. Phys.* **42**, 264(1963).
11. E. Erba, U. Facchini, E. Seatta Menichella and *Nuovo Cim.*, **22**, 1237(1961).
12. U. Facchini and E. Seatta Menichella, *Energ. Nucl.*, **15**, 54(1968).
13. A. K. Ignatyuk, G. N. Smirenkin, and A. S. Tishin, *Sov. J. Nucl. Phys.*, **21**, 255(1975).

14. A. G. W. Cameron, Can. J. Phys., **36**, 1040(1958).
15. P. E. Nemirovski, and Y. V. Adamchuck, Nucl. Phys., **39**, 551(1962).
16. H. Kummel, J. H. E. Mattauch, W. Thiele, and A. H. Wapstra, Nucl. Phys., **81**, 129(1966).
17. J. W. Truran, A. G. W. Cameron, and E. Hilf, CERN Conference, Vol. I, 275(1970).
18. J. Barden, L. N. Cooper and J. R. Schrieffer, Phys. Rev. 106, 162, 1957.
19. N. N. Bogoliubov, ZGETF **34**, 41, 1958.
20. A. Bohr, B. R. Mottelson and D. Pines. Phys. Rev. **110**, 963, 1958.
21. M. Sano, S. Yamasaki Prog. Theor. Phys. **29**, 397, 1963.
22. P. Decowski, W. Grochulski, Nucl. Phys. **A110**, 129, 1968.
23. J. L. Wile et al. Phys. Rev. C **35**, 1608, 1987.
24. U. K. Pal, Phys. Rev. C **51**, No. 6, 2942, 1995.
25. A. N. Behkami, Z. Kargar and P. Nazarzadeh, presented in the "Int. Nucl. Phys. Conf." 1995,
26. A. S. Iljinov, M. V. Mebel, Z. Phys. A **543**, 517, 1992.
27. A. Gilbert, A. G. W. Cameron, Can. J. Phys. **43**, 1446, 1965.
28. A. N. Behkami, Z. Kargar and M. Nasrabadi, Phys. Rev. C. **66** (2002) 064307.
29. S. K. Kataria, V. S. Ramamurhry and S. S. Kappor, Phys. Rev. C **18**, 549, 1978.

30. A. S. Jensen and J. Sandberg, *Physica Scripta* **17**, 107, 1978.
31. H. A. Bethe, *Rev. Mod. Phys.*, **9**, 69(1937).
32. C. V. Lier and G. E. Uhlenbeck, *Physica*, **4**, 531(1937).
33. J. M. Lang and K. J. Le Couteur, *Proc. Phys. Soc. Lond., A* **63**, 259(1958).
34. N. Rosenzweig, *Phys. Rev.*, **105**, 950(1957).
35. C. Bloch, *Phys. Rev.*, **93**, 1094(1954).
36. T. D. Newton, *Can. J. Phys.*, **34**, 804(1956).
37. N. Rosenzweig, *Phys. Rev.*, **108**, 814(1957).
38. A. A. Rose, *Phys. Rev.*, **108**, 720(1957).
39. T. Ericson, *Phys. Rev.*, **8**, 265(1958).
40. T. Ericson, *Nucl. Phys.*, **6**, 62(1958).
41. J. M. Lang and K. J. Le Couteur, *Nucl. Phys.*, **14**, 21(1959).
42. T. Ericson, *Advan. Phys.*, **9**, 425(1960).
43. L. Euler, *Opera mathematica*, Vol. II, p254, Berlin 1915, (1953).
44. C. L. Critchfield and S. Oleska, *Phys. Rev.*, **82**, 243(1951).
45. G. R. Grover, *Phys. Rev.*, **157**, 832(1967).
46. K. Kluge, *Nucl. Phys.*, **51**, 41(1967).
47. M. Hillman and G. R. Grover, *Phys. Rev.* **185**, 1303(1969).
48. F. C. Jr. Williams, *Nucl. Phys. A***133**, 33(1969).
49. F. C. Jr. Williams, G. Chan, and J. R. Huizenga, *Nucl. Phys. A***187**, 225(1972).

50. H. A. Bethe, Phys. Rev., **50**, 332(1936).
51. J. R. Oppenheimer, Phys. Rev., **50**, 391(1936).
52. J. H. D. Jensen, and J. M. Luttinger, Phys. Rev., **86**, 907(1952).
53. A. G. W. Cameron and R.M. Elkin, Can. J. Phys., **43**, 1288(1965).
54. L. Moretto, Nucl. Phys., **A182**, 641(1972).
55. H. Baba and S. Baba, Japan Atomic Energy Research Institute Report, JAERI-1183 (1969).
56. M. El Nadi and M. Wafik, Nucl. Phys. **9**, 22(1958/59).
57. H. Margenau, Phys. Rev., **59**, 627(1941).
58. W. Newson and M. M. Duncan, Phys. Rev. Let., **3**, 45(1959).
59. U. Mosel, P. G. Zint, and K. H. Passler, Nucl. Phys., **A236**, 252(1974).
60. A. N. Behkami and J. R. Huizenga, Nucl. Phys. A **217**, (1973) 78.
61. R. C. Duncan, S. L. Shapiro, and I. Wasserman, Ap. J. **309**, 141 (1986).
62. P. A. Seeger and R. C Perisho, Los Alamos Sci. Lab. Rep.LA3751 (1967).
63. I. Karstrom, Nucl. Phys. A **109** 625 (1968).
64. L. Henden M. Guttormsen, J. Rekstad and T. S. Tveter, Nucl. Phys. A **589**, 249 (1995).
65. Po-Lin Huang , S. M. Grime and S. M. Massey T N 2000 Phys. Rev. **62**, 024002.
66. A. N. Behkami and M. Soltani, Comm. Phys. Vol **43** No. 4 709 (2005).
67. D. Bucurescu and T. H. Von Egidy, J. Phys. G Nucl. and Part. Phys. **31** S1675 (2005).

68. J. R. Huizenga, A. N. Behkami, J. S. Sventek and R. W. Atcher. Nucl. Phys. A **223** (1974) 577.
69. A. N. Behkami and Z. Kargar, J. Phys. G Nucl. and Part. Phys. **18** 10 23-10-37 (1992).
70. M. Guttormsen, M. Hjorth-Jensen, E. Melby, J. Rekstad and S. Siem and A. Schiller Phys. Rev. C. **64** 034319 (2001).
71. A. K. Ignatyuck et. al. <http://www-nds.iaea.org/RIPL-2/>.(see DENSITIES - (ftp), Gilbert-Cameron Model, Data File (31kB), Last observed on July. 5, (2007).
72. A. K. Ignatyuck et. al. <http://www-nds.iaea.org/RIPL-2/>.(see DENSITIES - (ftp), Back-Shifted Fermi Gas Model (BSFG), Data File (27kB), Last observed on July. 5, (2007).
73. M. Gholami, M. Kildir and A. N. Behkami, Phys. Rev. C **75**, 044308 (2007).

CURRICULUM VITAE

MEHRDAD GHOLAMI

ADDRESS

Mehrdad Gholami
No.144, 7th Alley, Chehel Magham Blvd.
71467, Shiraz, Iran
Phone: +98 917 311 6685
Email: m.gholami@miau.ac.ir

PERSONAL DETAILS

Gender: Male
Date of birth: 3th of January, 1968
Place of birth: Shiraz, Iran
Present Citizenship: Iranian

EDUCATION

- | | |
|------------|---|
| 1985-1990 | Undergraduate Studies in Applied Chemistry at the Yazd I. A. University of Yazd, Iran |
| 1994- 1997 | Master in Marine Chemistry at the North Tehran I. A. University of Tehran, Iran
<i>Thesis: Measurement of Trace Elements and Radioactivity in Water, Fish and Bed Sediment of Bakhtegan Lake using NAA, ICP, AAS and Gamma Spectroscopy ; Supervisor: Prof. Dr. H. Ghafourian.</i> |
| 2002-2007 | Ph.D. in Chemistry at the Middle East Technical University of Ankara, Turkey.(CGPA= 3.69 from 4.00).
<i>Project title: Microscopic Study of Nuclear Level Density ; Supervisor: Prof. Dr. M.Kildir</i> |

PUBLICATIONS AND PAPERS

1. "Measurement of ^{137}Cs in Water, Fish and Bed Sediment of Bakhtegan Lake using Gamma Spectroscopy", 214th ACS, Division of Environmental Chemistry, National Meeting, Las Vegas, Nevada, September 7-11, 1997, Vol. 37, No.2, with S. M. Nojumi.
2. "Nuclear Level Densities and Spin Cut-off Factors Deduced from Low Energy Level Schemes", 1st International Nuclear Chemistry Congress, 22-29 May 2005, Kusadasi, Turkey, Abstract Book, Page 185, with M. Kildir, A. N. Behkami and M. Soltani.
3. "The Spin Cut-off of Nuclear Level Density", 2005, 2nd Joint Meeting of the Nuclear Physics Divisions of the APS and Physical Society of Japan, September 18-22, Maui, Hawaii., with M. Kildir, A. N. Behkami and M. Soltani.
4. "Nuclear Spin Cut-off Parameter and Effective Moment of Inertia" with M. Kildir and A. N. Behkami. Am. Phys. Soc. (four Corner section), Salt lake city Utah. Fall (2006).
5. "Microscopic Study of Nuclear Spin Cut-off Parameter" with M. Kildir and A. N. Behkami, Nashville, Tennessee, Oct. (2006).
6. "Nuclear Level Density with Non-zero Angular Momentum", with M. Kildir, A. N. Behkami and M. Soltani. Commun. Theor. Phys. (Beijing, China) 46 (2006) pp. 514-520.
7. "Statistical Treatment of Low Energy Nuclear Level Schemes", with M. Kildir, A. N. Behkami, Comm. Theo. Phys. (Beijing, China) 47 (2007) pp. 303-308.
8. "Microscopic Study of Spin Cut-off factor of Nuclear Level Density", with M. Kildir, A. N. Behkami, Phys. Rev. C 75, 044308 (2007).

WORKING EXPERIENCE

- | | |
|------------|--|
| 1996- 2001 | Faculty Member of Firuzbad I. A. University. |
| 1998- 2001 | Research Deputy of Marvdasht I. A. University. |
| Since 2005 | Faculty Member of Marvdasht I. A. University. |

LANGUAGE KNOWLEDGE

Farsi	Native
English	Speak fluently and read and write with high proficiency

TEACHING EXPERIENCE

Instructing following Undergraduate Courses:

1. Nuclear Chemistry.
2. Analytical Chemistry I, II and related laboratories.
3. Instrumental Analytical Chemistry and related laboratory.
4. Application of Electronics in Chemistry and related laboratory.
5. General Chemistry I, II and related laboratories.

Instructing following Graduate Courses:

1. Atomic Spectrometry.
2. Advance Electrochemistry.
3. Special Topics in Analytical Chemistry.

REFERENCES

These persons are familiar with my professional qualifications and my character:

Prof. Dr. M. Kildir

Thesis supervisor

Chemistry Department of Middle East Technical University
06531 Ankara Turkey

Phone: +90 312 210 3243
Fax: +90 312 210 1280
Email: Kildir@metu.edu.tr

Prof. Dr. A. N. Behkami

Thesis Co advisor

Physics Department of Shiraz University
71454 Shiraz Iran

Phone: +98 917 113 5323
Fax: +98 711 225 4594
Email: behkami@susc.ac.ir

Prof. Dr. O. Yavuz Ataman

Analytical Chemistry Instructor

Chemistry Department of Middle East Technical University
06531 Ankara Turkey

Phone: +90 312 210 3232
Fax: +90 312 210 12 80
Email: ataman@metu.edu.tr

Prof. Dr. R. Sezer. Aygün

Analytical Chemistry Instructor

Chemistry Department of Middle East Technical University
06531 Ankara Turkey

Phone: +90 312 210 3239
Fax: +90 312 210 1280
Email: saygun@metu.edu.tr

Prof. Dr. S. Özkar

Inorganic Chemistry Instructor

Chemistry Department of Middle East Technical University
06531 Ankara Turkey

Phone: +90 312 210 3212
Fax: +90 312 210 12 80
Email: sozkar@metu.edu.tr

Gholami, July 6, 2007